Features of Indian Summer Monsoon at its Gateway over Cochin using ST Radar, Radiosonde and Satellite Observations

Thesis submitted in partial fulfilment of the requirements

for the degree of

DOCTOR OF PHILOSOPHY

in

ATMOSPHERIC SCIENCE

By

Suresh N

Under the Guidance of

Prof. Dr. K. Mohankumar

DEPARTMENT OF ATMOSPHERIC SCIENCES

COCHIN UNIVERSITY OF SCIENCE AND TECHNOLOGY

COCHIN, INDIA

December 2017

Features of Indian Summer Monsoon at its Gateway over Cochin using ST Radar, Radiosonde and Satellite Observations

Ph.D. Thesis under the Faculty of Marine Sciences

Author

Suresh N
Research Scholar
Department of Atmospheric Sciences
Cochin University of Science and Technology
Cochin, India
email: narayasuresh@gmail.com

Supervising Guide

Prof. Dr. K. Mohankumar, M.Sc., Ph.D.
Advanced Centre for Atmospheric Radar Research
Cochin University of Science and Technology
ST Radar Facility, Cochin 682 022, Kerala, India
email: kmk@cusat.ac.in, kmkcusat@gmail.com

Advanced Centre for Atmospheric Radar Research
Cochin University of Science and Technology
ST Radar Facility, Cochin 682 022, Kerala, India

December 2017

This Slice of my academic life is dedicated to all my loving Students of Physics Chamber

ADVANCED CENTRE FOR ATMOSPHERIC RADAR RESEARCH
COCHIN UNIVERSITY OF SCIENCE AND TECHNOLOGY
ST Radar Facility, Cochin 682 022, Kerala, India

Prof. Dr. K. Mohankumar, M.Sc., Ph.D.
Director ACARR & Project Director, ST Radar Facility

CERTIFICATE

This is to certify that the Doctoral thesis entitled **Features of Indian Summer Monsoon at its Gateway over Cochin using ST Radar, Radiosonde and Satellite Observations**, submitted by **Mr. Suresh N** (Reg. No. 4510), is a bonafide record of research work done by the candidate under my supervision, and guidance in the Department of Atmospheric Sciences and the Advanced Centre for Atmospheric Radar Research, in partial fulfillment of the requirements for the Ph. D degree of Cochin University of Science and Technology. I further declare that this work is original and has not been formed the basis for the award of any Degree, Diploma, Associateship or any other similar title in any University or Institution.

I further certify that all the relevant corrections and modifications suggested by the audience during the pre-synopsis seminar and recommended by the Doctoral Committee of the candidate have been incorporated in the thesis.

K. MOHANKUMAR
UGC BSR Faculty

Tel: 91-484-2575241(Dir), Fax: 91-484-2575241 Mobile: 91 9447157370, 0484 - 2340995(Res): E-mail: kmk@cusat.ac.in, kmkcusat@gmail.com, kmkacarr@gmail.com

DECLARATION

I hereby declare that the thesis entitled **'Features of Indian Summer Monsoon at its Gateway over Cochin using ST Radar, Radiosonde and Satellite observations'** is an authentic record of PhD research work carried out by me under the supervision of Prof. Dr. K Mohankumar, Department of Atmospheric Sciences, Faculty of Marine Sciences, Cochin University of Science and Technology and that no part of it has previously formed the basis for award of any degree, diploma, associate-ship, fellowship or any other similar title or recognition in any University.

Cochin **Suresh N**
Date:

ACKNOWLEDGEMENTS

As a leading light showing the true path of advancement, my research guide and mentor Prof. (Dr.) K. Mohankumar, Director, Advanced Centre for Atmospheric Radar Research (ACARR), cannot be thanked only formally but should be considered as the spirit behind the whole effort I converged in the accomplishment of this thesis. May I extend my whole hearted gratitude to this motivating mind who at the outset was ready to accept me as one of the research students and thereafter moulded me with timely advices and suggestions.

I extend my sincere thanks to the S T Radar facility at ACARR funded through Science and Engineering Research Board (SERB) and Dept. of Science and Technology (DST), Government of India, for the extensive support they bestowed to me in making this project highly successful. The financial support given by Cochin University of Science And Technology (CUSAT) through University Fellowship is duly acknowledged at this moment.

To me, Department of Atmospheric Sciences (DAS) of CUSAT is always a centre of academic rejuvenation, and this prestigious department took me in confidence when it allowed me to associate with the series of GPS Radiosonde ascents as a pilot programme for the much awaited S T Radar project which got commissioned within a short time. I take this opportunity to present my thanks to the then Head of the Department Dr. C A Babu. Present Head of the Department Mr. Baby Chakrapani supported and motivated me throughout my work – thank you sir.

My entry into this leading department as a student was made possible with the loving support of Dr. C. K. Rajan, the former Head of the Department, who along with the graceful presence of the veteran scientist Dr. P. V. Joseph influenced me to taste the deeper nuances of the subject of Meteorology.

I am thankful to Dr. Santosh K. R, Dr. H S Ram Mohan, Dr. K G Anilkumar and the Faculty of the Dept. of Oceanography in bringing out my interest to this field of study. The special campaign event organized by SPL (VSSC) gave a new dimension to my work and I express my thanks to Dr. Sijikumar and Dr.Sunilkumar S V, for thier association.

I am much obliged to our former librarian of the Lakeside campus, Mr. Manuel who is always a good friend and motivator. The support and care offered by the computer lab Technical Officer Dr. M G Sreedevi and

Mr. G Yasodharan (Retd) helped me in this venture while all the present and past office staff members navigated me in the right direction - my sincere thanks to all.

The brotherly affection and guidance bestowed by Dr Venu G Nair is beyond all words of gratitude while Mr. Baburaj (India Meteorology Department) stood along with me during the experimental phase with befitting suggestions and professional transactions. Dr. Nithin Viswambharan truly gave initial guidance and practice in analyzing the radiosonde data – thank you dear friend. Dr. Johnson, Dr. G Bindu. Dr. Anu Simon, Dr. Madhu V, Dr. Abhilash S, Dr. K Satheesan, and so many friends in the campus played pivotal role in bringing out my affinity to this subject.

The nature of my research program was totally modified with the inception of a cream of youngsters in the scientific pool of ACARR – the brain child of Prof. Dr. K Mohankumar. Without the help and support of Dr. Manoj M G this venture would have never been accomplished, within the desired time. Also, the vital step provided by Dr. Ajil Kottayil as the corresponding author in publishing my research paper in the International Journal of 'Meteorology and Atmospheric Physics' paved my route towards the goal. Both, Dr. Manoj and Dr. Ajil deserve a great bouquet of gratitude for moulding me. I extend my love and affection to all executive and administrative members of ACARR at this time.

My university CUSAT made me to become a post-graduate in Meteorology and then supported me to undertake this research programme. No words and feelings would be sufficient to express my reverence and gratitude to this great national academic centre.

Nobody can do any fruitful effort, demanding a long term steady work, without the support of a loving family. I do accept the responsibility in putting directly or indirectly all my family under emotive pressure throughout the period of this project. My beloved wife and critic Dr. Anila supported me in advancing through this effort with timely suggestions and motivating compliments. My sons Niranj and Nikhil were role models for me to keep a vibrant mind in diving deep into the hidden realms of this subject. I thank all my well wishers and friends, especially Mr. Prasad kumar (Principal, Queen Mother's College, Aluva), for their help, suggestions and curiosity to see the productive culmination of this academic endeavor.

And……somewhere in the profound reality of Nature my mother and father are smiling at me with their blessings.

PREFACE

Kerala is the land of Monsoons. In fact, the first burst of the southwest monsoon over the Indian subcontinent takes place over Kerala. The timely onset, optimum duration and reasonable strength of the southwest monsoon are of vital importance to the life and economy not only of India but the entire South Asian region. The State constitutes a natural and unique geographic unit with oval mountains, verdant valleys, evergreen forests, cascading waterfalls and palm-fringed lagoons.

Cochin (10°N; 76.33°E) is located in the central part of Kerala is a meteorologically sensitive region. The rainfall over Cochin is influenced by both the coastal effect and the orographic effect, the region being lying within the boundary delineated by Arabian Sea in the west and mighty Western Ghats to the east. The highest mountain peak of Western Ghats, *Anamudi*, lies just 100 km in the same latitude belt of Cochin.

Cochin is considered as the Gateway of Indian summer monsoon. During this season, westerly flowing monsoon low level jet stream develops around 1.5 km, and the tropical easterly Jet stream forms at 14 km altitude. Both these jet streams oscillates north-south over Cochin, and modify the monsoon activity during summer.

A strong low level jet stream (LLJ) exists over Kerala during the southwest monsoon season. Over the peninsular region, the LLJ often intensifies on occasions of strong or vigorous monsoon conditions. This fast air current is a cross-equatorial jet stream and is the main artery feeding moisture for the monsoon rains over the entire south Asia. It has a core of wind speed 70 to 100 km per hour at an altitude of 1.5 km above sea level. The depth of the westerlies decreases northward progressively. The westerlies become easterlies at about 700 hPa level.

Tropical easterly jet stream (TEJ) is located above the Asian summer monsoon current between the equator and 20^{o}N latitude. It is most developed over the Indian peninsular region, overlying the southwest monsoon region. TEJ is seen from June to September only, over the north Indian Ocean. Maximum wind speed of TEJ is near to the tropopause region, between 14 and 16 km altitude. The core wind speed is of the order of 60 to 100 knots.

As Cochin being the entry region of the south west monsoon into India, a detailed understanding of the circulation and thermal characteristics of the entire troposphere and lower stratosphere is highly useful to understand the inter-annual and intra-seasonal

variability of monsoon rainfall over the coastal region on the southwest Peninsular India. Cochin is situated in the coastal region with moist enriched atmosphere over the Arabian Sea on one side and mighty Western Ghats mountain on the other side. The highest mountain peak of Western Ghats, just 100 km away from Cochin, orographically lifts the moist air flowing over the region produces intense clouding, which results heavy precipitation in the windward side during the monsoon season. Continuous monitoring of the atmosphere over Cochin is indeed necessary to understand the transformation of the atmospheric conditions as the moist air over Arabian Sea enters into the continental region. No attempt has been made in this region to monitor the circulation and temperature changes in the troposphere using high resolution GPS Radiosonde observations. Recently installed state-of-the art high resolution Stratosphere Troposphere Wind profiler Radar at Cochin University of Science and technology (CUSAT) gives continuous observations of the circulation pattern in this region, is expected to provide detailed information in the coming years.

As a first step to the comprehensive study for understanding the characteristics of the atmosphere over Cochin, regular high resolution GPS radiosonde observations were initiated at CUSAT, Cochin during the 2013 year monsoon onwards. Radiosonde observations were continued thereafter. Before realizing the main 205 VHF ST Wind profiler radar, a mini Wind Profiler radar with 49 antenna element system was operated in 2014 and 2015. The present doctoral thesis is the outcome of the studies obtained from the GPS radiosonde observations and mini Wind Profiler data during the period 2013 to 2016, with the major objective to identify the features of the coastal atmosphere over Cochin during the onset, active, break and withdrawal phases of monsoon. During this study period, good monsoon is experienced in the year 2013, whereas weak monsoon is observed in 2015. The nature of the atmosphere during the contrasting monsoon years (2013 and 2015) were studied and reported. In addition to the GPS radiosonde and mini Wind Profiler data, satellite observations were also used to supplement the observations.

The major objectives of the doctoral thesis work are: (i) to study the atmospheric characteristics over Cochin during monsoon period; (ii) to understand the diurnal and spatial variation of monsoon parameters; (iii) to compare the features of two distinct monsoon seasons at Cochin; and (iv) to explore the atmospheric circulation features over Cochin using ST Radar.

The first chapter of the thesis gives a detailed documentation of monsoon and its impact over Indian peninsular region. Chapter 2 unfolds the details of the experimental arrangements and procedures adopted in both Radiosonde and ST Radar observations.

The atmospheric features of south-west monsoon over Cochin were studied with Radiosonde experiments carried out by GPS loaded balloon ascents. Using the data from 54 such ascents, over a period of four and a half months, starting from 21st May to 16th October 2013, a detailed analysis of the time series of temperature, humidity, zonal and meridional winds were carried out and reported in chapter 3. Strengthening and weakening of monsoon low level jet (LLJ) in the lower troposphere and the tropical easterly jet (TEJ) in the upper troposphere are showing strong association with rainfall variations during monsoon.

A comparison between strong and weak monsoon years occurred in 2013 and in 2015 respectively is dealt in chapter 4. Using high resolution Radiosonde data gathered *in situ* by experiments, LLJ characteristics in Indian summer monsoon over Cochin was studied for two distinct monsoon years 2013 (strong monsoon)and 2015 weak monsoon). The LLJ core speed, core height and westerly depth vary significantly in these two contrasting years. During the afternoon, the LLJ core level is seen around 2 km and above. The moisture, momentum and kinetic energy fluxes during weak monsoon year are relatively low compared to that of the active monsoon year. The effect of LLJ on rainfall at Cochin was studied through multiple linear least square regression technique.

Chapter 5 deals with the special experimental campaign using radiosonde observations conducted simultaneously at three locations, viz., Thiruvananthapuram (8.63° N; 77° E), Cochin (10° N;76.33° E) and Coimbatore (10.9° N; 76.9° E) to learn the atmospheric characteristics during monsoon season. Two of the above stations are located in the coastal region, whereas the third one is an interior station. The diurnal changes in the atmosphere as well as the changes in the circulation patterns in the atmospheric region overlaying these triangularly located stations were studied and reported.

Preliminary studies of the lower tropospheric circulation patterns were studied utilising the mini Wind Profiler observations from Cochin and presented in Chapter 6 of the thesis. Two severe thunderstorm events observed during 2015 were studied utilising the high resolution and continuous observations from the mini Wind Profiler radar and narrated in this session. Intense vertical shear, strong ascending and descending circulation patterns are found associated with the growing, mature and decaying phases of the thunder storm cell.

The outcome of the study is depicted in Chapter 7 as summary and conclusions. Major findings of the doctoral thesis were presented. Future scope of the study, evolved from the present study, is given in this chapter. References are given at the end of the thesis in alphabetical order.

Contents

List of Tables

List of Figures

Chapter

1

An Overview of Indian Summer Monsoon with Special Reference to the Weather and Climate of Kerala

Contents

1.1 Background

The Indian Summer Monsoon is one of the most decisive factors for at least one fifth of the world's population in providing drinking water, food security, livable climate and their daily livelihood. The word 'monsoon' means seasonal reversal of pressure and wind systems (Ramage, 1971). This terminology is used for climate that has an apparent seasonal shift of prevailing winds between winter and summer, notably in tropical Asia, Australia, Africa, and the Indian Ocean. Monsoon systems represent the dominant variation in the climate of the tropics with profound local, regional, and global impacts (World Climate Research Programme Report, 2006). The Indian Summer Monsoon or simply the southwest (SW) monsoon which sets in around the first week of June and lasts until September contributes to about 75% of the annual rainfall (Kaur and Purohit, 2015) received by the country. About 60% of the agricultural production is directly dependent on the strength of the summer monsoon. The SW monsoon shows large variability on both spatial and temporal scales, and the inter-annual standard deviation of rainfall is estimated to be about ten percent (9 cm) of its seasonal mean (~89 cm). Within a season itself, the monsoon is manifested as strong and weak (active-break cycle) spells, and their amplitude and frequency decide the vigour of both intra-seasonal and inter-annual variabilities of summer monsoon precipitation over the region.

The monsoonal circulation is a planetary scale phenomenon, and the link between the seasonal reversal of winds over the north Indian Ocean, their cross-equatorial flow and relationship with the commencement of summer rains over South Asia began to be investigated with the classical work of Halley (1686), based on the analysis of data collected during the transit of ships over the vast Indian Ocean (Sikka, 2012). With the establishment of the India Meteorological Department (IMD) in 1875, scientific studies on the southwest (summer) and northeast (winter) monsoons in India were systematized with lot more ground based and air-borne observations. Based on some 20 years of data, Blanford (1886) emphasized the prominence of seasonal surface heat low over now Pakistan region, and the monsoon trough stretching from undivided northwest India to Bay of Bengal in regulating the processes in SW monsoon and regulating rainfall over the Indian region.

In a climatological sense, the SW monsoon for the entire country sets in over Kerala around the first week of May. The monsoon onset over Kerala (MOK) occurs over the southern part of Kerala, especially over the region between Thiruvananthapuram and Kochi (also known as Cochin). In general, Cochin is qualified as the gateway of Indian summer monsoon (ISM). Subsequent rate of northward propagation of rain bands, its active and weak phases, and final withdrawal from the southern peninsula is of utmost importance to the ultimate existence of the flora and fauna over the continent. It is to be emphasized that the ISM is typically considered to be the 'model' one among the global monsoons due to its semi-permanent features and systematic seasonal behaviour (Charney and Shukla,1981). In a simplified manner, the monsoon can be viewed as a large-scale sea-breeze circulation (Gupta, 2006) modified by the rotational effects of the Earth (Coriolis force), and also forced by the topography of the country with several background teleconnection patterns. The huge circulation pattern extending right from the Earth's surface (planetary boundary layer-PBL) and extending to the lower stratosphere and the associated instability determine the quantum of rainfall received during each monsoon season. Probing into the characteristics of monsoon commencing from entry at the Gateway and its withdrawal at the exit point offers us an exceptional opportunity to portray its complex characteristics during different

years, and to comprehend its dynamics and thermodynamics. The unique topography of Kerala (see Fig. 1.1) provides a favourable condition for strong rainfall along the west-coast of southern peninsular region.

This chapter tries to narrate the general characteristics of monsoon including the semi-permanent features, the strong jet-like circulation pattern and their role in inducing deep convection, the intraseasonal and interannual variabilities, and finally the withdrawal of the gigantic convection.

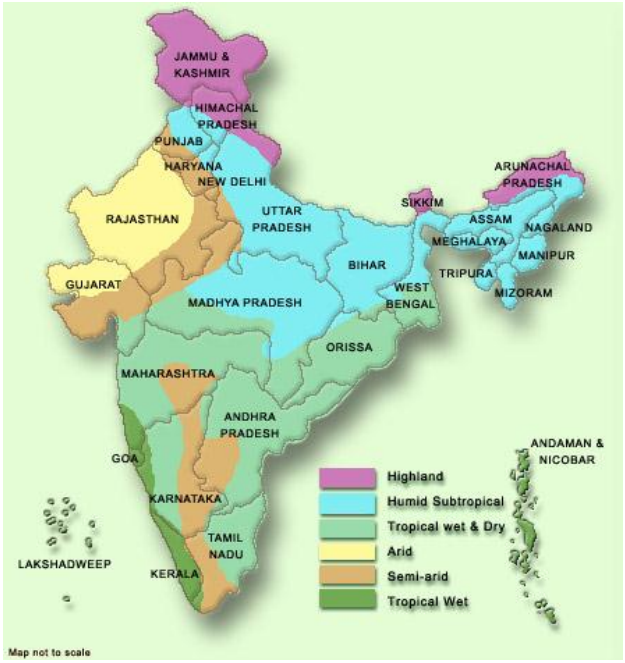

Fig.1.1: Climatic Zone Map of India

1.1.1 Large-scale Aspects of Indian Monsoon

Several works in the past have addressed new large-scale components of the SW monsoon since 1950. The significant points among them are:

(a) Traditionally, south-west monsoon is considered to be a large-scale sea breeze circulation, that results from the differential heat capacity of the land and ocean water during the northern hemisphere summer, modified by the rotational effects of the Earth. The Indian Summer Monsoon current is formed due to a high-pressure area near a small island in the southern hemisphere over the South Indian Ocean called Mascarene, located at 30 degree south latitude and 70 degree east longitude, at about 4,000 km away

from the Indian mainland. Winds from this high-pressure area, termed as Mascarene High, start blowing towards the northern hemisphere along the east Somalia coast under the Coriolis force. The east Somalian coast has a north-south oriented hilly area from where these winds turn eastwards towards Kerala and Karnataka in the Indian peninsular region in the form of a Low-Level westerly Jet known as 'Findlater Jet'. The winds go towards the Bay of Bengal and from here make another turn towards the North-East and enter the northern plains through an east-west oriented Monsoon trough which runs along the Indo-Gangetic plains. Indian Ocean provides energy to the monsoon circulation, and the importance of Indian and western Pacific warm pools to monsoon processes has been much emphasized.

(b) Heat Low that decides the temperature and pressure difference between land and the sea. In case of India, the Heat Low is centered around Pakistan, a low-pressure area that doesn't have moisture, but which controls the sea-breeze flow towards the land.

(c) Tibetan high in the upper troposphere (Koteswaram, 1958; Flohn, 1960; Yanai and Song, 1992; Wu et al., 2004 etc.) that acts as an elevated heat source for pulling in the monsoon current deep inland.

(d) Upper tropospheric easterly jet stream (Koteswaram, 1960) that helps in kick-starting the south-west monsoon by increasing the surface pressure over the south-western Indian Ocean through its strong descending motion.

(e) Low level jet (LLJ) off Somalia coast (Findlater, 1969) and its extension over peninsular India (Joseph and Raman, 1966), which is the main artery of moisture supply for monsoon in the troposphere (Sikka, 2012); shown in Fig. 1.2

(f) Global scale east-west divergent circulation in the upper troposphere (Krishnamurti, 1971) with wave number two structure with two divergent centres over Tibetan and Mexican highs, and two convergent centres over the mid-Atlantic and mid-Pacific troughs.

(g) Monsoon trough over India (Keshavamurthy, 1968; Chaudhary and Krishnan, 2011), heat and moisture budget of the monsoon trough (Anjaneylu, 1969), and dynamics of tropospheric circulation during contrasting monsoon seasons (Kanamitsu and Krishnamurti, 1978).

(h) Mascarene High (Krishnamurti and Bhalme, 1976; Ogwang et al, 2015)

(i) Presence of temperature inversions in the lower troposphere over the Arabian sea (Colon, 1964; Muraleedharan et al, 2013), and their role in widespread subsidence over the Arabian sea and even inside northern and central India (Bhat, 2006; Rao and Sikka, 2005)

(j) Role of double equatorial trough, the first being the northern hemisphere equatorial trough and the second being the southern hemisphere equatorial trough over the Indian ocean (Raman and Dixit, 1964)

(k) Heat sources and moisture sinks fluctuations (Bhide et al., 1997).

Apart from the above studies, there is a deluge of studies exploring the multi-scale interaction among different scale of processes such as the interaction between planetary-scale waves, medium scale waves and short scale waves in the maintenance of circulations.

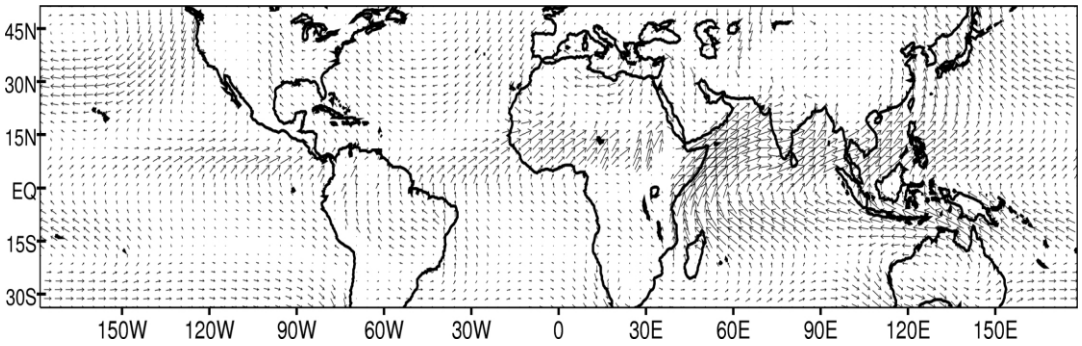

Fig. 1.2: shows the monsoon wind pattern at a level 925 hPa (WCRP)

1.1.2 Monsoon Onset and Advance

Monsoon Onset over Kerala (MOK) has been active topic of research since the work of Ananthakrishnan et al. (1967). It is now well established that the Onset is also connected with the 30-50 day oscillation (Joseph et al., 1994). Formation of monsoon vortex associated with the onset was investigated by Krishnamurti et al.

(1981) using aircraft data, and further investigation on its dynamics was performed with numerical model (Krishnamurti and Ramanathan, 1981). It was demonstrated that one of the precursors to monsoon onset was the build-up of moisture up to mid-tropospheric heights about two weeks in advance of MOK. It is understood that most of the precursors related to rainfall, winds and seasonal reversal of temperature and pressure systems are dynamically inter-related. These changes occur in a slow manner in the upper troposphere, mid-troposphere and lower troposphere at different rates beginning from mid-March to get fully organized by mid-May when the much awaited Onset is about to take place.

Several investigators have suggested different criteria for defining Onset. Goswami and Xavier (2005) emphasized the change in mid/upper tropospheric meridional temperature gradient as an important parameter for objectively defining MOK. There are several studies on this line. From the point of MOK, formation of a synoptic scale disturbance (low pressure area, onset vortex, mid-tropospheric vortex along 8°-10° N between 70°-90°E) brings about the burst of rains over Kerala, which is in line with the public perception of jump in rainfall and strong winds (See Fig. 1.3a and 1.3b). However, in most of the years, the objective indices-based MOK and the IMD's operational MOK data differ by 2-3 days of each other. The mean date of MOK is 01 June with a standard deviation of one week. The processes such as burst of rainfall over Kerala, enhanced moistening of lower and middle troposphere over peninsula, building up of the meridional temperature gradients in the middle and upper troposphere, appearance of the tropical easterly jet over southern India, shift in the large-scale trough patterns in mid-tropospherical global scale, and disappearance of sub-tropical westerly jet stream etc. are interlinked dynamically and take place within about a week of each other and coincide with the date of MOK.

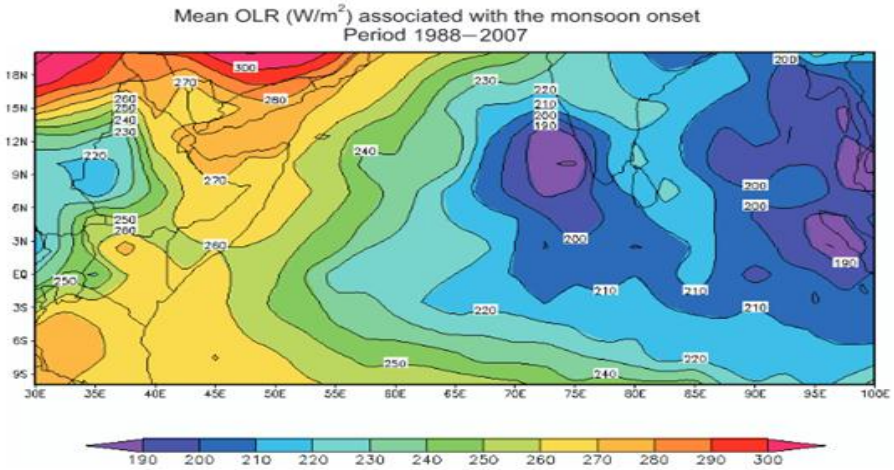

Fig. 1.3a: The variation of mean OLR and the mean wind during the onset from 1988 to 2007 (Pai and Nair, 2009)

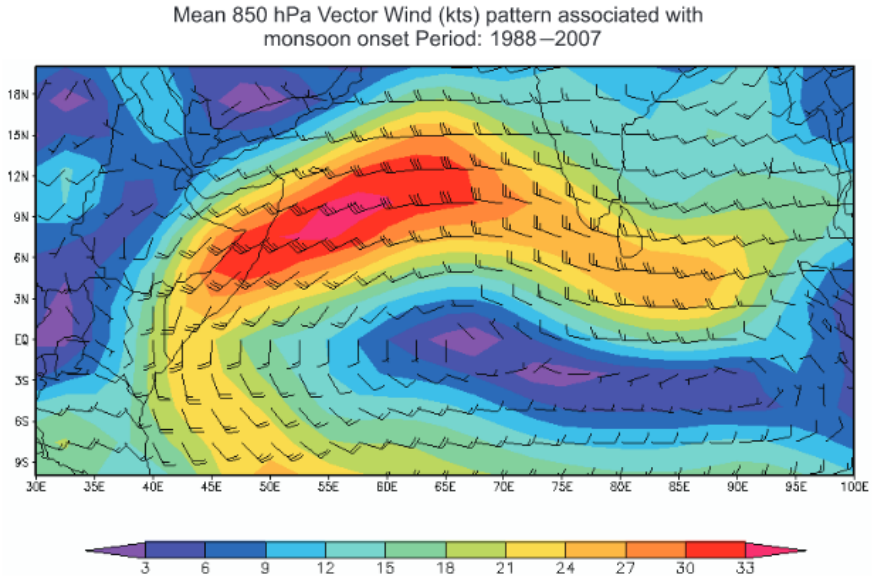

Fig. 1.3b: The vector wind pattern during the monsoon onset (Pai and Nair, 2009)

Based on an analysis of the past 60 years (1948 – 2007) record, Wang et al. (2009) show that the onset date can be objectively determined by the beginning of the sustained 850 hPa zonal wind averaged over the southern Arabian Sea (SAS) from 5˚-15˚N, and from 40˚ - 80˚E. The rapid establishment of a steady SAS westerly is in agreement with the sudden commencement of the rainy season in India. Before the onset, on the biweekly timescale, it is seen that there is a westward extension of the centre of convection from the equatorial eastern Indian Ocean to the southeast Arabian Sea. On the intra-seasonal time scale, the onset tends to be led by

north-eastward propagation of an intra-seasonal convective anomaly from the western equatorial Indian Ocean.

1.1.3 Monsoon Intra-seasonal Oscillation

Although the summer monsoon season is the 'rainy season' over most of the Indian region, it does not rain every day, at any place during the season. Naturally, on the all-India scale also, there are large fluctuations in the quantum of daily rainfall (Rajeevan et al., 2008). Subsequent to the onset phase of the monsoon, the continental tropical convergence zone (CTCZ) gets established over the core monsoon zone of India, around the beginning of July. During the peak monsoon months of July and August, the rainfall primarily occurs over this zone, and its amplitude fluctuates between active episodes with continuous rainfall interspersed with weak spells of rain or no rain (break spells). This sub-seasonal oscillation with time-scales longer than synoptic, yet shorter than seasonal is known as the Intra-seasonal Oscillation (ISO).

The ISO is manifested as active-break cycles that have tremendous impacts on every aspects of life. These intra-seasonal variations occur with a typical period between active and break phases of 30-60 days, known as Madden Julian Oscillation (MJO; Madden and Julian,1994), and with periodicity of 10-20 days, otherwise known as the Quasi-biweekly Oscillation (Kikuchi and Wang, 2009). The Indian/Asian monsoon can, in fact, be viewed as a series of active-break cycles, which often originate over the equatorial Indian Ocean that spread pole wards over land and eastward over the tropical ocean. The MJO is related with cloudiness and active-break cycles, and can influence the entire monsoon season. The quasi-biweekly mode is related with variation in convective activity, and propagates westward. The 5-6 day variability (tropical disturbances such as tropical cyclones) which move westward from the Pacific and can deliver large amounts of rain in a short period also contributes to intra-seasonal variability. Prediction of the intra-seasonal rainfall variations is of prime importance as these variations can have dramatic impacts, affecting the timing of crop planting and crop selection, and the management of water resources in the affected regions. The prediction of active-

break cycles has been improved in recent years, with skill for up to 20 days in advance using weather forecast models, though many challenges remain (WCRP).

Several studies have identified the conditions leading to active/break cycle (Blanford, 1886; Ramamoorthy, 1969; Raghavan, 1973; Keshavmurti et al, 1986; Krishnan et al, 2000; Annamalai and Slingo, 2001; Gadgil and Joseph, 2003; Rajeevan et al., 2008 etc.). Ramaswamy (1965) demonstrated the incidence of break monsoon as a consequence of interaction between sub-tropical westerly circulation and tropical easterly jet stream. Keshavmurti (1980) investigated the shift in quasi-stationary large-scale features of tropospheric circulation in active-break monsoon. Recent review by Sikka (2012) points out to the fact that short or moderate break monsoon episodes can be viewed as a part of the oscillations of the monsoon trough (MT), but longer breaks lead to the disappearance of the MT or shifting its quasi-stationary position north of the sub-Himalayan belt. The latter leads to a sustained shift in the SW monsoon rainfall regime for over a week and it is in such epochs that above-normal surface temperatures, lower tropospheric inversions, strong north-westerly dusty winds and lower tropospheric anti-cyclonic vorticity persists over the Gangetic plain. The understanding on prolonged break or active cycle has immense impacts as these can lead to severe drought or flood in the country.

1.2 Local Exchange Processes during Monsoon

Study of the interactions between the SW monsoon and the atmospheric boundary layer (ABL) gained importance from the International Indian Ocean Experiment (IIOE; 1963-1966) onwards. Over the Arabian Sea, the near-surface winds are strong and the surface is very rough, and hence the sea surface and the lower troposphere monsoon are exchanging fluxes of momentum, latent heat and sensible heat in energetically more complex manner. In another study of the ABL across the Orissa coast, it was found that strong low-level air stream impinges on the coast after travelling over peninsular and Central India and emerges over the North Bay of Bengal, which is the seat for active convection, warm SST and genesis of low pressure systems. These studies showed that ABL over the entire east-west extent of the MT has a significant influence on monsoon physics. Some of the interesting points are given below:

(i) Increased instability in the ABL during weak/break monsoon under suppressed condition, and decreased instability (increased stability) under active monsoon and organized convective conditions.

(ii) Momentum, sensible heat and latent heat exchanges are much influenced under the changing wind condition as the monsoon oscillates between active and suppressed convective episodes. Such interactions are more marked along the western margin of the MT. Air-sea fluxes are enhanced at the time of formation of monsoon depressions in Bay of Bengal (Sivaramakrishna et al., 1992).

Other processes to be examined include: (iii) local feedbacks between ABL and monsoon, and diurnal variation, (iv) role of ABL for supply of moisture for formation of cloud systems, (v) cloud scale processes and role of ABL etc.

The sea surface temperature (SST) of the Arabian Sea and the Bay of Bengal and its influence on monsoon through air-sea interaction is another major process that controls the monsoon. The impact of the monsoon onset over the west and central Arabian Sea is large as the SST abruptly falls at the time of monsoon onset (Rao, 1986). During July and August too, the Arabian Sea continues to cool but a much slower rate with episodes of slight warming during weak monsoon and slight cooling during active monsoon as the monsoon oscillates on intraseasonal time scales (Rao and Goswami, 1988; Vinayachandran, 2004). The more vigorous circulation in the Arabian Sea, forced by stronger mean surface winds, cools the surface layer by exporting heat through southern boundary and into deeper ocean.

Studies by Rao and Shivkumar (1999) and others have emphasized on the build-up of a mini warm pool over the south-east Arabian Sea from January to April, which was invoked to monsoon onset over Kerala through formation of even monsoon onset vortex. It is highlighted that south-east Arabian Sea in winter and pre-monsoon season is a location for important air-sea interactions which affect the ocean as well as the atmosphere with possible consequences on the build-up of the summer monsoon.

During the summer monsoon season, a quasi-stationary trough, in which sometimes northward moving vortices are embedded, persists off the coast of southwest India (Rao, 1976). Nearly half the number of active to vigorous monsoon situations in Konkan and three quarters of such occasions in coastal Karnataka are associated with troughs off the west coast (Rao 1976). Jayaram (1965) found that for the case of the offshore trough during 3-6 July 1962, the highest rainfall occurred to the south of the apex of the trough and this belt moved slowly northward with the trough. The offshore trough-upper air cyclonic circulation is a combination that has the potential for fetching the monsoon flow further north along the west-coast.

1.3 Jet Streams and Monsoon

a) *Tropical Easterly Jet*

The summer months witness the development of cold Easterly jet stream centered between 5° N (during active monsoon) and 15°N (during break condition) latitude over peninsular India (Sathiyamoorthy et al., 2007). It is strongest over the peninsula, and the wind speed sometimes reaches 150-175 km hr^{-1}. Flohn (1964) had examined the climatology of TEJ and demonstrated that it is confined to within the 200-100 hPa layer. Koteswaram (1958) demonstrated that the existence of the TEJ is due to the north-south temperature difference between the Tibetan Plateau region and the Equatorial Indian Ocean in the upper troposphere. During monsoon onset and revival, the axis of TEJ is located over the equatorial region, and as the monsoon progresses further, it shifts northward (Sathiyamoorthy et al., 2007). In a broader sense, the TEJ completes the air flow set by the cross equatorial wind generating the low level jet (LLJ), and is an important deciding factor of the strength of the ISM.

b) *Westerly Jet Stream*

During winter, over the sub-tropical zone, at about an altitude of 8 km a westerly jet stream is developed. This bifurcates into two branches – one flowing along the northern side of Himalayas and the other taking a route along the southern side. It is believed that the latter branch brings the western disturbances from the Mediterranean region into the sub-continent. The occurrence of occasional heavy

rain and cold wave over north western planes can be attributed to this western disturbance. Ramaswamy (1962) had shown that during break monsoon condition, two jet streams exists with entirely different characteristics - the easterly jet and the sub-tropical westerly jet - within a short latitudinal distance of each other and dynamically interacting with each other and influencing the ISM. These Jet streams are effective in exchanging heat in the meridional direction. With the help of 20-years simulation of a high resolution AGCM forced with climatological SSTs, Krishnan et al. (2009) has shown the interaction of monsoon-midlatitudewesterlies during droughts in the Indian summer monsoon droughts. Prolonged monsoon breaks that occur on sub-seasonal time scales involve dynamical feedbacks between monsoon convection and extra-tropical circulation anomalies. Recent study by Xavier et al. (2017) has shown the crucial role of mid-latitude westerlies in inducing a heavy flood over the Uttarakhand in 2013.

c) *Characteristics of Low Level Jet and its impact on Monsoon*

During summer, the shifting of Intra Tropical Convergence Zone (ITCZ) towards northern part of India – known as *Utharayanam* in Kerala, heats up the north Indian region and pulls the moisture laden air mass to set the SW Monsoon. The Low Level Jet (LLJ) provides favourable background circulation and abundant water vapour for vigorous monsoon (Hongbo, 2014). LLJ is regarded as the fast moving ribbon of air with wind speeds greater than 12 m s^{-1} in the boundary layer or the lower troposphere. Strong to vigorous monsoon conditions occur in Kerala on about 15% to 20% of the occasions in the first two months of the season. In the second half of the season active to vigorous monsoon conditions rapidly decrease and they become rare (only 5% of the occasions). Normal monsoon is a common feature in Kerala occurring on about 40% to 50% of the occasions. Since, LLJ has a strong bearing on the vigour of monsoons,Scientists have carried out a large amount of studies regarding the characteristics of LLJ (Fig. 1.4), and its influence on monsoon.

Findlater (1969) conducted a series of observational analyses on the characteristics of Somali Jet, and its relation with summer monsoon rainfall. It is generally believed that the summer monsoon rainfall activity is directly correlated

with the strength of LLJ, as it is the strength of the latter that is bringing in ample moisture in to the land area for the triggering of cloud formation and precipitation. By analysing 5 years'of wind data obtained from radiosonde/radio-wind network, Joseph and Raman (1966) established the existence of a westerly low-level jet over peninsular India with strong vertical and horizontal wind shears. Using monthly mean wind data, Findlater (1971) showed that the LLJ splits in to two branches over the Arabian Sea, one branch passing south-eastward toward Sri Lanka and the other eastward through peninsular India. Hoskins and Rodwell (1995) employed a time dependent primitive equation model with specified zonal flow, mountains and diabatic heating. The east African highlands and a land-sea contrast in surface friction are shown to be essential for the concentration of the cross-equatorial flow in to a LLJ (Joseph and Sijikumar, 2004). LLJ with its large shear vorticity field in the boundary layer has a prominent control on monsoon rainfall. To the north of the jet axis, the rainfall is found to be large, with the precipitation maximum a few degrees latitude to the north of the jet axis, and to the south of the axis, the rainfall is suppressed.

Observational capabilities of directly estimating the strength of LLJ is limited in the country except satellite and re-analysis data sets, whose accuracy is less compared to ground-based measurements. However, the emergence of state-of-the-art facilities such as network of Doppler Weather Radars, Wind Profiling Radars, GPS based Radiosonde measurements etc. has filled such a data gap to certain extent in the recent decades. Turner and Stein (inCOMPASS Field Campaign, 2016) outlay the scope of employing DWR data across India to examine the strength of monsoon convection.
(http://www.met.reading.ac.uk/nercdtp/home/available/desc/entry2018/SC201811.pdf). Routray et al. (2010) used the DWR-derived radial velocity and reflectivity data in a meso-scale model for prediction of Bay of Bengal monsoon depressions. The 24-hour forecast errors for wind, temperature and moisture profiles were analyzed, and it is deduced that the cycling mode assimilation enhanced the performance of the WRF 3-D variational data assimilation.

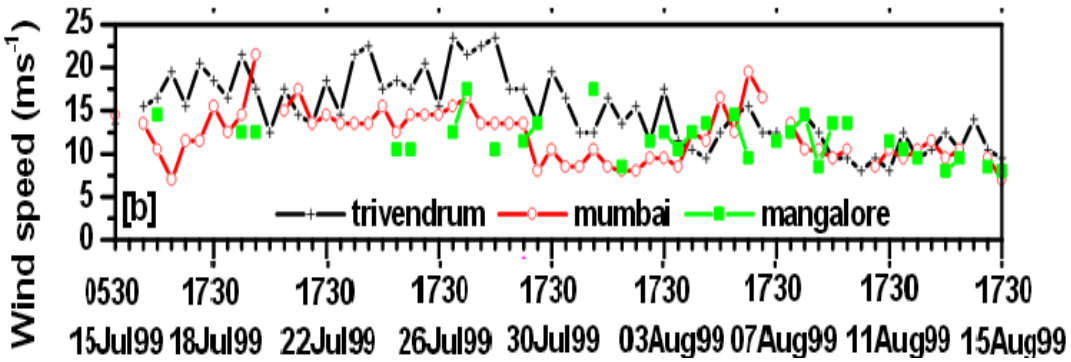

Fig. 1.4: Zonal wind speed observations in IMD stations (*Courtesy*: *IMD*)

Remote sensing of horizontal and vertical winds using wind profiling Radars is emerging as a powerful tool for characterizing and predicting the winds and weather worldwide. Using the Indian MST Radar at Gadanki (13.47°N, 79.18°E), Vasantha et al. (2002) studied the characteristics of monsoon winds during June through September, and it was found that the westerlies prevailed up to 8 km, with a clear change in direction beyond this height. Using the same MST radar, and high resolution GPS Radiosonde observation, Raman et al. (2011) report some new aspects of LLJ as regards its vertical position. They showed that the LLJ existed at around 710 hPa over south-eastern peninsular India, rather than at 850 hPa as reported by earlier classical papers. In addition, the LLJ has been reported to show distinctive features during active-break cycle of ISM.

The 404 MHz wind profiler at Pune (18.38°N, 73.58°E; Joshi et al. 2006) in India was employed to examine the LLJ in the month of July especially during the active phase of monsoon. The time series of the height/intensity of the observed LLJ appears to be periodic. The LLJ is observed throughout the day with wind maxima in the range 15 – 20 ms^{-1} and the wind direction for all the cases is about 275˚ (± 20˚).These wind maxima occur between the height ranges of 1.65 – 3.0 km. Wind shears observed beneath LLJ core shows a strong increasing tendency while a slowly reducing nature is found above the core. The energy dissipation rates derived from the observed spectral widths on intense LLJ day is stronger than weak LLJ day and they peak near the level of the core of LLJ. Also it is observed that LLJ is present with upward directed clear air vertical velocities probably supporting the development of convective system. Doppler Lidar observations conducted at an

Indian station (Mahbubnagar; 16.73°N, 77.98°E, 445 m above mean sea level) by Ruchith et al. (2014) revealed the time evolution of LLJ during south-west monsoon season, and showed that westerlies predominantly existed up to a height of 3000 m above ground, and there was a wind speed maximum at around 500 m during night time in most of the observational days. It was also reported that this jet core maximum gets lifted up immediately after sun-rise, and the day time maxima were observed between 2000-2500 m without much change in its magnitude. Kalapureddy et al. (2007) demonstrate that the observed diurnal structure of LLJ depends on the local convective activity, wind shears and turbulence associated with boundary layer winds. Additionally, the day-to-day change in the LLJ structure depends on the latitudinal position of the LLJ core.

1.4 Recent trends in Monsoon winds and precipitation

Given that the national economy depends critically on the variability of monsoon, its comprehensive understanding is warranted. The food grain production of the country is strongly dependent on the monsoon, with its critical dependence on the onset, duration distribution, and the periods of active-break conditions of the ISM (Singhvi and Krishnan, 2014). Significant spatio-temporal variabilities of the amount, intensity and distribution of rainfall exist, with consequent impact on the occurrence and frequency of floods and droughts. The long-term average of the seasonal monsoon rainfall, however, remains largely constant (Goswami et al., 2006). Several factors such as the Sun-Earth geometry, the North Atlantic Oscillation, the El-Nino Southern Oscillation, extent of Eurasian snow cover, change in vegetation, SSTs in the Indian Ocean, anthropogenic activities etc. contribute to the monsoon variability, but an assessment of their exact influence and the long-term stability is difficult (Singhvi and Krishnan, 2014).

In addition to the increase in greenhouse gases and anthropogenic aerosols, the tropical Indian Ocean has experienced rapid warming of the SST at a rate of 0.5-1.0 °C with the strongest warming during JJAS in the past five decade, and this warming is clearly related to the weakening of south-westerly winds (Swapna et al., 2013). Roxy et al. (2015) showed that the drying of Indian sub-continent by rapid Indian Ocean warming leads to a weakening land-sea thermal gradient, and hence

the monsoon. They used long-term observations and coupled model experiments, and demonstrates that the monsoon Hadley circulation and hence the strength of LLJ is weakened as a result of the increased ocean warming and subdued warming of the continent.

However, some studies have pointed out that the monsoon circulation and rainfall have intensified in a changing climate (Wang et al., 2013). Using various observational data sets, Jin and Wang, (2013) showed a contrasting result that the Indian monsoon rainfall has increased at a rate of 1.34 mm day^{-1} $decade^{-1}$ since 2002, due to increase warming of the Indian landmass and subdued warming over the Ocean. Loo et al. (2015) states that the precipitation anomalies are consistent with the increasing trend in global temperature anomalies for the post-1970 period. By using daily rainfall data, Goswami et al. (2006) showed that there is a significant rising trend in the frequency and magnitude of extreme rain events over the core monsoon zone of central India for the period 1951-2000. They also argued that there is a significant decreasing trend in the frequency of moderate events during the same period so that the increasing contribution from heavy events is offset by decreasing moderate events, unravelling the critical question of why the Indian summer monsoon has been stable and does not show any significant trend.

Ghosh et al. (2016) has also published a study in the same line as that of Goswami et al. (2006), stating that the trend in spatial variability of mean monsoon rainfall is decreasing as exactly opposite to that of the extremes. Krishnamurthy (2011) conducted a study of the trends in low pressure systems, rainfall and temperature using long records of daily data. It reports that the number days when low-pressure exists has an increasing trend during 1930-2003. However, in the recent years, the number of days with depressions decreases while those with low pressure systems or cyclonic circulations increase. Recent study by Vishnu et al. (2016) reveals that the number of monsoon depressions in the Bay of Bengal decreases attributed to the weakening of monsoon circulation. They also report that the mid-tropospheric humidity and the intensity of LLJ have decreased in the recent epoch over the eastern Arabian Sea, the head BoB, and the land over east Asia while it has increased over the northwest Pacific. Several modelling studies using

sensitivity experiments have shown that the changes in the land-sea thermal contrast can modulate the monsoon cross-equatorial flow in a global warming scenario (Alavez et al, 2014; Kamae et al., 2014 among several others). Sandeep and Ajayamohan (2014) report a poleward shift in the Indian summer monsoon low level jet under a globally warming environment. Consistent with the northward shift, a drying (wetting) trend of the southern (northern) part of the west coast is also suggested.

Using the MST radar observation at Gadanki, Ratnam et al. (2013) reported that there is a sharp strengthening of TEJ during the recent warmer decade (2001-2010). They also showed that this change is reflected in the tropical cyclone systems and ultimately on the precipitation patterns over the Indian region. In another study, it is shown that there is a significant reduction in the spatial extent of TEJ between 1960s and 1990s (Sathiyamoorthy, 2005). Bansod et al. (2002) also demonstrated a decreasing trend in the strength of TEJ, and there are studies saying that the number of tropical convective systems over Bay of Bengal is also decreasing (Srivastava et al 2000, Rao et al., 2008).

In a recent study, Balaji et al. (2017) utilized the collocated observations of Wind profiling Radar and Microwave Radiometer to study the dynamics and thermodynamics associated with rainfall characteristics in the premises of the Indian Institute of Tropical Meteorology (IITM), Pune, Maharashtra for the year 2015. Continuous vertical profiles of winds, temperature and humidity showed significant promise for exploring the LLJ, its periodicity (~9 days), and its association with moisture transport, clouds and precipitation embedded within the monsoon large-scale convection. High resolution data of horizontal wind profiles from UHF Wind Profiling Radar over Pune for a 3-year period was utilized by Ruchith et al. (2016) to study the seasonal and intra-seasonal variation of low level winds. It was found that the westerly wind maxima occurred at a height between 1.5 km and 3.0 km, with a clear turning in the easterly direction beyond 4-5 kilometres. In addition, the rainfall was seen to be directly related to the strength of LLJ.

With the backdrop of several studies mentioned above, the present doctoral thesis intends to address the peculiar characteristics and dynamical aspects of

monsoon low-level jet observed right over the Gateway of monsoon – Cochin, and bring out significant results pertaining to the onset, its advancement into the landmass, and contrasting features during weak and strong monsoon years. Chapter 2 provides the details of atmospheric observational facilities, instrumental data sets, and the general methodology. Chapter 3 specifically explores the characteristic features of monsoon circulation and associated meteorological parameters over Cochin during an active monsoon year - 2013. Chapter 4 brings out the salient but distinctive features of dynamical parameters and its periodicity during contrasting monsoon years. The investigation of dynamical fields such as vorticity and divergence, and its relation with monsoon convection performed with the help of data from a dedicated field campaign using Radiosondes, is presented in Chapter 5. Chapter 6 encompasses diagnostic study of local convection events over the west coast of India-Cochin- by employing an advanced Stratosphere-Troposphere (S-T) Wind Profiling Radar operating at the VHF range of 205 MHz, which is the world's first Radar working in this frequency range, followed by Summary and Conclusions provided in Chapter 7.

****

Chapter

2

Location, Data and Methodology

Contents

2.1 Location and Meteorology

Kerala State, having an area of 38863 km², and comprising of about 1.18% of India's landmass, is situated between the Arabian Sea to the west and the Western Ghats to the east. Located at the extreme southern tip of the Indian subcontinent, Kerala has a coast running about 580 km in length, while its width varies by about 35–120 km. Geographically, Kerala is roughly divided into three climatically distinct regions: the eastern highlands (rugged and cool mountainous terrain), the midlands (rolling hills), and the western lowlands (coastal plains). The topography consists of a hot and wet coastal plain gradually rising in elevation to the high hills and mountains of the Western Ghats (see Fig. 2.1). Kerala, being very close to the Equator, has a wet and maritime tropical climate, heavily influenced by the seasonal heavy rains brought by the monsoon, and is one of the wettest areas on the Earth. Anamudi (2694m), the highest peak in India after Himalayas, is situated in the Munnar division of the Western Ghats. Most of the rivers of Kerala originate from the Western Ghats. Kerala has four distinct seasons:

- Pre-Monsoon starts from March and extends to May with hot temperatures (sometimes up to 39° C) and occasional thundershowers.
- The south-west monsoon season is in place from June until late September, bringing about 70-75% of the annual rainfall (3000 mm/year), with widespread heavy rains spanning all over the State.

- Post-Monsoon season extending from October through mid-December with heavy thunderstorms accompanied by lightning and occasionally gusty winds. This rainy season is otherwise known as the North-East monsoon, mainly due to the prevailing winds that brings in the rain.
- Winter season spanning mid-December through February, with clear nights and calm winds, and the night time temperatures most often going below 20° C.

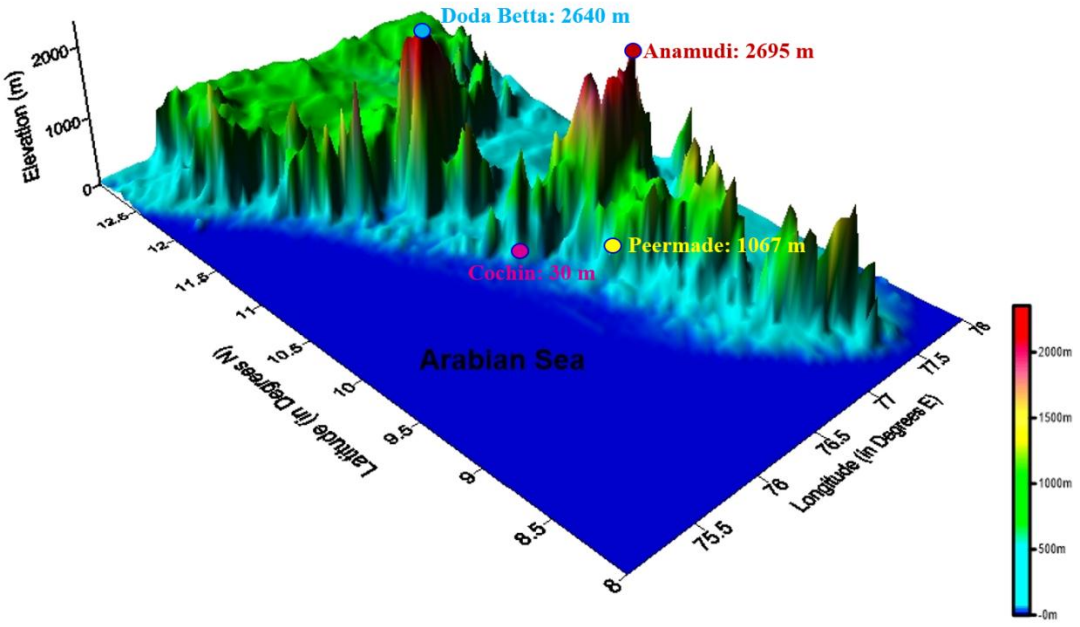

Fig. 2.1: Topographic map of Kerala (*Courtesy*: *Mohankumar et al., 2017*)

2.1.1 Kochi- the Gateway to Southwest Monsoon

Kochi, the major port-city of Ernakulam district considered to be the gateway of Indian Summer Monsoon, is situated between Northern Latitudes 9˚47' and 10˚17' and Eastern Longitudes 76˚9' and 76˚47', has the following physical parameters.

a. Temperature: The average atmospheric temperature ranges from 23.8˚C to 34.52˚C with minimum and maximum values in January and May, respectively. The average relative humidity varies from 35% in January to 93.66% in September (Rajan, 1989).

b. Rainfall: The climate is very much tropical in nature and the average monthly rainfall (SW monsoon) ranged from about 5 mm in March to 240 mm in July.

c. Tides: Cochin estuary has perennial connection with the Arabian Sea near the main entrance of Cochin harbour. This region is subjected to semi-diurnal tidal influence with a variation about 1 m.

d. Winds: The wind speed varies from 2 m s^{-1} in winter to 10 m s^{-1} in monsoon season.

2.2 Data and Methodology

The present study is mainly centered at Kochi, by employing a variety of observational facility such as the in situ data taken from the GPS Radiosonde ascents, the wind data from a state-of-the-art 205 MHz VHF wind profiling Radar, Automatic Weather Station data from a 32-m meteorological tower, Satellite-derived wind products and Re-analysis products. The main period of the study is from 2013 to 2016.

2.2.1 GPS Radiosonde (GRAW)

A Radiosonde is a disposable, balloon-borne device that measures the vertical profile of meteorological variables and transmits the data to a ground based receiving and processing station (Fig. 2.2). These profiles are typically obtained twice each day and are the core of the global weather observing system that provides inputs to numerical forecast models. The sensor package routinely measures the variation with altitude of temperature, humidity, and pressure as the balloon ascends from the surface to heights up to about 30 km. When the device also measures winds, it is more properly called a rawinsonde, although the term radiosonde is commonly applied to both.

Since 1957, globally all stations made their soundings at the same times, 00:00 and 12:00 UTC. Shortly after an operational upper-air sounding is completed, a standard data message is prepared and made available to all nations using the Global Telecommunications System. These messages are transmitted in a universal format that reports meteorological conditions at various significant levels, which represent levels where prescribed changes in meteorological conditions occur.

The radiosonde is carried aloft by a balloon as part of a flight train. Hydrogen is the gas most commonly used to inflate the balloon and provide its

lifting capacity, although helium and natural gas are sometimes used for special applications. The flight train consists of five components: (1) the balloon; (2) a parachute to bring the radiosonde safely back to Earth after the balloon bursts; (3) 30 m of nylon separation line that isolates the radiosonde's sensors from water vapor and thermal contamination by the balloon; (4) a de-reeler to let out the nylon line after launch; and (5) the radiosonde itself.

The radiosonde is an electronics unit that comprises three major sections: a suite of sophisticated meteorological sensors; signal-processing electronics; and a radio transmitter to relay the measurements back to a receiver at the radiosonde launch station. The meteorological measurements are made at intervals that vary from 1 to 6 s, depending on the type and manufacturer of the radiosonde. The meteorological community has been assigned two radio frequency bands for use in transmitting meteorological data: 400–406 MHz and 1675–1700 MHz. All of the world's radiosondes are required to meet certain performance standards that have been established by the WMO.

Fig. 2.2: View of ascent of GRAW Radiosonde

In addition to the graphical output, Graw system provides numerical data in ascending time, Pressure, Temperature, Relative Humidity, Wind speed and Direction, Longitude and Latitude, Altitude, Azimuth, Elevation, Range, for every position of the Balloon.

2.2.2 Technical specifications of GRAW GPS Sonde:

The specification of Grawradiosonde is given in Table 2.1.

Table 2.1: Specifications of GrawRadiosonde

Weight	< 90 g
Wind finding	GPS (48 Channel)
Temperature resolution	0.1°C
Temperature Random Error	<0.2° C
Humidity resolution	1% RH
humidity Random Error	<4 % RH
Pressure accuracy	< 0.3 hPa
Geopotential height accuracy	< 10 m
Wind speed accuracy	<0.2 ms^{-1}
Accuracy of horizontal position	< 5 m

2.2.3 Special Field Campaign

A special field campaign by utilizing concurrent Radiosonde ascents over three stations in centered around Cochin was conducted during the monsoon month of August in 2013. The observational procedure to collect the radiosonde data is detailed as below: On every third day at 17:30 hrs (12:00 GMT)a hydrogen filled balloon carrying a GPSonde was released from the Main campus of Cochin University of Science and Technology (CUSAT), from 21st May to 30th October 2013, making altogether 54 successful ascends and about >10 failures. More than 50% of the successful ascends marked maximum altitude above 25000 m and the 3-sonde program on 12th August in association with Space Physics Laboratory (SPL, ISRO) attained a maximum altitude 36230 m.

Another special CAMPAIGN program in association with SPL Thiruvananthapuram and Amrita University, Coimbatore, conducted during August 26-29 in 2013 provided a comparison in atmospheric data at Kochi, Coimbatore and Thiruvananthapuram, with twelve ascends starting from 1130 IST on 26th Aug to 0530 IST on 29th Aug, with six hours interval.

2.2.4 205 MHz Stratosphere-Troposphere Wind Profiling Radar

Wind profiler radars play an important role in experimental atmospheric research (Balsley and Gage, 1980). Their ability to measure wind with a high temporal and spatial resolution makes them well suited for the investigation of processes that are important for understanding the atmosphere including climate variability (Samson et al., 2016).

Conventionally, the wind profiler radars were developed around three frequency bands, Viz., 50 MHz, 400 MHz and 1000 MHz, and these systems typically operate in two modes, viz., low mode with shorter pulse and low altitude, and high mode with longer pulse and high altitude, which negotiate height coverage for resolution (ITU-Report, 2013). A feasibility study conducted by NASA for monitoring the wind for space shuttle launch suggested that frequencies of 50 MHz, 225 MHz and 400 MHz are suitable for stratospheric and tropospheric probing (NASA Technical Report, 1984). No attempt has been made to design and develop a Wind Profiler Radar (WPR) in the frequency near to 200 MHz, because this frequency range is widely used for the radio and TV broadcasting, especially in the US and European countries (Samson et al., 2016). The 200MHz radar has got the advantage of height coverage from 0.5 km to 20 km and the range resolution of 45 meter. It is highly cost-effective compared to 50 MHz radar and requires only lesser real estate. Frequency allocation is being provided on specific requirement for the wind profiler radars in the frequency band of 200-220 MHz as a case-by-case basis.

The weather observation instruments that can observe the air motion of the troposphere with high degrees of accuracy and time resolution, are necessary for the remote sensing and weather forecast. Wind profile radar (WPR) is one such instrument which provides the three-dimensional measurements of wind velocities and wind directions of each layer of atmosphere in real time, and has become indispensable for high accuracy weather prediction. It also provides almost continuous measurement of wind simultaneously and nearly continuously over a range of altitudes, it provides detailed information on vertical structure and wind variability. In addition to wind variability, it also provides measurement of signal strength and Doppler spectral width. Signal strength is influenced by the intensity of

inhomogeneities in the radio refractive index, which depends upon the gradients of atmospheric temperature and humidity as well as the intensity of turbulence.

2.2.4.1 Wind Profile Measurements from ST Radar

(a) Horizontal Velocity Measurement

The Doppler wind profilers measure horizontal wind from two or more fixed beams directed obliquely in orthogonal planes. The profiler measures the radial component of the wind in each beam direction. The oblique beams are typically directed about 15 degrees off the zenith (vertical). Since mean vertical motions are typically less than about 10 cm/s, vertical motions are usually ignored in determining the horizontal wind from the radial component. But, such vertical components are still taken into consideration for calculating horizontal component at high precision.

Wind profiles are typically deduced from a consensus of many samples of individual wind measurements taken over about 10 to 30 minutes. Individual samples are typically obtained on each beam in about one minute. When three beams are used for wind profiling, about ten values will be in a consensus to form the profile for the zonal and meridional components of the velocity. The consensus process compares velocities and discards outliers that do not agree with other values.

(b) Vertical Velocity

Vertical velocity is measured with the vertically directed beam of a wind profiler. Unlike the horizontal velocities the expected range of vertical velocities is usually less. Thus it is possible to adjust the maximum unambiguous velocity to be much less than that required for measurement of horizontal velocities. As a consequence, the spectral resolution is much better for vertical velocity measurement.

2.2.4.2 Radar Equation

The vertical range and temporal availability of wind and temperature measurements are important criteria for an operational use of wind profiler. Especially, the maximum range depends not only from technical properties of the system but also from the meteorological conditions. Therefore, the maximum range

shows significant temporal variations. The maximum range is determined by the strength of the back-scattered power and its ratio to the noise. The dependence of the back scattered power on the atmospheric properties is described by the radar equation. Gathering all system parameters in the constant β, the radar equation can be written in the following simple form:

$$P_r \propto \beta \frac{P_T \eta}{r^2 l^2} \quad \ldots (2.1)$$

where

$P_T$is the transmitting power,

$\eta$is the volume reflectivity,

$r$is the range and

$l$is a attenuation parameter.

It is obvious that the back scattered power is directly proportional to the transmitting power $P_T$and the volume reflectivity η as well as inversely proportional to the square of range and the attenuation parameter. Furthermore, the detectability of the signal depends on the strength of noise.

For given system parameters in the available range, especially in the maximum range, the changes in received signal power are caused by variations of volume reflectivity and/or the attenuation of the electromagnetic and acoustic waves in the atmosphere. Received power for clear air radar from radar range equation

$$P_r = \beta \frac{P_r A_e \pi C \tau \eta F}{128 R^2 a_t a_r} \quad \ldots (2.2)$$

Where,

Pr = *Receiver Power (in dBm)*

Pt = *Transmit Power (in dBm)*

A_e = *Effective Aperture Area (in sqm)*

C = *Velocity of electromagnetic waves in space (in m/s)*

t = *Pulse Width (in s)*

h = *Volume Reflectivity*

R = *Range (in m)*

a_t = *Transmission Loss (in dB)*

a_r = *Receiver Loss (in dB)*

F = *Antenna Weighting Factor*

If the characteristic length of back scattered structures are within the inertial sub-range, the volume reflectivity is given by the following equation:

$$\eta = C_n^2 0.38 \lambda^{-1/3} \quad \ldots (2.3)$$

Where,

λ = Wavelength (in m)

Cn^2 = Refractive Turbulence Structure Constant

2.2.4.3 Hardware Description

The Wind Profiling radar uses Doppler technique that obtains its echoes from turbulent inhomogeneities in the atmospheric radio refractive index field.

Fig. 2.3: ST radar Facility at ACARR

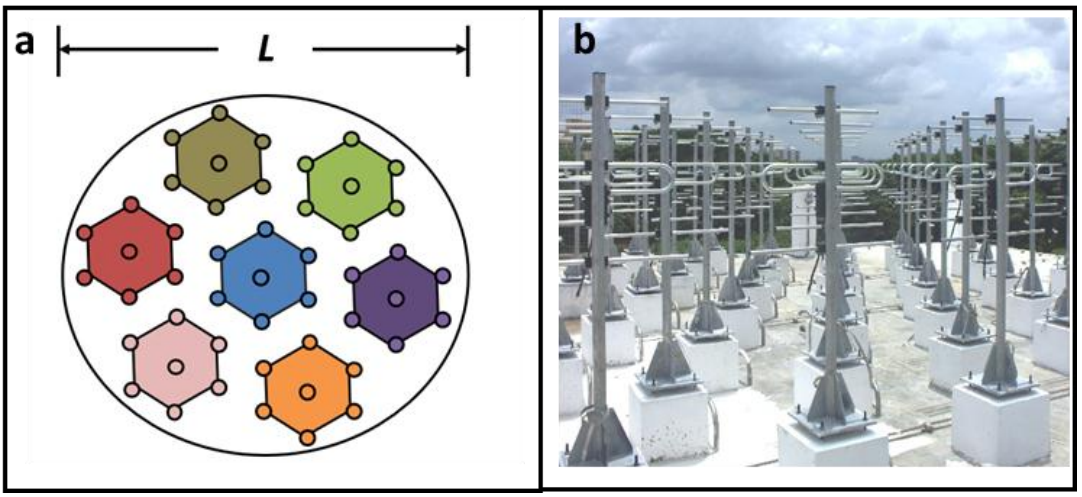

Fig:(**2.3a**): Schematic of antenna arrangement. Each hexagon represents a cluster of 7 antennas. (**2.3b**): Installed antenna in 49 element profiler.

In the lower troposphere, the radio refractive index is dominated by water vapor and echoes are fairly strong, especially in the humid tropics, while sensitive radar systems are required to observe well into the free troposphere. It uses Yagi-Uda antenna arranged in near circular pattern (Fig. 2.3).

The Doppler spectrum provides the meteorological information content from which almost all measurements are made by Doppler Wind Profilers. Profilers receive back-scatter returns from atmospheric features (turbulence, clouds, precipitation) and non-atmospheric features (insects, birds, trees, airplanes, radio frequency interference). The challenge in signal processing is to avoid the returns from non-atmospheric scattering targets and focus on the atmospheric returns. To do this, signal processing section of profilers integrates thousands of consecutive samples to boost the signal-to-noise ratio (SNR) of the atmospheric returns, through a process known as coherent integration. A set of coherent integrations is processed via Fast Fourier Transform (FFT) to produce a single Doppler velocity spectrum, and a set of spectra are averaged together to improve the detectability of the spectral peak. Doppler Spectra are produced typically with about a one minute sample of data. Spectra are produced at each range gate.

The FFT done in Signal Processing module of the profiler is characterized by the number of spectral points in the FFT, the maximum unambiguous velocity of the

spectrum and the resolution of the spectrum. The spectral peak is analyzed to produce a set of Doppler spectral moments. The lowest moment (zeroth moment) yields the area under the spectrum and determines the signal power of the spectrum. The first moment gives the mean radial velocity. The second moment gives the spectral width.

System Specifications

The specification of ST Radar is detailed in Table 2.2.

The basic block diagram of ST Radar is shown in Fig.2.4a. To obtain a lowest range resolution of 45 m, a shorter pulse of 0.3μs is used. RF bandwidth of 5MHz is employed. The master clock of 10 MHz is distributed to all subsystems.

Table 2.2: Specification of ST Radar

Sl. No.	Parameters	Specification
1	Operating Frequency	205MHz
2	Bandwidth	5MHz
3	Peak Power Aperture product	$2.2 * 10^8$ Wm^2
4	Height Coverage	0.5 to 20km
5	Height Resolution	45 to 300 meters
6	Horizontal wind velocity	Up to 70 ms^{-1} with accuracy of $1ms^{-1}$
7	Vertical wind velocity	Up to 30 ms^{-1} with accuracy of $0.1ms^{-1}$
8	Off-Zenith angle	0^0 - 30^0programmable in steps of 1^0
9	Azimuth angle	0^0 - 360^0programmable in steps of 1^0
10	Pulse Width	Baud of 0.3μs, 0.6μs, 1μs, 2μs

RF signal is generated by coherent signal generator and routed to Transmit Receive Module (TRM) through switching and synthesizer unit and feeder network. Transmit/Receive pulse (TRP) is generated by I/O controls and communication unit, and routed through digital distribution card to TRM. Based on the TRP each TRM will generate its own control signal to control the transmitter path, the receiver path, the T/R switch, attenuators, limiters, phase shifter etc. The T/R switch which is enabled by TRP helps to use the same antenna for transmission and reception. During the transmitting time the receiver is disabled to protect sensitive receiver from the high energy RF pulse. The received signal is amplified using a series of amplifiers to a level at which digital receiver can detect the signal.

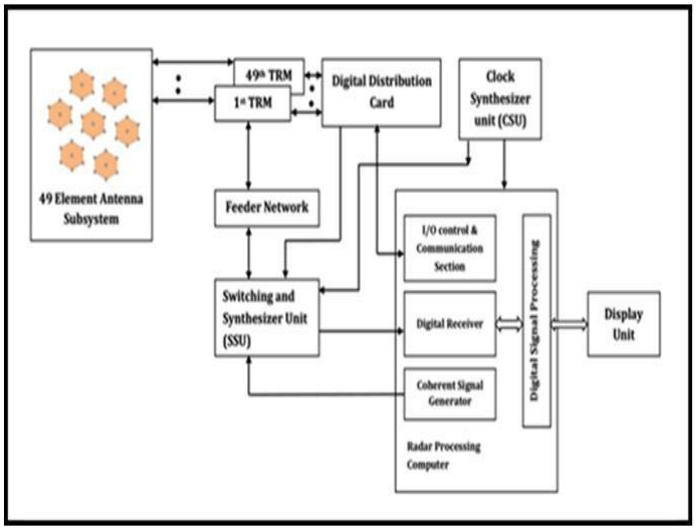

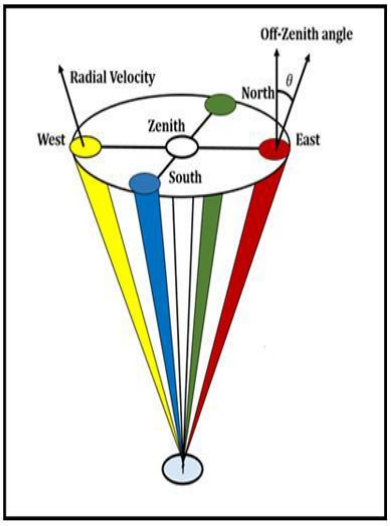

Fig. 2.4a: Basic block diagram of Mini wind Profiler

2.4b: Five beam configuration of mini profiler for wind measurement.

The reflected signal is modulated by the velocity of wind at each height. Radial velocity at each height range is calculated from the received echo.

$$V_r = fd * \frac{\lambda}{2} \quad \ldots (2.4)$$

Where

V_r = Radial Velocity (ms^{-1})

f_d = Doppler shift (Hz)

In the five beam configuration (Fig. 2.4b) the main lobe is tilted in 5 different orthogonal to zenith beam with an off-zenith angle θ. It is assumed that the atmosphere is homogeneous across the radar observational volume. The horizontal wind components at different height range are derived from the radial velocities(V_r). Let the radial velocities measured in East, West, North, South and Zenith are $V_{rE}, V_{rW}, V_{rN}, V_{rS} and V_{rZ}$ respectively then

$$V_{rE} = U * cos\theta + Wsin\theta \quad \ldots (2.5)$$

$$V_{rN} = V * cos\theta + Wsin\theta \quad \ldots (2.6)$$

$$V_{rW} = -U * cos\theta + Wsin\theta \quad \ldots (2.7)$$

$$V_{rS} = -V * cos\theta + Wsin\theta \quad \ldots (2.8)$$

$$V_{rE} = W \quad \ldots (2.9)$$

From the equation, the *u* (zonal Wind), *v* (meridional wind) and *w* (vertical wind) can be calculated (Samson et al., 2016). Fig. 2.5a shows the normalized power spectrum for east and west beam observed on March 24, 2015. It is clear that the power spectrum of the two beams are mirror images to each other as expected, confirming the robustness of the technique. Fig.2.5b shows the comparison of Zonal and Meridional winds for the same day, compared with a simultaneous Radiosonde observation. From the plots it is very clear that the Radar is giving comparable results. The detailed validation of winds obtained from this Radar is published in a separate research paper (Kottayil et al., 2016).

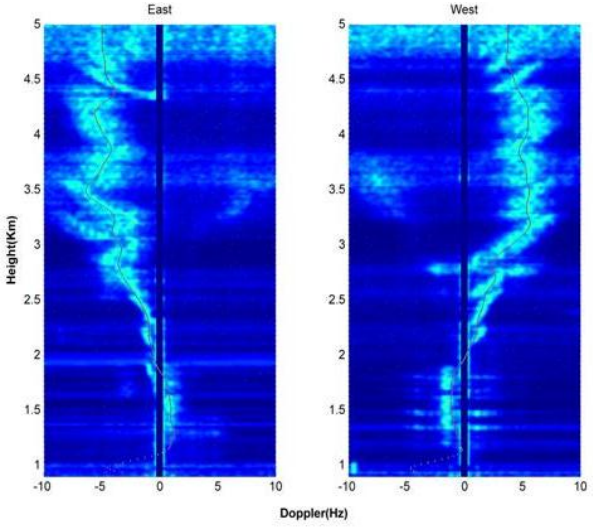

Fig. 2.5a: Power spectrum observed for East and West beam on March 24, 2015

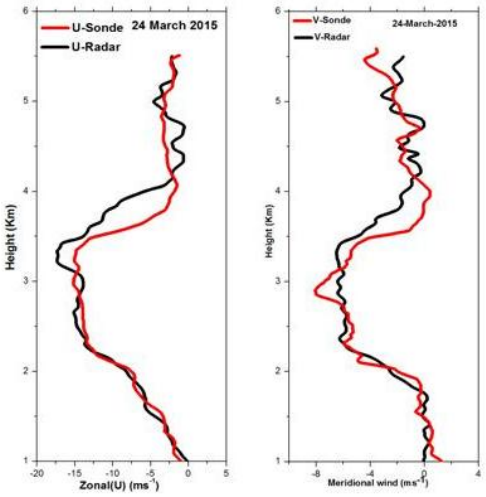

2.5b: Comparison of zonal and meridional winds

2.2.5 Advanced 32-m Meteorological Tower

Advanced Centre for Atmospheric Radar Research (ACARR), CUSAT and has signed an Agreement regarding the Institutional framework and sharing of responsibilities with CSIR-CMMACS and regarding the installation, maintenance and operation of Meteorological tower and sensors in the premise of ACARR at CUSAT Main campus. CSIR C-MMACS under Institutional arrangement has established an instrumented 32 metres meteorological tower at CUSAT as a part of the CSIR Climate Observation and Modelling Network (COMoN). The CUSAT location was recommended as one of the sites for augmentation of existing Comon

instrumentation. Accordingly, the following additional sensors instruments are being installed at the CUSAT sites.

3D sonic Anemometer integrated to H_2O open path Gas Analyzer and sonic temperature, Net Radiometer, Soil Heat Flux plate, Disdrometer, Cielometer, Photosynthetically Active Radiation (PAR) sensor, Evaporimeter, and 3-level instrumented meteorological profilers.

2.2.6 Satellite and Re-analysis Products

The Microwave Humidity Sounder (MHS) onboard NOAA-18 satellite provides the data to assess the humidity variation over the Indian peninsular region, which was used during the ISM in 2013 and 2015. This Polar Orbiting Environmental Satellite (POES) keeping an altitude 854 km above the Earth, is sun-synchronous with a period of 102 minutes (14 times daily) and use a transmission frequency 137.9125 MHz. MHS is a five channel self-calibrating microwave scanning radiometer. The instrument is providing a humidity profiling capability in the frequency range of 89-190 GHz. The measured signals are also sensitive to liquid water in clouds, graupel and large water droplets in precipitating clouds (https://directory.eoportal.org/web/eoportal/satellite-missions/n/noaa-poes-series-5th-generation).

Over a wide region surrounding Cochin, the satellite data collected during the same monsoonal period is analyzed to compare the study that is done with radiosonde. For this, ERA-Interim data at 0.75° resolution is analyzed.

Brief Description:

- ERA-Interim is a global reanalysis of recorded climate observations over the past 3.5 decades (Dee et al, 2011). It is presented as a gridded data set at approximately 0.7 degrees spatial resolution, and 37 atmospheric levels. ERA-Interim is produced by the European Centre for Medium-Range Weather Forecasts (ECMWF).

Temporal Coverage:

- 4 times daily, January 1979 to December 2012 (currently).
- Pressure level files are currently updated through October 2013.

Spatial Coverage:

- Global grid, 0.7 degrees approximate resolution.
- 89.5°S - 89.5°N, 0°E - 359.3°E.
- Grid dimensions are 256 latitudes x 512 longitudes.
- Grid type: N128 Gaussian grid. Equal spacing on longitudes.

Levels:

- All 37 original pressure levels, 1 to 1000 hPa, quasi-logarithmic.
- Levels: 1, 2, 3, 5, 7, 10, 20, 30, 50, 70, 100, 125, 150, 175, 200, 225, 250, 300, 350, 400, 450, 500, 550, 600, 650, 700, 750, 775, 800, 825, 850, 875, 900, 925, 950, 975, 1000 hPa.

The above information of data and location is common to all the working chapters. However, the detailed methodology for each Chapter is described in the respective places.

****

Chapter

3

Features of Monsoon Circulation and the Associated Meteorological Parameters over Kochi, Kerala during an Active Monsoon Year, 2013

Contents

3.1 Introduction

Kerala is the land of Monsoons. The timely onset, optimum duration and reasonable strength of the southwest monsoon are of vital importance to the life and economy of India. Cochin, qualified as the Gateway of Monsoon, is the industrial capital of Kerala State, located on the southwest coast of India at 10° 02′N 76°13′E, with an area of 94.88 km^2.

Cochin also known as the *Queen of the Arabian Sea*, is a coastal metropolitan city, located on the west coast of India. It is considered as one of the 28 Indian cities among the emerging 440 global cities that will contribute 50% of the world GDP by the year 2025 (McKinsey Global Institute, 2011). Cochin is flanked by the Arabian Sea on the west and criss-crossed by backwaters, of which the most prominent is Vembanad Lake. Many portions of the region are water logged for most part of the year. This coastal region includes the backwaters, encompassing the northern end of a peninsula, several islands and a portion of the mainland. To the east lies the urbanized region in the rest of the mainland area. Much of Kochi lies at sea level, with a coastline of 48 km.

Cochin features a tropical monsoon climate. Cochin's proximity to the equator along with its coastal location results in little seasonal temperature variation, with moderate to high levels of humidity. Annual temperature ranges from 23° to 31°C, with the record high being 36.5 °C, and record low 16.3 °C (IMD Report, 2013). From June to September, the south-west monsoon brings in heavy rains as Cochin lies on the windward side of the Western Ghats. From October to December, Cochin receives lighter, yet significant rain from the northeast monsoon, as it lies on the leeward side. Average annual rainfall is 2,978 mm with an annual average of 125 rainy days (IMD Report, 2017).

Meteorologically, Cochin is a sensitive region and the climate is dominated by heavy rainfall during the southwest monsoon season and moderate rainfall during the post monsoon months. Being a coastal station, the city is influenced by the effects of land and sea breezes. Winds are generally light to moderate throughout the year. The weather at Cochin is moderately hot and humid round the year. Heavy showers, with thunder and lightning, occur during the pre- and post monsoon seasons. December to February is comparatively cooler than the rest of the year. About 75 % of the annual rainfall is contributed by the southwest monsoon. During the summer, March-May, the temperature hits a usual high of 35°C while the mild winter high is 28°C. The temperature range is usually 20°C-35°C.

3.2 Relevance of the study

In association with the installation of a powerful Stratosphere-Troposphere Wind Profiler Radar at Cochin, a pilot study utilising high resolution GPS radiosonde observations and other surface meteorological parameters over Cochin is conducted to understand the detailed information of atmospheric conditions over this region. Accordingly, regular observations of GPS Radiosonde observations along with surface meteorological observations from a 32 m Meteorological Tower installed at the ST Radar site at Cochin University of Science and Technology (CUSAT) Campus, near Thrikkakara from 2013 Monsoon season year onwards were taken. The present study reported in this Chapter is based on GPS radiosonde

observations to understand the wind characteristics at various levels in the entire troposphere and lower stratosphere during an active monsoon year - 2013.

Cochin is located in the near-equatorial site at 10° N latitude and 76° E longitude position. From the climatological mean of wind around 850 hPa level shows that the mean location of the Monsoon Low Level Jet (MLLJ) is situated over this latitude region. Similarly, the Tropical Easterly Jet stream (TEJ) observed during the monsoon season around 14 km altitude region also swings around the latitude belt of 10° N. Thus monitoring of the vertical profiles of wind during the monsoon season over Cochin will provide interesting information about the spatial and temporal changes in the zonal wind structure over Cochin in modulating the activity of summer monsoon circulation pattern.

In most of the studies concerned with the monsoon behaviour over Indian peninsular region, the vertical profile over a specific area, at different levels, is not much treated in detail. It is that segment of atmospheric understanding, especially over Kochi, is addressed in this work. This analytical observation plays a role in understanding the monsoon influenced by both the *Coastal effect* and the *Orographic effect,* as Kerala lies within the boundary defined by Arabian Sea and Western Ghats. While the Arabian Sea serves as a reservoir of water vapour pumped into the land region under the forcing of strong westerly reaching to a maximum speed of 15 to 22 m s^{-1}, the presence of mighty Western Ghats reaching to an altitude of about 2 km and extending over a span of more than 1000 km decelerates the zonal wind speed (Ananthakrishnan and Soman, 1988). This blocking of humid air-mass strengthens the cloud formation and the following precipitation over the land with an average positive elevation of about 2 km from west to east. The highest peak in the Western Ghats Range is 'Anamudi' lying in the same latitude of Kochi, 10^0 N. Hence the location of our study region is so vital in probing the varied and subtle characteristics of Southwest monsoon.

A characteristic study of Low Level Jet (LLJ) was conducted at Kochi located at 10° North latitude and 76° East longitude during the southwest monsoon period - June, July, August and September - of 2013, with GPS installed Radiosonde balloon

ascents. The development and properties of LLJ during the whole monsoon period over the peninsular region of India are well observed by various studies, started with Joseph and Raman (1966), continued with more details by Findlatter (1969), and enriched by several others (eg: Ramage and Raman, 1972; Joseph and Sijikumar, 2004). It is experienced that deep convection generating cloudiness is associated with LLJ (Remedio, 2013). During the monsoon period LLJ is formed below 6 to 7 km altitude with the core existing in between 1.5 to 5 km height.

It is observed that LLJ is present up to 20° N latitude with highest frequency of occurrence taking place in the month of July and maximum wind speed existing below 2.4 km. Joseph and Raman (1966) defined LLJ with certain specific conditions such as wind speed maximum below 6 km, wind direction 270 ± 40° and wind shear changing rapidly on either sides of the core of LLJ, yet sharper over the lower side (Joseph and Raman, 1966).

The vertical profile of various atmospheric parameters could be gathered and analyzed with this four month long series of observations, for the first time at Cochin. Meteorological parameters such as wind speed, wind direction, Relative Humidity, temperature, geo-potential height, dew point temperature and derived properties such as momentum flux, moisture flux, kinetic energy inflow are compared with the corresponding rainfall data, and are presented in this Chapter.

3.3 Geographical Location of the Site

Indian peninsular region is surrounded by Arabian Sea on the western side, Indian Ocean over the southern side and Bay of Bengal over the eastern side. It is at the southern part of the Western coast of India that the state Kerala is located within the latitudes 8° N and 13° N. The observational site is at Kochi (earlier it was known as Cochin), located at 10.02^0 N latitude and 76.32^0 E longitude. The launching site is shown with reference to the Indian subcontinent in which Kerala being the southernmost state along the west coast and Cochin is the most advanced city in Kerala.

The southwest monsoon seasonally found in Indian peninsular region enters into the main land through Kerala - the southernmost state of India, and Kochi is normally the gateway of this entry. The monsoon wind taking a clockwise turn along the Somali coast in the Arabian Sea is hitting the western coast of India from second half of May, every year, till the middle of October. The humid air developed over the Indian Ocean is pulled into the land by the trough developed in an East-West orientation across north India. Western and central India gets 90% of annual precipitation while southern and north western India gets 50 – 70% of rainfall during this season and 18-28N is considered as the *core monsoon zone* receiving heavy rainfall (IMD Monsoon Report, 2013).

The wind during the monsoon season over the Indian ocean and Arabian Sea has two major components i) Low Level Jet (LLJ) or Somali Jet stream at 850 hPa bringing moisture to the subcontinent from the Arabian Sea, and ii) the Tropical Easterly Jet (TEJ) at the level 100 hPa widely distributing the rainfall (Ramage, 1971).

3.4 Data and Methodology

Wind profiles during the Southwest monsoon period (June, July, August and September) in 2013 was studied with GPS Radiosonde system, by German made GRAW Radiosonde. The periodicity was about once in three days and the launch was at 17:30 IST. The GRAW system provided data on Atmospheric Pressure, Temperature, Relative Humidity, Wind speed, Wind direction, Geopotential height, Dew point, Elevation and Range of balloon at various altitudes, with an interval of 5 seconds.

The Graw radiosonde system provides graphical details, such as Profile Data diagram, Altitude diagram, Emagram, Hodograph, Refractive Index variation, Tephigram, Skew-T diagram etc. Most of the ascents reached altitudes more than 25 km and hence various atmospheric properties in Troposphere and Stratosphere could be observed during this monsoon period.

The wind data collected from radiosonde experiments are computed as the horizontal wind components, such as zonal (u) and meridional (v).Vertical profiles of the horizontal wind components show the nature of the variability of the circulation at different altitudes and also gives information on the wind shear and the related properties.

The temperature data against altitude provides temporal and spatial values and Lapse rate. The level of tropopause and temperature inversion, if any, could also be detected. From the Relative humidity data the specific humidity and hence the real amount of water vapour present at different levels could be assessed.

The rainfall data of India Meteorological Department during the same period is used to compare the intensity of rainfall with height and core-speed of westerly LLJ domain. The correlation between the rainfall and various properties of LLJ are determined. The turbulence effect in the lower troposphere is analysed with the wind shear calculation. The liquid water content up to various levels are calculated to account for the amount of moisture entering into the peninsular region. Also from the zonal wind data, integrated over a specific height, gives the momentum per unit mass, in the moisture transport over Cochin.

Major objective of the study reported in this Chapter is to understand the atmospheric characteristics including the circulation pattern up to the mid-troposphere during an active monsoon year over Cochin, and to study the intra-seasonal variability with special attention to the monsoon Low Level Jet stream over this region. Within the Planetary Boundary Layer the surface roughness influences the atmospheric conditions so that the inherent nature of wind structure gets modified. The topographic feature of Kerala with elevation towards East, across its width, helps the lifting of moisture-impregnated air-mass, during monsoon, to condense and precipitate above the land mass.

The details of Balloon Ascent are given in Table 3.1, below.

Table 3.1: Details of Balloon ascents

			Ascent Time line				
Ascent No	Date	Surf Press (hPa)	Surf Temp (°C)	Surf Rel. Hum(%)	TropoHt(m)	Max. Ht(m)	Problem
1	21-May-13	1003.6	33.6	45	18197	26275	
2	24-May-13	1004.6	31.3	68	17755	28820	
3	27-May-13	1005.5	30.4	65	data not available(dna)	11714.5	Sensor failure
4	30-May-13	1002.5	30.8	64	17031	26121	
5	1-Jun-13	1003	25.3	87	17943	24949	
6	7-Jun-13	1003.5	25.1	87	15998	24857	
7	10-Jun-13	1003.6	29.8	69	dna	15947	
8	13-Jun-13	1001.5	28.8	74	16692	18775	
9	19-Jun-13	1005	27	90	16821	29278.5	
10	22-Jun-13	1005	25.6	89	16835	23473	
11	25-Jun-13	1005	26.5	83	16322	26570	GPS failure
12	28-Jun-13	1006	29.5	80	dna	8971	
13	1-Jul-13	1007	24.8	66	16241	27396	
14	4-Jul-13	1002.7	25	93	dna	8351	GPS failure
15	7-Jul-13	1003	23.7	93	16349	28151	
16	13-Jul-13	1005	28.4	83	dna	15784	Sensor failure
17	16-Jul-13	1005	23.3	70	dna	13425	GPS failure
18	19-Jul-13	1003.8	25	91	18292	29382	
19	22-Jul-13	1005	27.3	84	16654	27304	
20	25-Jul-13	1005.7	27.7	71	17002	27362	
21	28-Jul-13	1007.5	28.6	70	dna	15764	balloon bursted
22	31-Jul-13	1003.6	29	71	dna	10207	GPS failure
23	3-Aug-13	1005.5	24.2	91	18353	21642	
24	12-Aug-13	1004.1	28.8	70	16911	36263	
25	15-Aug-13	1004.6	29.2	70	dna	8916	GPS failure
26	21-Aug-13	1004.7	28.8	69	dna	15690	GPS failure
27	24-Aug-13	1004.2	28.5	71	16749	23079	GPS failure
28	26-Aug-13	1003.7	28.9	68	15795	15931	GPS failure
29	27-Aug-13	1005.7	30	72	16163	26270	
30	28-Aug-13	1006.5	28.8	76	16362	27097	
31	30-Aug-13	1005	30.8	67	16655	28968	
32	2-Sep-13	1006	31.6	66	15820	25498	
33	5-Sep-13	1006	31	66	15660	28079	
34	8-Sep-13	1009	30	73	15817	29463	
35	11-Sep-13	1004.9	28.7	77	15359	22210	
36	14-Sep-13	1005.4	28	88	15799	28647	
37	17-Sep-13	1003.3	26	91	16269	29181	
38	20-Sep-13	1003.7	29.3	82	16743	19612	GPS failure
39	23-Sep-13	1004.6	32.1	62	17225	26424	
40	26-Sep-13	1008.2	31.5	66	16745	23375	
41	29-Sep-13	1006.2	28.6	80	16591	28887	
42	2-Oct-13	1005.5	31.6	69	17011	29858	
43	9-Oct-13	1007.7	29.6	75	16317	29744	
44	16-Oct-13	1004.6	30.6	77	16894	24018	GPS failure
45	30-Oct-13	1007.3	31.8	64	16672	27874	

3.5 Results and Discussion

3.5.1 A typical Balloon Track

A typical balloon track in Radiosonde experiment is shown (Fig 3.1) in red, against Longitude (A), Latitude (B) and Altitude (C) in metres**.** The initial position of the track, which is the launching point is lat - 10.05° N and lon – 76.32° E.

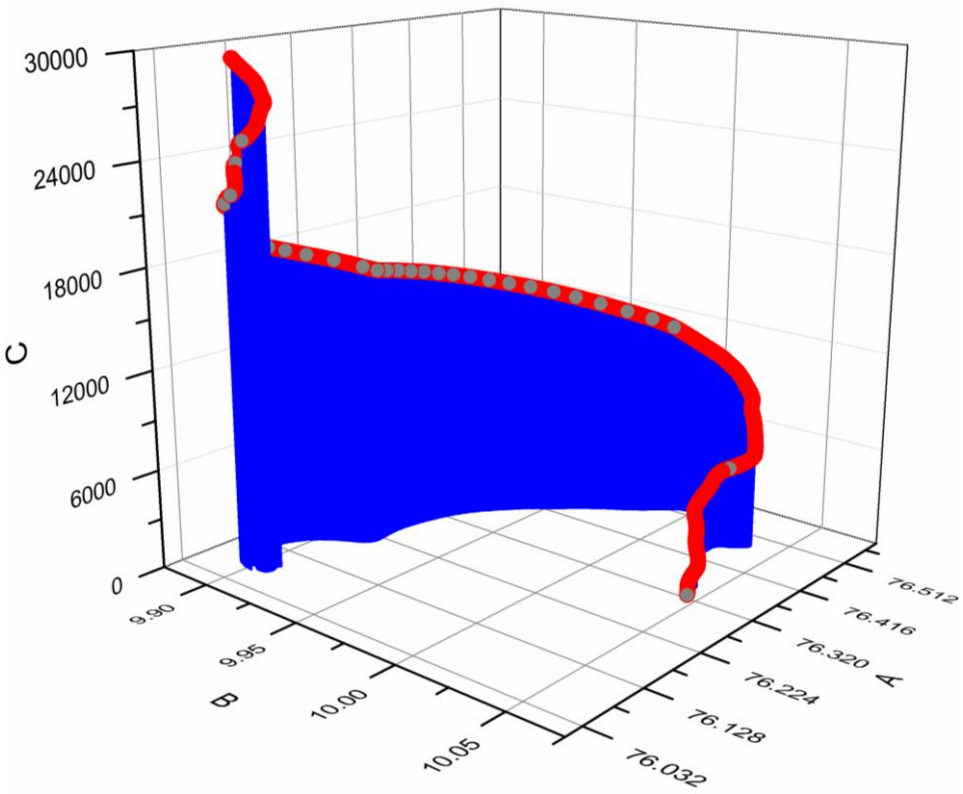

Fig 3.1:Balloon Track of a Typical Radiosonde Observation on June 01, 2013

From the ground level the balloon is ascending under the influence of westerly and hence drifting towards south-east direction until it is turned around by the Easterly. The balloon covers a few kilometres towards east (Fig. 3.2) but it is drifting around 50 km towards west under the forcing of easterly. The balloon track varies with, the change in rising rate depending on the buoyant force and air drag - with Reynold's number in the range 3 x 10^5 to 4 x 10^5 (Andras et al., 2013). The presence of cloud and air pockets affect the motion of balloon.

As it crosses the Tropopause its movement is quite random within the stratosphere (Fig. 3.1).

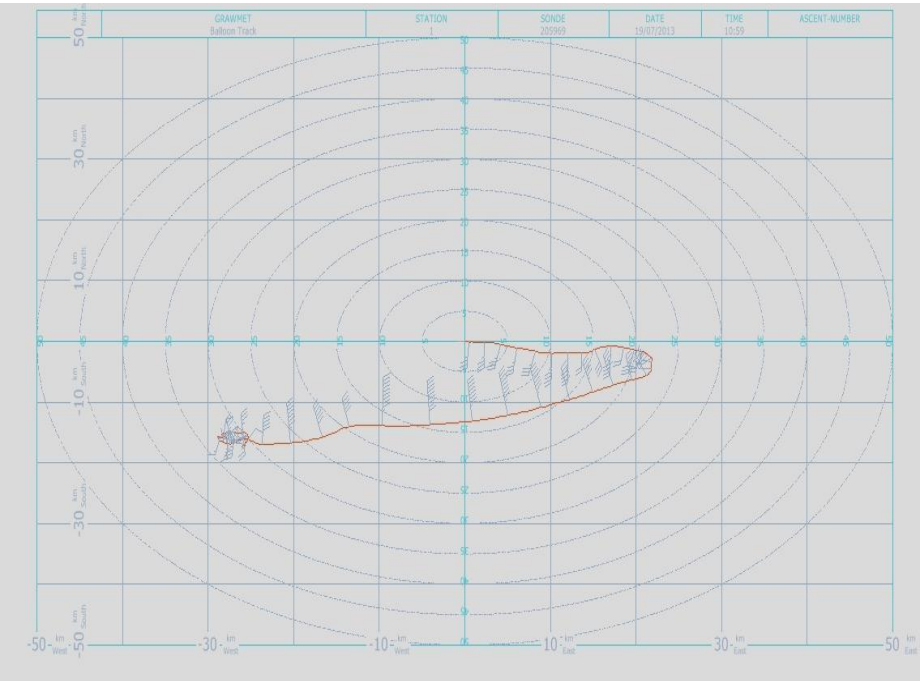

Fig. 3.2: Balloon Track showing the horizontal coverage

The series of GPS monitored Radiosonde ascents, designed to cover the entire Southwest Monsoon period of 2013, took off with a periodicity of once in three days, was a great experience for the 'Atmospheric Sciences' community of the University, since it provided 'in situ' data collection facility to work and understand the atmosphere in which we are living.

Such an ascent frequency was chosen because the study was targeted for the whole season lasting over four-month period, covering the entire south-west monsoon. No abrupt change was expected in the features of the monsoon.

3.5.2 Maximum Height reached by Radiosonde balloon during the experimental period.

Fig. 3.3 illustrates the bar diagrams of the maximum height covered by the Radiosonde observations during the 2013 Monsoon period. The maximum height reached by Radiosonde system depends on various factors, such as: (a) the hydrostatic thrust depending on the difference in density of air and that of gas filled in the balloon, (b) total weight of the balloon and the payload, (c) the elastic property of the balloon, and (d) the thermodynamic state and instability of the atmosphere

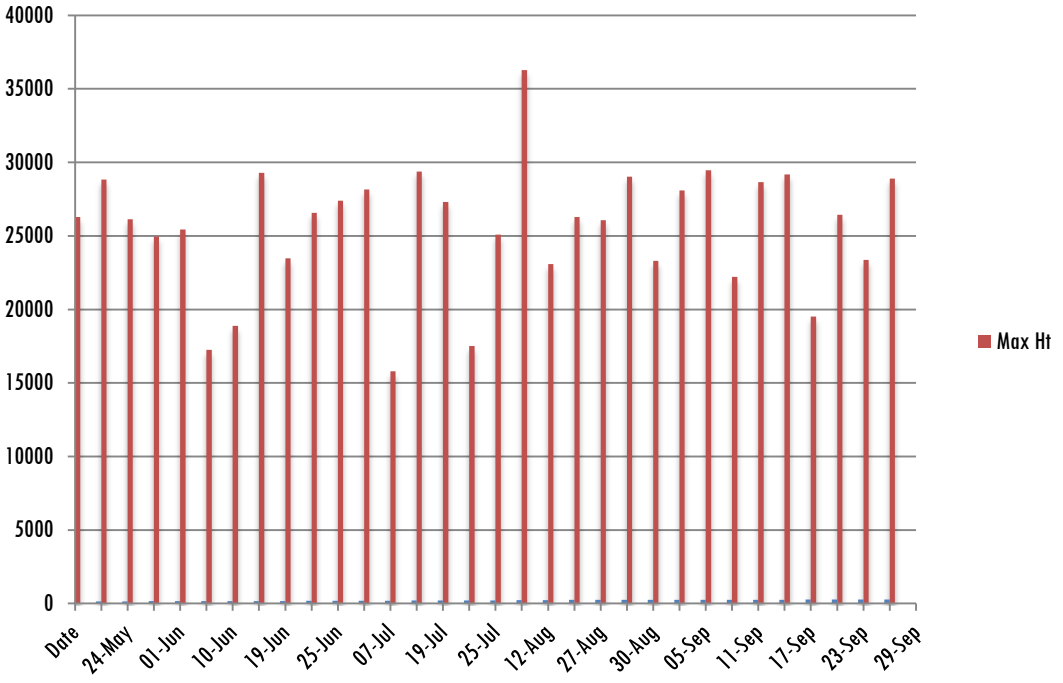

Fig. 3.3: Maximum height attained by radiosonde observations during 2013 Monsoon

In the ascents during 2013 monsoon period, more than 50% of the ascents recorded a maximum height above 25 km and the one that reached over 35 km is the ascent conducted in collaboration with Space Physics Laboratory (Thiruvananthapuram) for comparing the three sondes – Graw, Pisharoty and Messie. Grawsonde was found to be highly reliable, sensitive and accurate. Almost all ascents covered the tropopause level and hence major studies in weather features could be carried out.

3.5.3 Vertical Profiles of temperature, relative humidity, zonal and meridional winds on 1st July 2013 at 17:30 IST – An active monsoon day

The behaviour of the atmosphere is represented with the vertical profiles of temperature, relative humidity, zonal and meridional wind components during an active monsoon day is illustrated in Fig. 3.4.

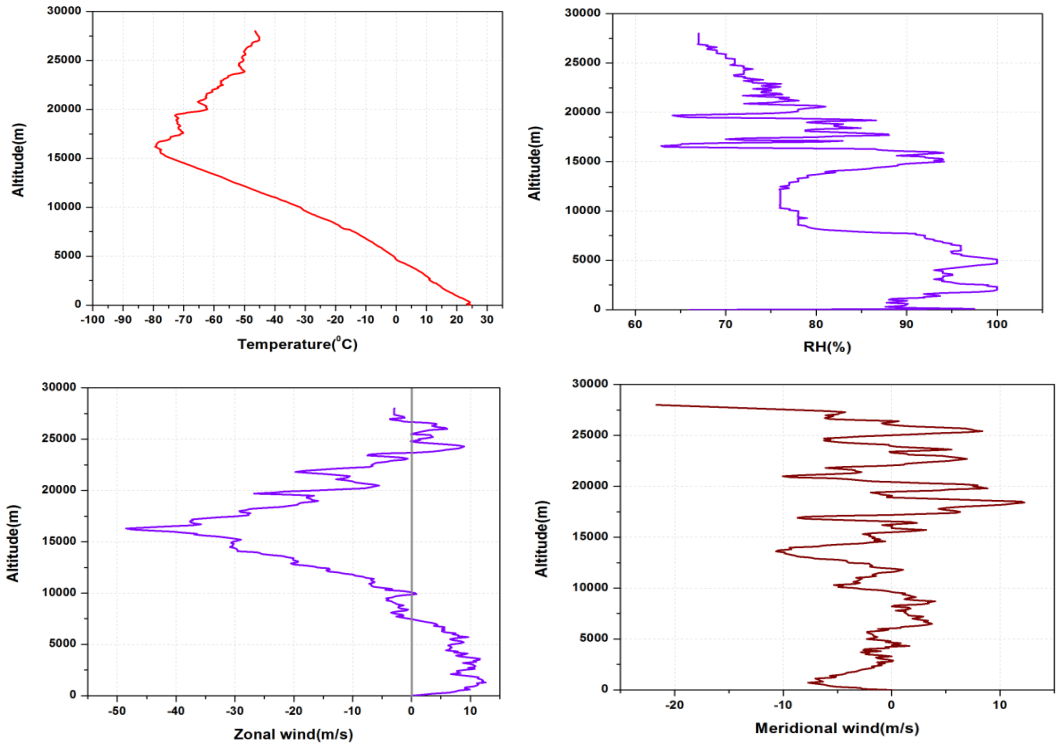

Fig. 3.4: Vertical profiles of (a) Temperature. (b) Relative Humidity, (c) Zonal Wind and (d) Meridional Wind during an Active Monsoon day.

Temperature profile - giving the variation of temperature with altitude, presents a number of features: 1) The tropopause temperature is almost -80°C and the tropopause height is 16300 m, (2) The environmental lapse rate is about - 6.44 °C/km up to the level of tropopause.

The relative humidity within 6 km touching almost 100% with strong LLJ is marking a deep convection. At an altitude of about 10 km, the relative humidity decreases to 76% featuring cloudiness in the lower part of troposphere above Cochin.

By July, as the monsoon gets well established, the LLJ core speed at an altitude 1.5 km, becomes 14 ms^{-1} and the TEJ core achieves almost 50 ms^{-1} speed, close to the tropopause. The vertical height of westerly is more than 6 km indicating a very large column of water vapour being transported onto the land. From 2 to 16 km there is gradual change in the magnitude of wind speed from + 14 ms^{-1} to -50 ms^{-1}, providing an average wind shear of -4.5 x 10^{-3} s^{-1}.

In the meridional wind profile below 6 km it is northerly and from 6 to 10 km it is southerly. Thus taking the zonal and meridional components below 6 km, the resultant monsoonal wind over Cochin is not ‘south-westerly’ but ‘north-westerly’.

3.5.4 Variation of Temperature during Monsoon 2013

The temporal variation of temperature throughout the monsoon season of 2013, over Cochin is plotted up to an altitude 10 km (Fig. 3.5), representing the atmospheric structure below the mid-troposphere. There is a gradual decrease in temperature within this troposphere region and almost a homogeneous thermal state is recorded at each pressure level over the entire period. Yet, a wave effect that makes a pulse of change in temperature with a short time period could be seen descending here.

It could also be noted that in between 14th June and 18th July in 2013, the surface temperature dropped below 24°C on certain days showing the cooling effect due to continuous raining. After this period weakening in the intensity of rainfall (Rainfall report by IMD) keeps the surface temperature above 24°C.

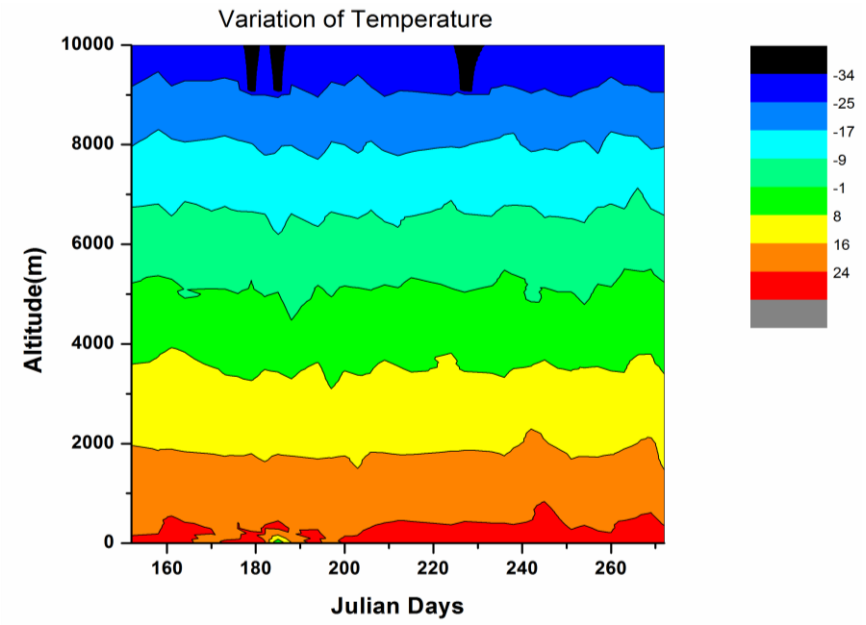

Fig. 3.5: Temporal variation of Temperature up to mid-troposphere

3.5.5 Variation of Specific Humidity with Altitude

Specific humidity is described as the ratio of mass of water vapour in a unit mass of moist air, usually expressed as grams of vapour per kilogram of air. It is an extremely useful quantity in determining the weather systems of a region. The rate of evaporation of water from any surface is directly proportional to the specific humidity difference between the surface and the adjoining air. Specific humidity does not vary as the temperature or pressure of a body of air changes, as long as

moisture is not added to or taken away from it. This stability of the specific humidity makes it useful as an identifying property of a moving air mass. The specific humidity of saturated air increases rapidly with increasing temperature.

From the radiosonde observations, the vertical profiles of specific humidity were computed for the entire 2003 monsoon season and are displayed in Fig 3.6. During June and July, it is almost within 0.012 to 0.016 with an initial high value exceeding 0.016, which gradually decreases to 0.012. In the first week of August it again reinstates its magnitude back to 0.016 even up to an altitude around 1 km due to the heavy raining in July. After the first week of August the specific humidity is consistently above 0.01657 and the altitude within which that value of specific humidity is decreasing gradually, due to the slow weakening of rainfall intensity. It can also be observed that the height to which positive specific humidity measured is decreasing as the season advances, showing the weakening of the inflow of moisture flux.

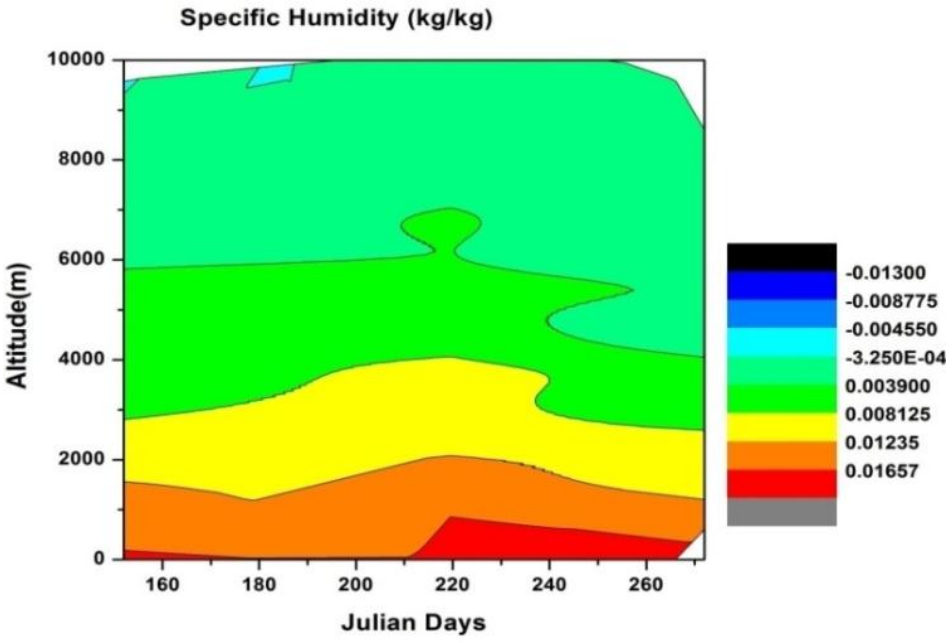

Fig. 3.6: Temporal variation of Specific Humidity (2013)

3.5.6 Vertical Profiles of Zonal Wind

The vertical profiles of zonal wind up to 10 km altitude over Cochin from radiosonde observations conducted during the southwest Monsoon of 2013 is shown in

Fig. 3.7. The variation of zonal wind shows periodical peaks in velocity going beyond 18 m s^{-1}.From 1st June 2013, that is the onset period of southwest monsoon in Kerala, the velocity of Low Level Jet is found to be changing both in level and strength.

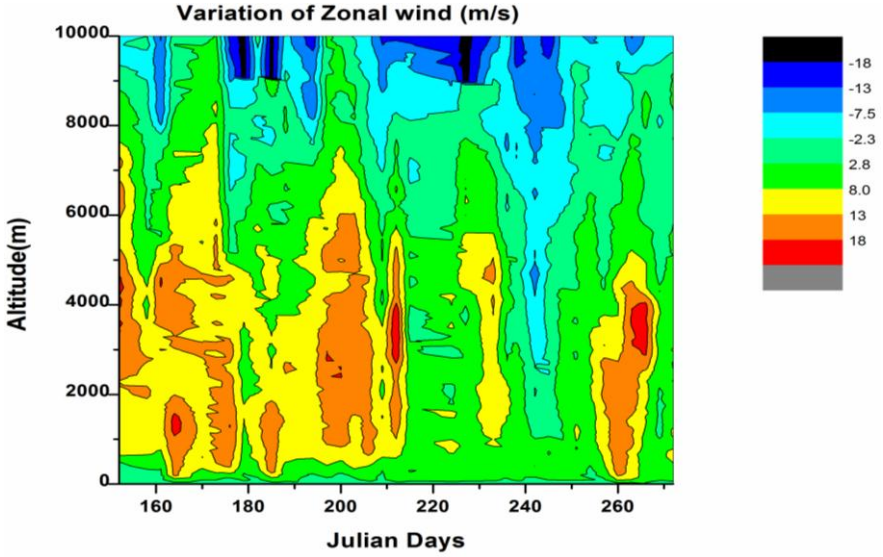

Fig. 3.7: Variation of Zonal wind in Time series over the Monsoon period of 2013

LLJ reaches a maximum altitude of about 8 km in the last week of the same month and its level decreases to 3.6 km by 6th July 2013. Again in the last week of July the height of LLJ ascends to 7.3 km which further decreases to an absence of LLJ in the first half of August. But during the second half of August the vertical extension of LLJ is observed up to a height of 5.5 km. A relatively weak LLJ in the first quarter of September strengthens and takes a vertical span up to 5 km by the last week of the same month. A periodicity of 30 to 60 days is observed for the variation of wind speed. Hence throughout the Monsoon period the vertical extension of LLJ is varying at a periodicity of 30 days in agreement with Madden-Julian oscillation. The maximum height of LLJ is found to be decreasing from 8 km to 5 km over the period June to September, which then withdraws along with the cessation of South-West Monsoon.

Furthermore, it is found that as the core level increases, the level of 8 m s¯1 speed limit of the wind is descending. The days within which the wind speed stays at more than 8 m s¯1 is also decreasing with the advancement of Monsoon. That is, the monsoon spell is lasting for longer period at the initial phase than in the latter span of the season.

3.5.7 Development of LLJ during the onset of Monsoon over Kochi

In the observation taken during the last week of May and first week of June revealed the nature of development of LLJ, as shown in Fig.3.8. Westerly wind is plotted on the right side and easterly on the left side of the zero line of zonal wind velocity. From 21st May to 27th May the westerly core velocity is quite less than 10 m s^{-1}, and the vertical width of westerly is gradually increasing. By 30th May, the core velocity becomes clearly more than 10 ms^{-1} and the transition level of westerly to easterly becomes almost 8 km (Joseph and Raman, 1966).

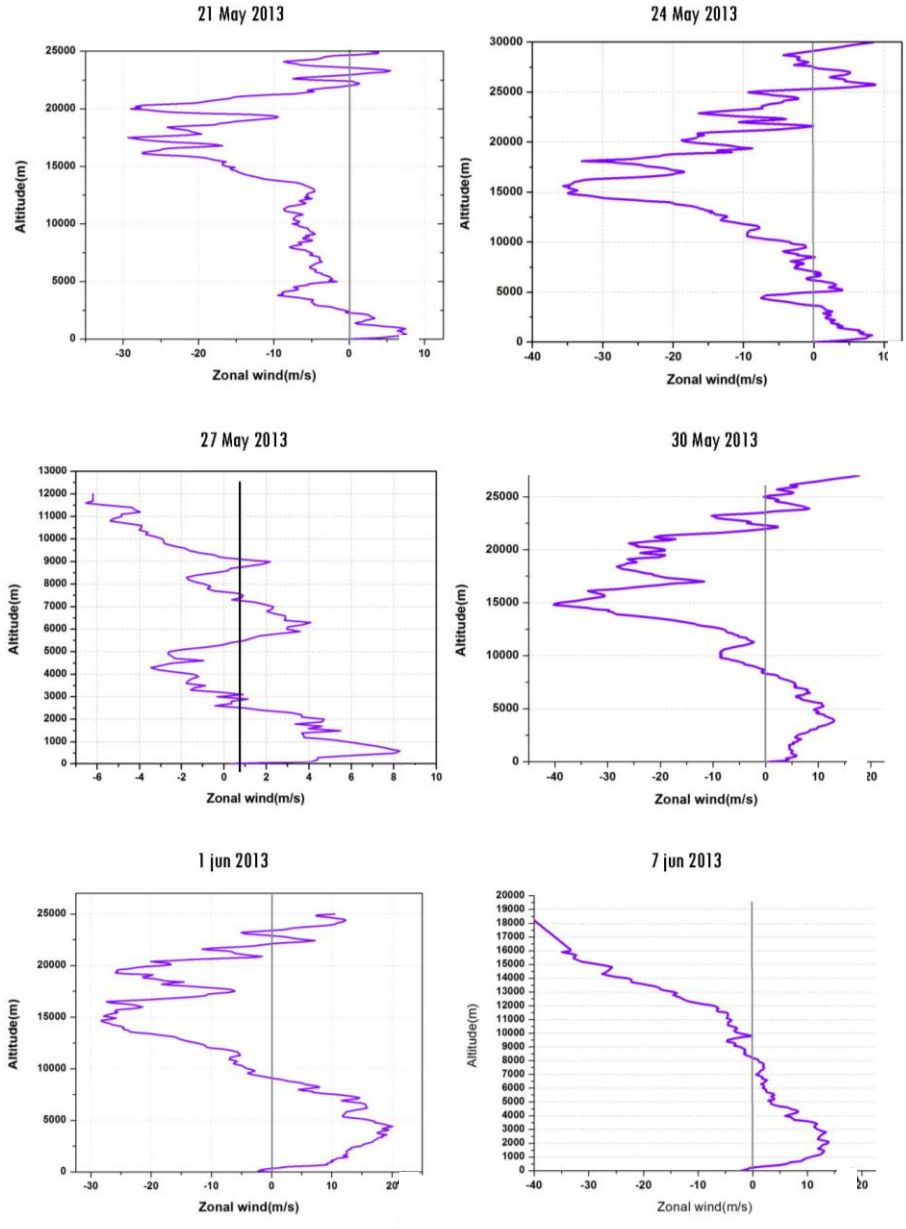

Fig. 3.8: Development of LLJ during the onset of south west monsoon 2013

3.5.8 Budyko's Index (BI)

Budyko's index of turbulence measured as the ratio of difference in temperature across two levels in the atmosphere to the square of the average wind velocity within the two levels.

$$BI = \left(\frac{\Delta T}{\overline{u}^{2}} \right) \qquad \text{--(3.1)}$$

BIis taken for 1st June 2013 and shown below (Fig. 3.9). The minimum the BI value, the maximum would be the turbulence, indicating a strong jet core and high vertical shear (Murthy et al, 2002). From 1 km to 7.5 km, the Budyko's Index is found to be less than 10^{-2}, showing the range of altitude where the turbulence due to westerly is maximum.

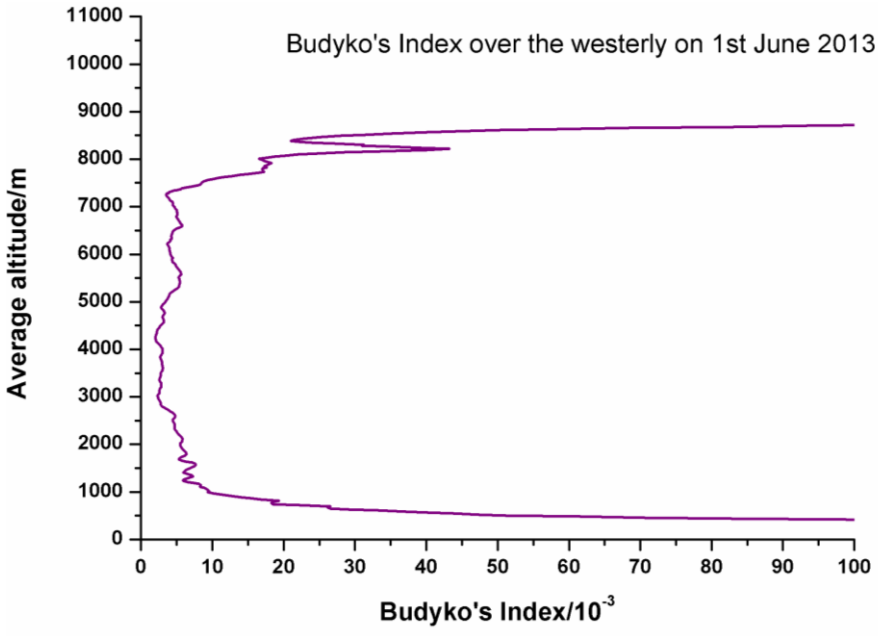

Fig. 3.9: Vertical profile of Budyko's Index

3.5.9 Temporal Variation of Vertical Shear of Zonal wind

From Fig. 3.10, it is seen that above 500m, the wind shear is almost within 0.005 -> -0.009 s^{-1} up to the upper tropospheric levels. Wind shear above the surface is high (0.01 -> 0.03 s^{-1}) in June-July and low in August – (below 500m) implies high instability and strong possibility of convection. In the monsoon period this shear is showing a decreasing trend even at altitudes within 2 to 4 km. This

descending and subsequent weakening of shear can be attributed to the gradual decreasing strength of westerly related to the lowering of the differential heating across the land and sea.

Specific humidity during June and July is almost within 0.012 to 0.016 with an initial high value exceeding 0.016, which gradually decreases to 0.012. In the first week of August it again reinstates its magnitude back to 0.016 even up to an altitude around 1 km due to the heavy rain in July. After the first week of August the specific humidity is consistently above 0.01657 g kg^{-1} and the altitude within which that value of specific humidity experienced is decreasing gradually, due to the slow weakening of rainfall intensity.

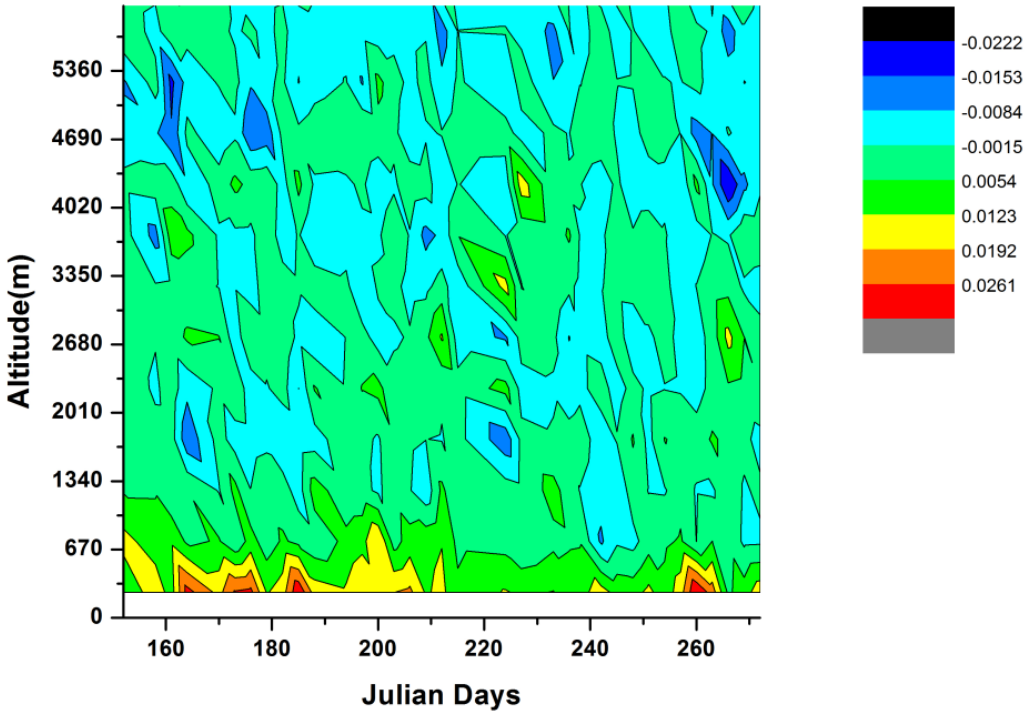

Fig. 3.10: Temporal variation of vertical wind shear of Zonal wind.

The wind shear below and above the core level on these six days are shown in Table 3.2 (also represented graphically in Fig. 3.11) and found that with the onset of monsoon it is increasing below the core level.

Table 3.2: Wind shear below and above LLJ core

	Below LLJ core level			Above LLJ core level		
Date	**Δz/m**	**Δv/ms^{-1}**	**Wind shear/s^{-1}**	**Δz/m**	**Δv/ms^{-1}**	**Wind shear/s^{-1}**
21-May	924	7.49	0.008106	1228	7.49	0.006099
24-May	666	8.6	0.012913	1690	8.6	0.005089
27-May	584	5.12	0.008767	1979	8.65	0.004371
30-May	3847	9.03	0.002347	4478	9.03	0.002017
01-Jun	4023	20.03	0.004979	4713	20.03	0.00425
07-Jun	1836	13.9	0.007571	6055	13.9	0.002296

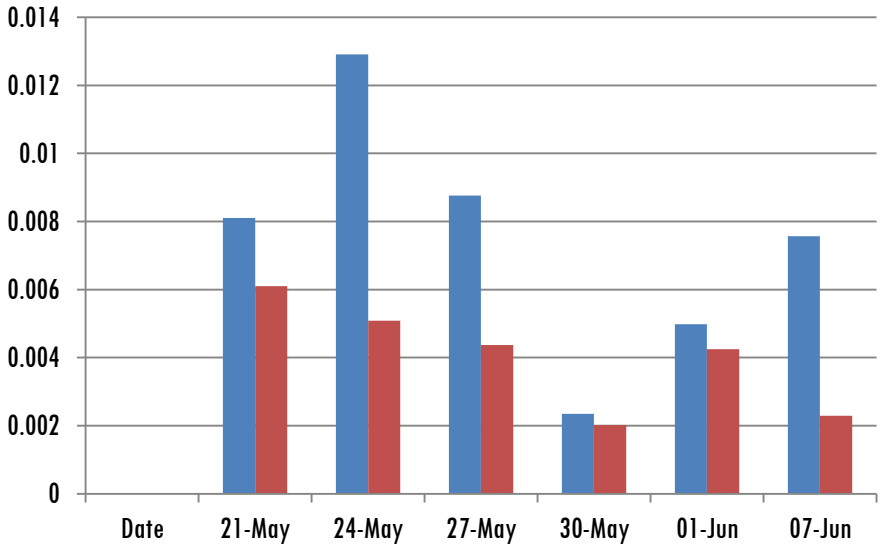

Fig. 3.11: Wind shear below (blue) and above (red) the core level of LLJ

3.5.10 Rainfall during Monsoon 2013 at Kochi

The Rainfall intensity during this period, recorded by India Meteorological Department, is given in Fig.3.12. It clearly shows that there is a downward trend in the intensity with periodic surges. While there is no rain during the second half of August, an intensity hike occurs in September, which goes beyond 30 mm per day.

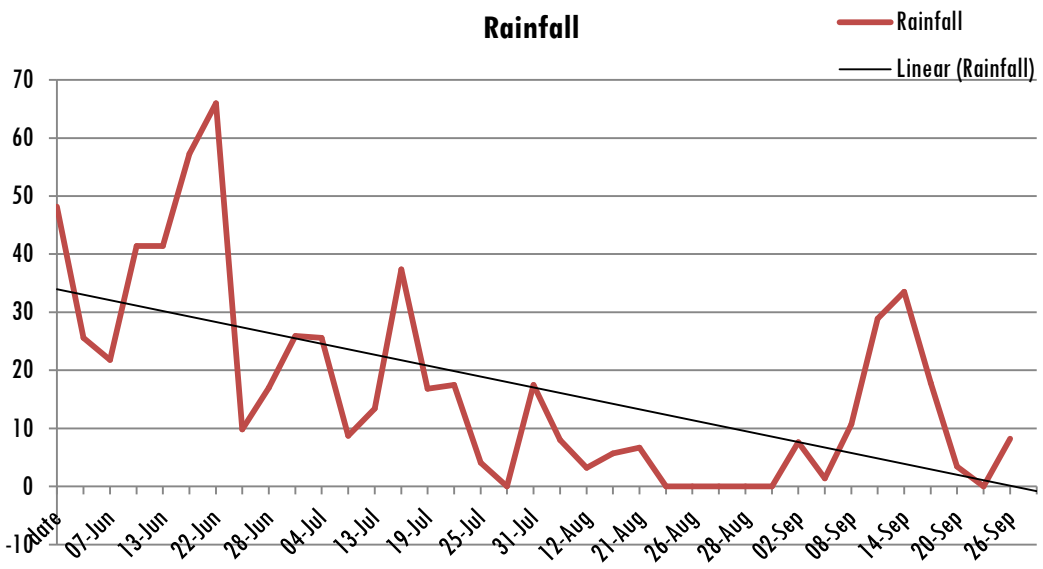

Fig. 3.12: Rainfall during SW Monsoon (2013) at Kochi (*courtesy: India Met Dept*)

3.5.11 Level of maximum velocity of LLJ

The active presence of Low Level Jet (LLJ) is a major feature in the Indian summer monsoon, which carries the moist air from Indian Ocean into the main land. Over the entire period of Monsoon, the level of LLJ core makes a periodic variation in altitude. The onset of Monsoon show a high value in the core level, and within the month of June it drops to an altitude less than 1.5 km from 4.5 km. In the month of July again a rise in level occurs, reaching to almost 4.2 km and then swinging back to 1 km by the end of July. The height at which the maximum velocity of LLJ recorded in time series is represented in Fig. 3.13. The core level of LLJ is moving up from 4 km at the beginning of June to a maximum of 4.5 km within one week and then shifting down to a minimum height of 1.2 km within a month. The next hike starts by the end of first week of July, crossing 4 km height and falls down to 1.2 km within one week. The last rise in the core level during this monsoon season occurs by the end of the first week of August. Thus, altogether there are three prominent rises in the LLJ core level occurred during the entire Monsoon period of 2013.

In the Fig.3.13, it can be noted that, on considering minor hikes in core level over the three months June, July and August, a periodicity of 15 days in between two consecutive hikes is clearly present. In most of the days the LLJ core stays above 1000 m altitude which can be attributed to the warming up of lower part of atmosphere during the day, on all days.

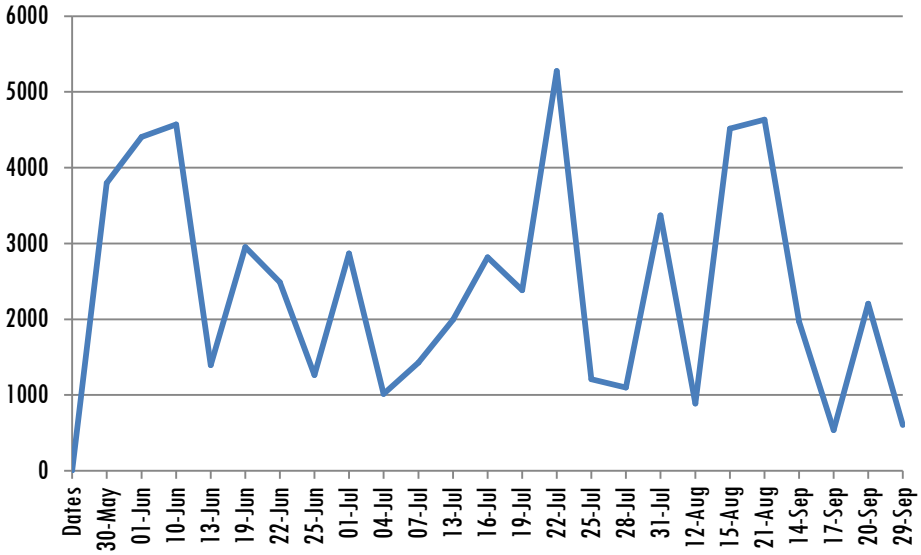

Fig. 3.13: The variation of the height of core level of LLJ in time-series.

On comparing the level of core of LLJ with rainfall data, it is observed that as the level of the core changes, rainfall is decreasing and vice versa (Fig 3.14). This observation shows that the lowering of the jet core is spreading the cloud cover within the lower layer and suppressing the development of convective clouds. This also highlights the fact that the presence of wind shear close to the surface plays a role in enhancing the intensity of rainfall. The negative correlation between the height of core level and rainfall intensity proves our observation.

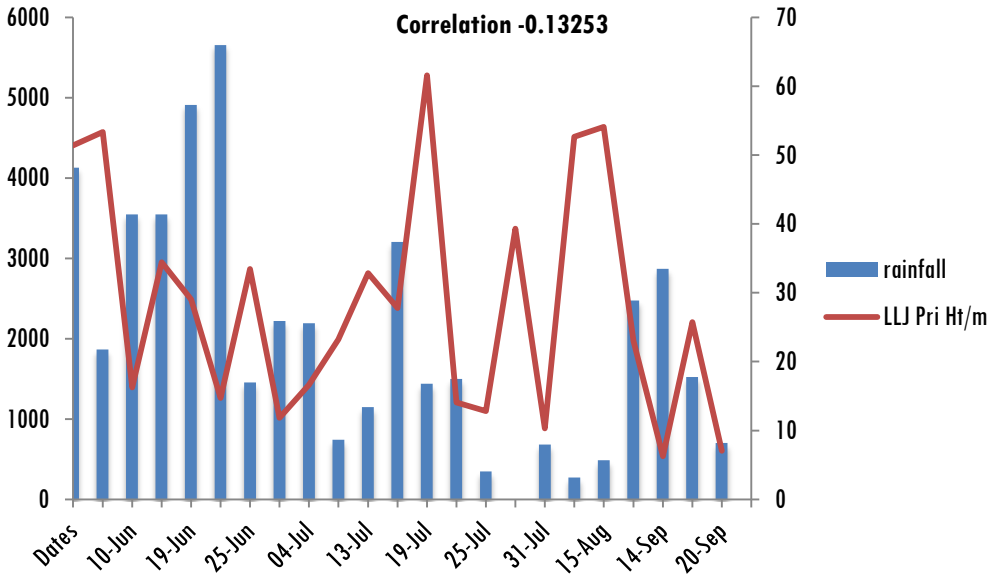

Fig. 3.14: Core level height and Rainfall

The core speed of LLJ in time-series is represented in Fig. 3.15. After the onset of Monsoon, the core speed shoots up from 14 m s-1 to 19.5 m s-1 in a week. Within a periodic time interval of 10 days, sudden increase in core speed could be noticed over a period covering June, July and up to mid August. In the whole Monsoon period, five major increases in core speed occurred, showing strength above 17 m s^{-1}.

In comparison between the core speed of LLJ and rainfall (Fig 3.16), the first half of Monsoon season presents a high correlation while the lack of moist air makes the rainfall intensity low in the second half.

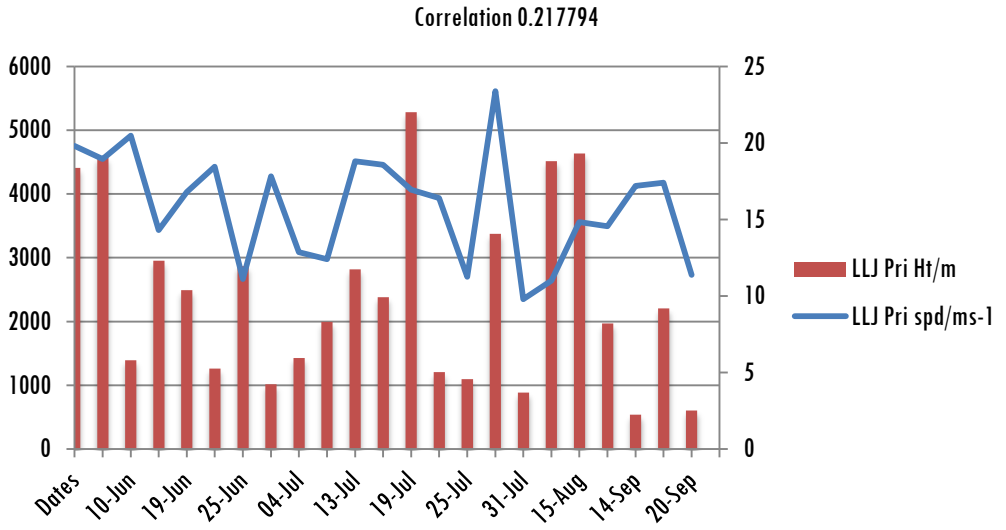

Fig. 3.15: Variation of LLJ core speed and level

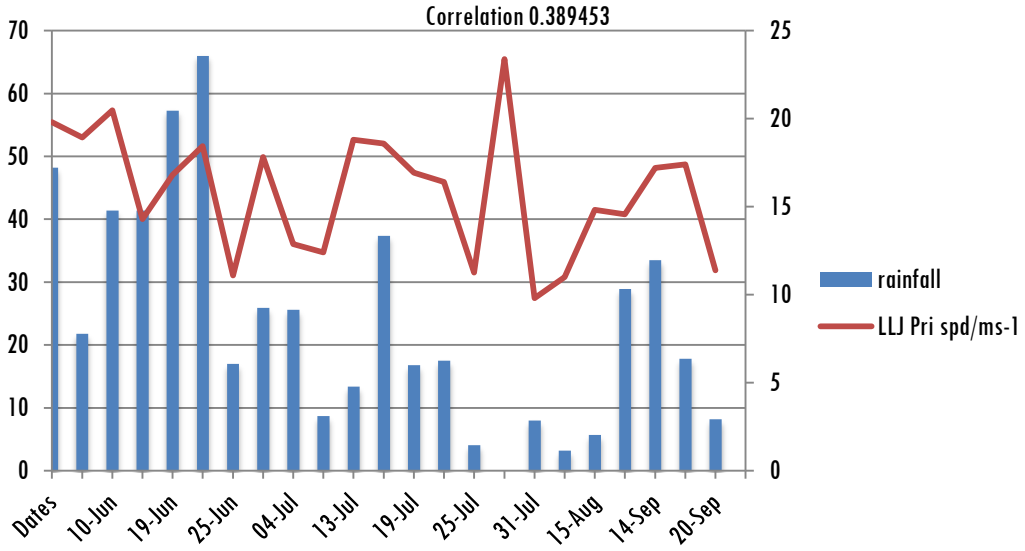

Fig. 3.16:Core speed and rainfall intensity

There is no appreciable influence on rainfall from core speed. Of course on certain days, there are proportional trends. Yet, in total, the two factors are not much related to each other.

3.5.12 Transition of Westerly to Easterly Regime during Monsoon

The height of westerly regime in the lower troposphere over Cochin during the 2013 monsoon season is represented in Fig 3.17. The vertical span of westerly regime shows clear intra-seasonal variations. In every month, during June to September of 2013, the height of westerly rises and falls. For every surge of active monsoon conditions, the altitude of westerly domain peaks and its level decreases when the intensity of monsoon weakens. This peaking trend is maximum in June and July while August and September showed relatively low level of peaks. Both in June and July, the vertical extent of westerly goes beyond 10 km height (see Fig 3.17). The correlation between the height of the westerly and rainfall is 0.510, which is statistically significant at 95% confidence level. The decrease in the vertical span of westerly shows a corresponding decrease in rainfall in most of the cases. Hence it can be understood that the vertical extension of westerly is vital in strengthening the rainfall by bringing larger amount of moist air.

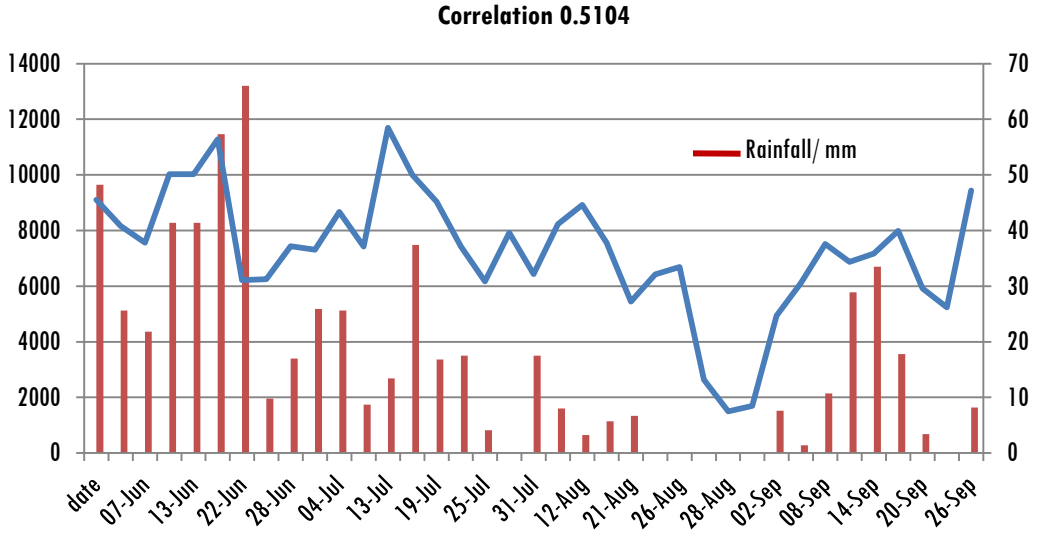

Fig. 3.17: Level variation of 'Westerly – Easterly' boundary

3.5.13 Tropical Easterly Jet Core Level Temperature and Speed

An attempt has been made in the study to understand the circulation features in the upper troposphere using Radiosonde data. The tropical easterly jet stream (TEJ) is an important meteorological phenomena observed in the upper troposphere over Indian Peninsular region during the summer monsoon season. The time series of TEJ core and the temperature of the TEJ core level is plotted and displayed in Fig 3.18. It can be seen that the temperature of the TEJ core shows moderate association with the speed of wind at this level. The fluctuations in temperature is somewhat reflected in changing TEJ core speed. As per the thermodynamic point of view, this association is possible. It indicates that the variation in temperature is contributing to the strengthening/weakening of TEJ.

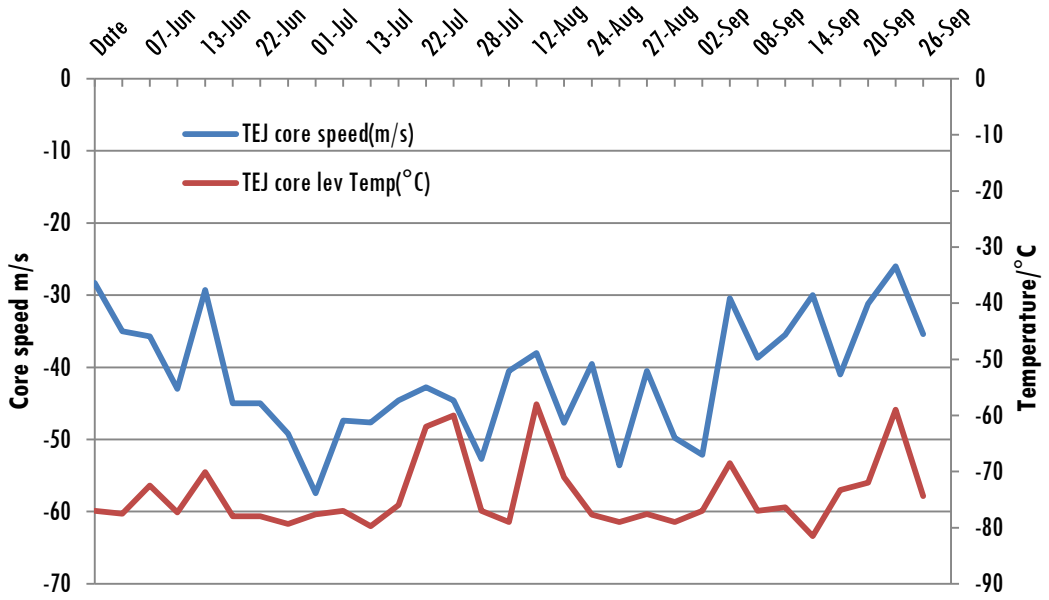

Fig. 3.18: Association between temperature and speed of Jet core

3.5.14 Vertical Shear of Wind between Low Level Jet and Tropical Easterly Jet

Vertical wind shear is an important factor for the development of convective systems at a region. A weaker vertical shear makes the convection grow faster vertically into the air. If the vertical shear is too strong, the convection cannot grow vertically and its energy becomes spread out over larger area. In this context, it is

interesting to see the vertical shear of zonal wind between the monsoon low level westerly Jet stream in the lower troposphere and the Tropical easterly Jet stream in the upper troposphere over Cochin during the monsoon season.

Fig. 3.19 illustrates the time series plot of the height of the core of LLJ (lower part) and TEJ (upper part). The core levels of LLJ and TEJ are showing a variation in opposite phase. As the height of LLJ goes up during an active monsoon condition, the core of TEJ moves down, causing strong shear. On the other hand, during weak monsoon conditions, the height of LLJ core become lower, and the core of TEJ goes up resulting in weak wind shear. This favours vertical growth of convection, causing localised rain, but suppress widespread rain. This indicates that the vertical shear of zonal wind becomes stronger during the active phases of monsoon, thereby suppressing the vertical growth of convection and spreads horizontally, causing widespread rain. Such an undulating mode of change in opposite phase in the core levels is a notable feature depending on the weather condition of the troposphere (Rai and Dimri, 2017).

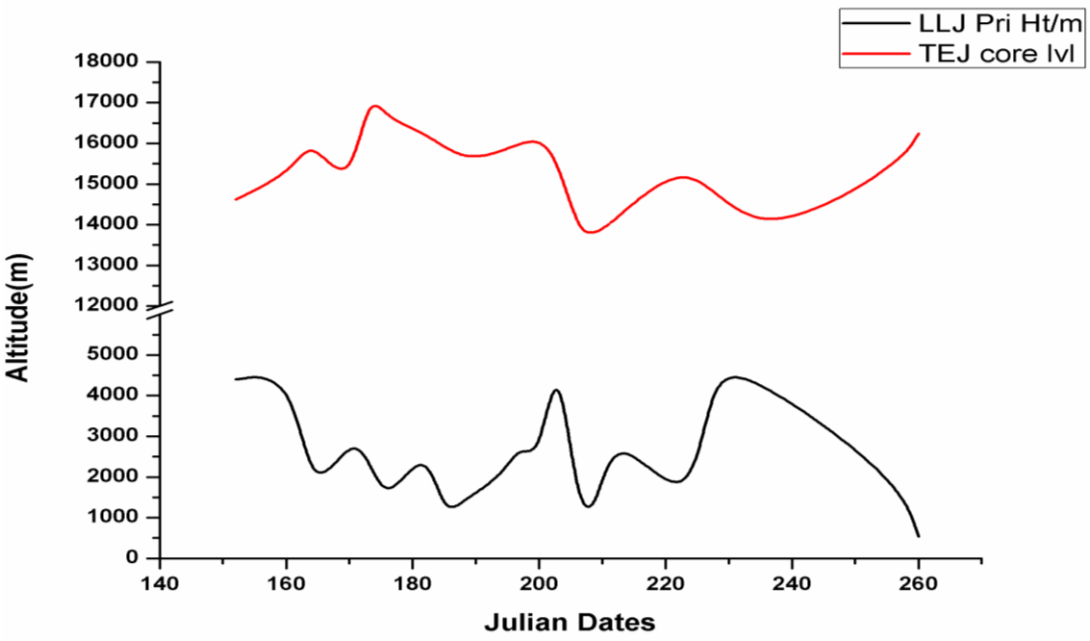

Fig. 3.19: LLJ and TEJ core levels.

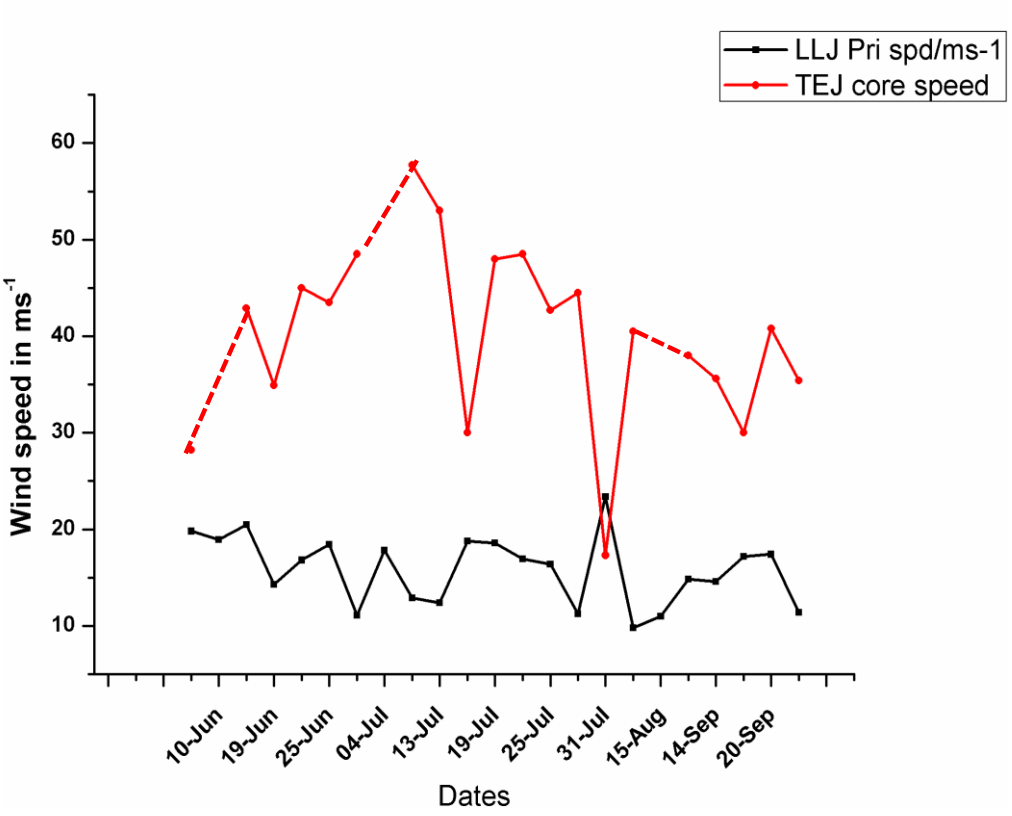

Fig. 3.20: Temporal variation of core speeds of TEJ and LLJ.

Also, it is seen that the temporal variation in core speeds of LLJ and TEJ are almost in opposite phase (Fig. 3.20).

3.5.15 Wind shear across LLJ and TEJ and its impact on Rainfall

On analysing the wind shear across LLJ and TEJ and comparing with the intensity of the rainfall, a strong correlation is observed as shown in Fig 3.21. During the active period of Monsoon both wind shear and rainfall intensity show almost a proportional variation and in certain time span wind shear has a leading phase, which is needed for the development of convection (Hua et.al, 2009).

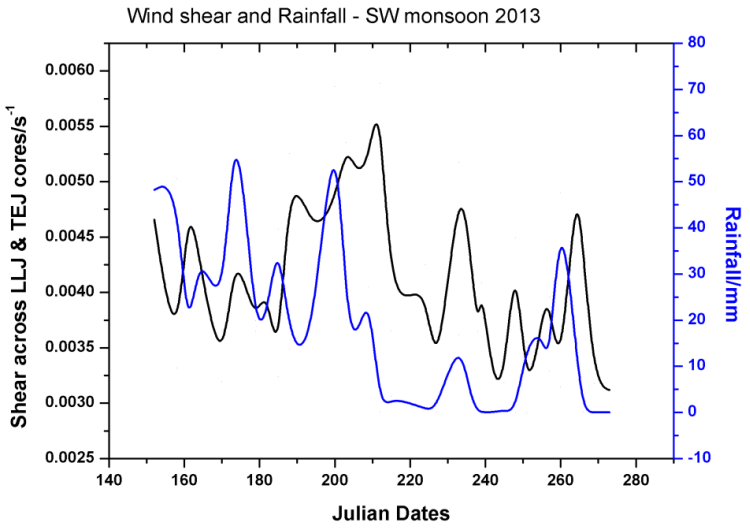

Fig. 3.21: Comparing wind shear and Rainfall intensity.

The wind shear across the TEJ and LLJ core are very much correlated by their phase, during the July-August period of the monsoon regime. But at the beginning and at the end, this phase correlation is not present.

3.5.16 Tropopause Height Variation

It has been reported that the height of the tropopause and its variation contributes to the variations in the underlying weather and climate (Misra et al., 2011).Using a three-dimensional general circulation model, they reported that the differences in moisture have been the reason for tropopause variations. Their study further suggested that the eddies and weather patterns on the surface of Earth are significantly influenced by processes in the atmospheric layers above. Thus the height of the tropopause at a region is an indicator of the weather disturbances in the lower troposphere.

As per the tropopause defined by World Meteorological Organisation, the height of the tropopause is the lowest level at which the lapse rate decreases to 2 K/km or less, provided that the average lapse rate between this level and all higher levels within 2 km does not exceed 2 K/km. Tropopause height measured as the lowest temperature level at the top of the troposphere found to be varying between 15.5 km to a maximum 18.2 km during the entire monsoon period under observation is given in Fig 3.22. Either due to the failure in the balloon ascent in reaching such a height on certain days or technical problem in encountered in GPS system data on certain days are not presented. Yet, systematic change in tropopause height can be

noticed and it can be connected to the variation of land surface temperature during the wet and dry sessions in the monsoon (Geerts and Linacre, 1997).

In the early phase of the monsoon, associated with the summer solstice, the altitude of the tropopause over Cochin is found to be situated at higher altitude, whereas, the tropopause height is lower during the active monsoon conditions. It is associated with the surface cooling due to high clouding and strong wind in the lower troposphere. More precisely, as temperature of the land surface decreases with the continuation of rain, there is high possibility for the rise in the density of lower atmosphere which in turn brings down air mass and that leads to the lowering of tropopause height.

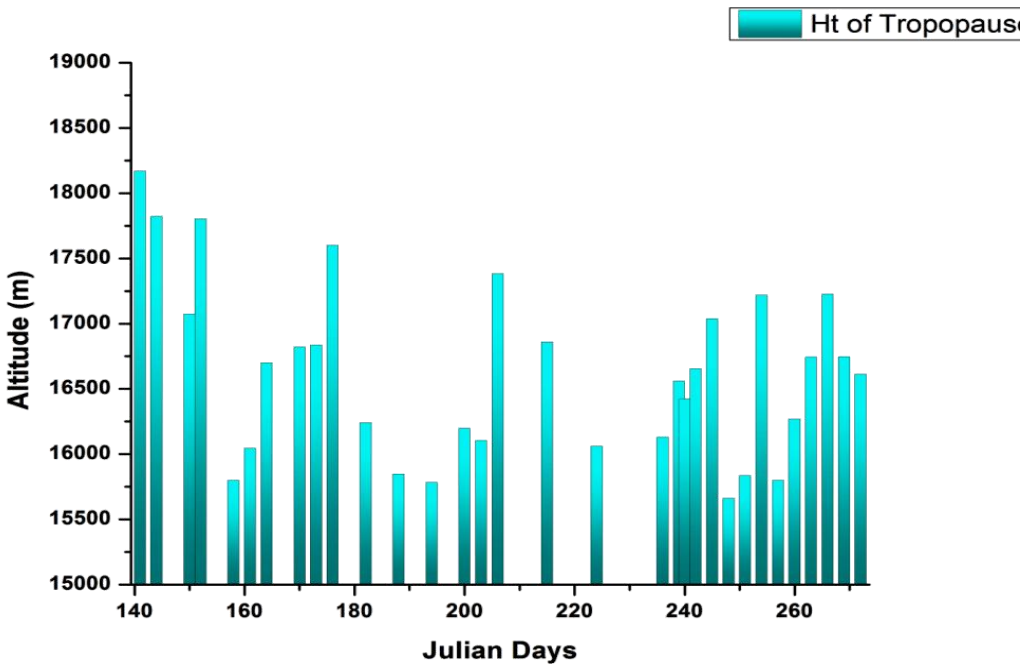

Fig. 3.22: Variation of Tropopause height during the experimental period.

3.5.17 Zonal Momentum Flux during the 2013 Monsoon Period

During the entire summer monsoon season, the westerly wind dominates in the lower troposphere. It is therefore interesting to search the depth of the westerly regime covering the entire lower troposphere and its associated weather systems. Momentum flux is calculated for unit area over the SW Monsoon season, using the relation

$$\int_{z1}^{z2} \rho u.dz \qquad \text{--(3.2)}$$

where **ρ** is the density of air and **u** zonal velocity, over the entire height of the Westerly.

The momentum flux per unit volume, over the entire vertical span of westerly (Fig 3.23), depending on the zonal velocity, gives a picture of the forcing of vapour from the Indian Ocean. As the upper limit of westerly moves up, there is corresponding hike in momentum flux. The momentum flux shows a lowering trend with periodical variations. The momentum flux reaches maximum values beyond $8x10^4$ kg/m/s during a number of occasions in the months June and July, also comes down to lowermost value less than 10^4 kg/m/s when there is no rain. The forcing, developed from the momentum flux, acting over the orographically inclined land mass of Kerala produces intense turbulence to establish convective cloud system.

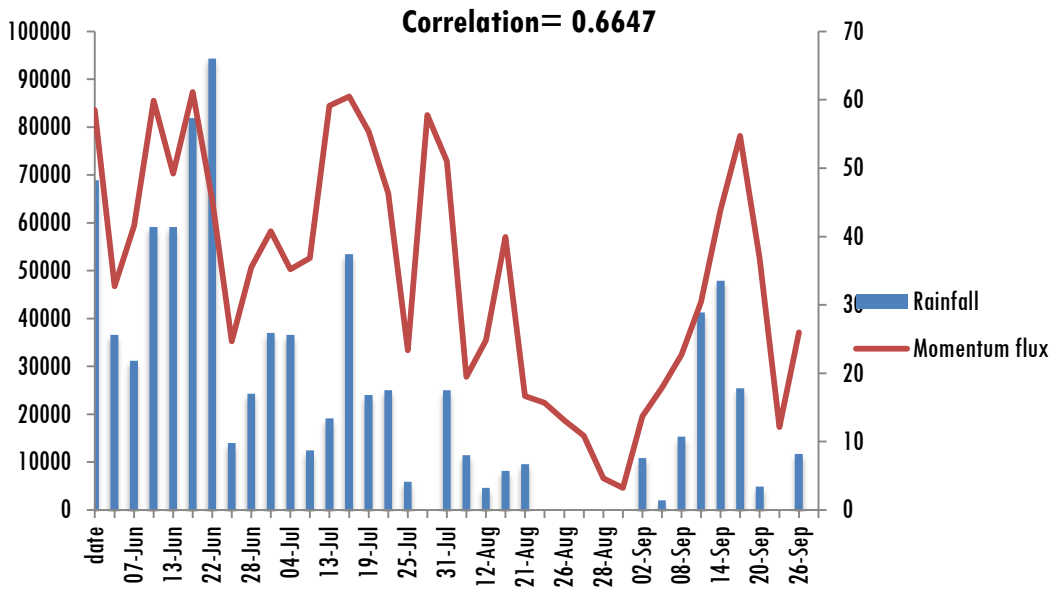

Fig. 3.23: Momentum Flux per unit volume

3.5.18 Zonal Kinetic Energy Flux

The zonal kinetic energy (KE) flux during Monsoon period of 2013 over Kochi is studied (Fig 3.24) with the radiosonde data from the zonal velocity component, using the relation,

$$\int_{z1}^{z2} \frac{1}{2} \rho u^2 .dz \qquad \text{--(3.3)}$$

for unit volume, where ***v*** is the zonal wind speed and ρ is the density of air, for each level, over the entire height of the westerly. The Kinetic energy transport shows the energy transfer linked with the strong differential heating across land and ocean. This large quantity of energy pulses with periodicities of 30 to 50 days can be partially trapped to transform into mechanical and electrical energy forms.

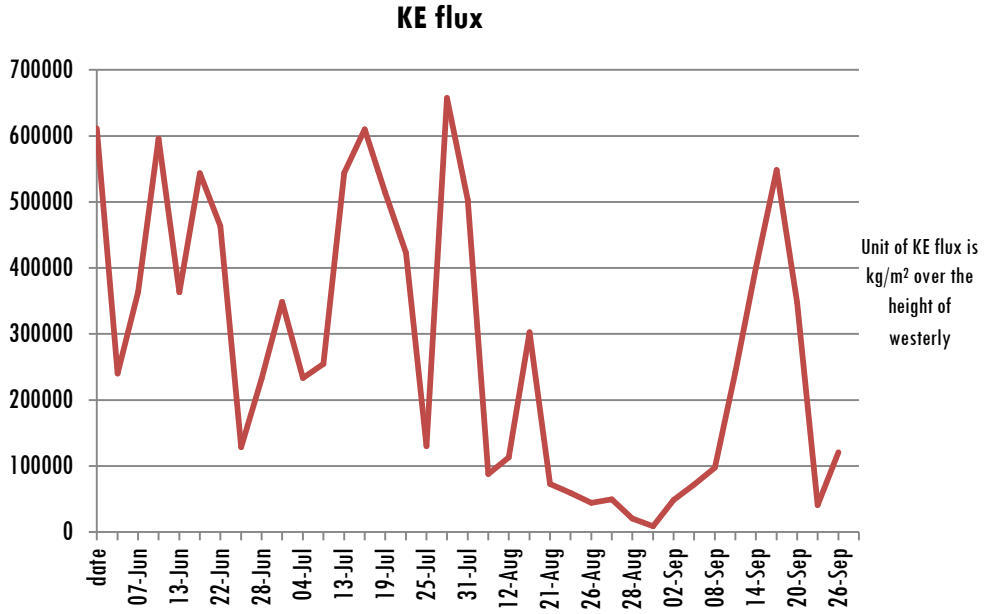

Fig. 3.24: Variation of Kinetic Energy flux during the Monsoon period.

It is clear from the data of kinetic energy flux (Fig. 3.24) that the transfer of energy is appreciably high in the month of July and in mid September. August recorded a rather less energy flux which can be attributed to the weakening of wind speed. The zonal kinetic energy transport shows the forcing from the Arabian Sea linked with the strong differential heating across land and ocean. The large quantity of moisture pulled into the atmosphere presents a great challenge over the orographic structure lying from the coastal belt at Kochi to the Western Ghats towered by Anamudi, over a distance of more than 100 km.

The kinetic energy variation occurring in a period of few days can set in gravity waves which can modify the cloud formation and distribution, and hence the rainfall pattern over the region (Lane and Reeder, 2001).

3.5.19 Influence of Kinetic energy on Rainfall

To examine if the zonal KE has any influence on the precipitation pattern over this coastal station, the time series of zonal KE per unit mass and the rainfall observed over Cochin is plotted as shown in Fig 3.25. The zonal KE per unit mass on each corresponding day is found to be varying to a maximum value of 10^6 J/kg and a minimum below 2×10^5 J/kg. It is observed that the KE per unit mass during the summer monsoon period shows considerable association with the rainfall pattern over Cochin. The correlation between the KE and rainfall is quite high over Cochin. The computed correlation coefficient between these two parameters showed a value of 0.639, which is statistically significant at 5% significance level. The increase in westerly wind speed during the monsoon season over Cochin, results in an increase in moisture transport and hence the intensity of rainfall.

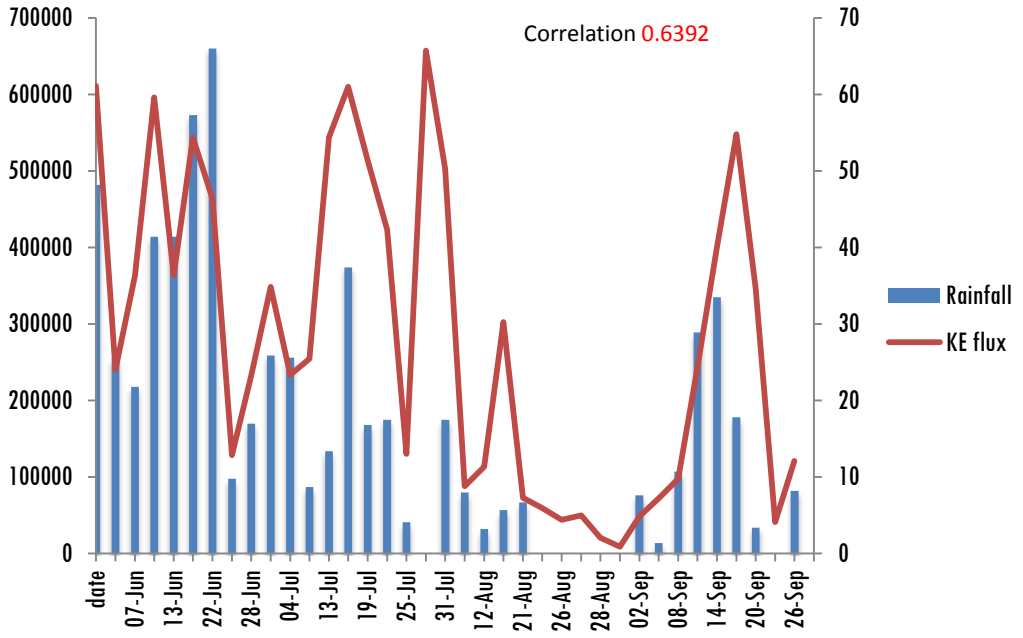

Fig. 3.25: Comparison of KE flux and Rainfall

3.5.20 Moisture Flux

Atmospheric moisture advection is the horizontal transport of water vapor by the wind. Determining the atmospheric water vapor at a region is significant in the prediction of all weather elements, such as clouds, fog, temperature and rainfall. Vertically integrated moisture flux convergence is an important component of the atmospheric water balance equation. Considering the relevance of moisture advection in the weather systems at a place, we computed the vertically integrated moisture flux over Cochin utilizing the Radiosonde available during the monsoon season using the equation

$$\int_{z1}^{z2} (\rho.q.u).dz \qquad \text{--(3.4)}$$

where $\boldsymbol{z_1}$ is the near surface height, $\mathbf{z}_2$ is at 10 km; ρis the density of air and $\boldsymbol{q}$ the specific humidity, and u is the zonal wind at each level. The specific humidity $\boldsymbol{q}$ at various levels in every ascent is calculated using the equations:

Saturated vapour pressure, $e_s = 611x \exp[(17.27x\ t)/(237.3 + t)]$

Vapour pressure, $e = U \times e_s/100$

Sp. Humidity, $q = 0.622 \times e/(p \times 100)$

The computed vertically integrated moisture flux over Cochin is plotted with time as shown in Fig 3.26. The moisture transported from the Indian Ocean after the onset of Monsoon till the end of July is very high; subsequently another pulse of a similar situation is occurring in the second half of September. Even within that high moist flux period, a periodic variation is notable. The moisture flux study made with the specific humidity and zonal wind components present in the westerly reveals, a 30 days periodicity in the peak value going beyond 800 kg/ms and a decreasing trend till the end of August. It is interesting to note that a similar periodicity is observed in the rainfall during the same period.

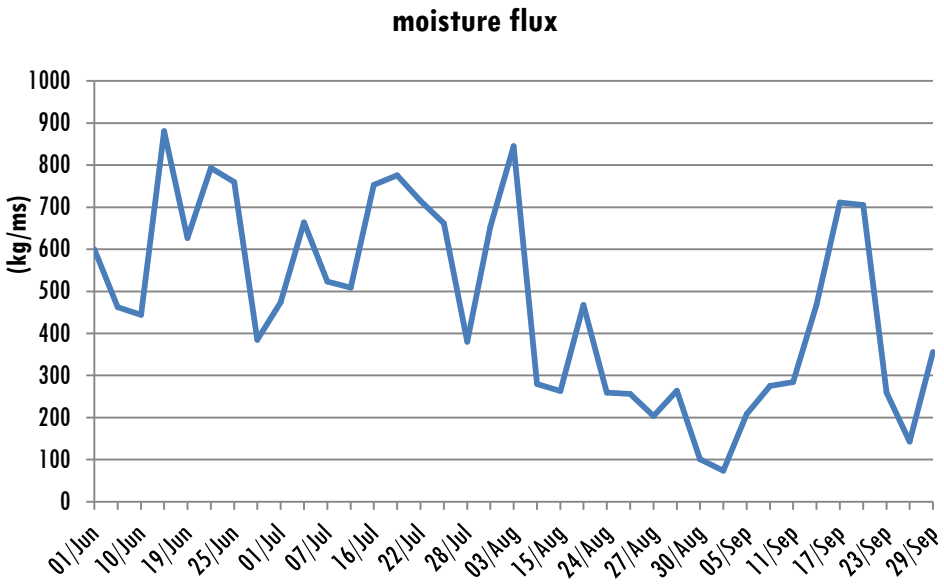

Fig. 3.26: Moisture flux variation

3.5.21 Vertically Integrated Moisture Flux and rainfall

Fig 3.27 is a plot of vertically integrated moisture flux and rainfall over Cochin during the monsoon season. The moisture flux shows significant association with rainfall. Strong positive correlation coefficient (0.719) is computed between the vertically integrated moisture flux and rainfall. When the moisture flux is less than 600 units, the rainfall shows strong association. Large fluctuations in the rainfall pattern can be observed above this optimum moisture flux. It infers that the link between moisture flux and rainfall is not purely linear, but varies after a cut off limit.

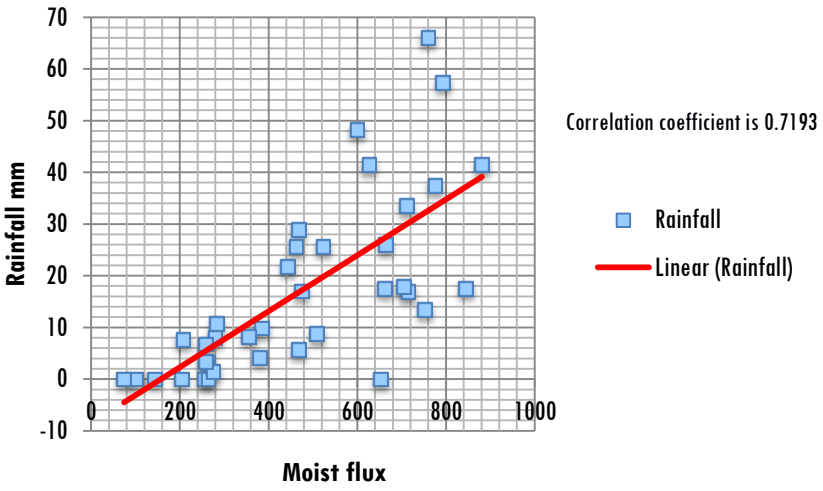

Fig. 3.27: Correlation between Moist flux and Rainfall

3.5.22 Integrated Angular Momentum for both Westerly and Easterly about the Boundary between westerly and Easterly

During the data analysis, an attempt was made to find the angular momentum of unit volume of air at each level, both in Westerly and Easterly, about the boundary level separating the two zonal winds, by taking the product of momentum of unit volume of air at a level and the perpendicular distance of this air parcel to the boundary (Fig. 3.28). And finally, this quantity is integrated for all the levels in both the winds.

The total **Angular Momentum** is

$$L = \sum \rho * U * (\hat{Z} - Z) \qquad \text{- (3.5)}$$

where **ρ** – density of air at the level **z**, moving at the zonal wind speed **u** and $\hat{\mathbf{z}}$ is the height of the boundary level between Westerly and Easterly from the ground level.

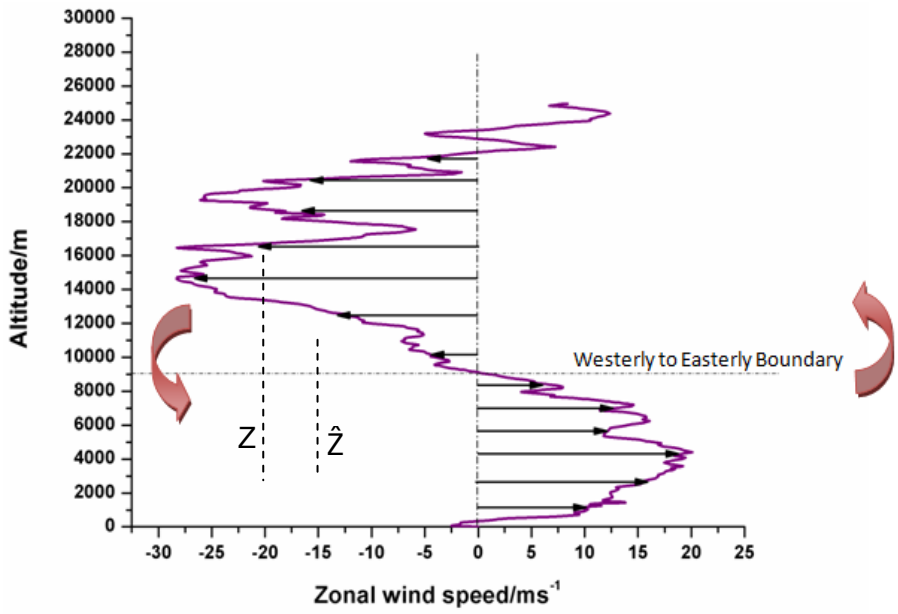

Fig. 3.28: Zonal wind speed variation with altitude, representing the factors used to calculate the angular momentum.

On evaluating the possibility of any impact of this Angular Momentum upon the intensity of Rainfall (Fig. 3.29, and Table 3.3), it was found that a strong correlation did exist in between them.

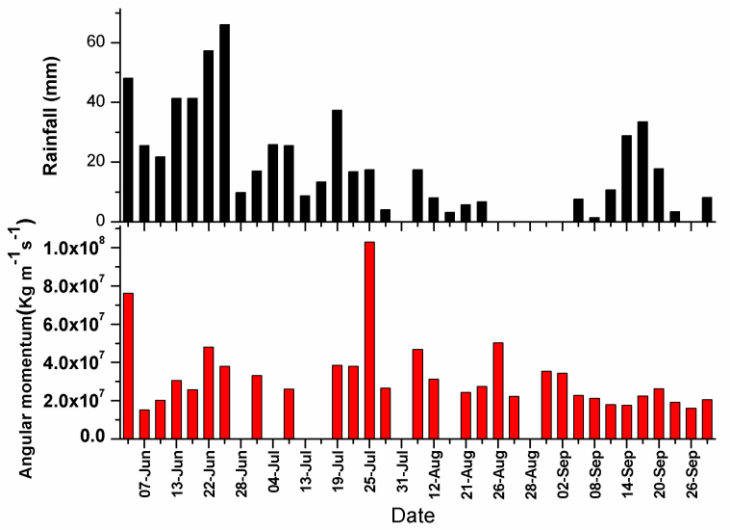

Fig. 3.29: Comparison between Ang. Momentum and Rainfall intensity (Correlation between Ang. Momentum and Rainfall = 0.76).

Table 3.3: The angular momentum calculated on every ascending day with the Era-interim data of vertical velocity of air at the 500hPa level and the corresponding Rainfall.

Date of ascent	Angular Momentum/10^7	Vertvel (w) of air at 500hPa/cms^{-1}taken from Era-interim	Rainfall/cm
01-Jun-13	2.3393152	1.293740495	4.82
07-Jun-13	1.6228135	3.627644099	
10-Jun-13	1.0240618	0.630406921	2.18
13-Jun-13	0.9740155	0.626243583	4.14
19-Jun-13	2.2166591	3.141349744	4.14
22-Jun-13	3.0218012	2.203698562	5.73
25-Jun-13	2.7839	2.516958005	6.6
01-Jul-13	0.886627	0.156777606	1.7
07-Jul-13	1.0196656	-0.315	2.56
13-Jul-13	0.9740155	-2.348	0.87
19-Jul-13	1.3685527	2.8242	3.74
22-Jul-13	1.2881127	2.3651	1.68
25-Jul-13	1.3041041	0.9428	1.75
28-Jul-13	1.1326184	0.9411	0.41
03-Aug-13	1.13	1.5695	1.75
12-Aug-13	0.945	0.3915	0.8
21-Aug-13	0.979	-1.965	0.57
24-Aug-13	1.02	0.7102	0.67
26-Aug-13	0.909	0.3941	0
27-Aug-13	1.01	0.6303	0
30-Aug-13	1.47	2.5212	0
02-Sep-13	1.28	0	0
05-Sep-13	0.858	2.26	0.76
08-Sep-13	0.735	0.815	0.14
11-Sep-13	0.8	1.4	1.07
14-Sep-13	0.767	-0.946	2.89
17-Sep-13	0.948	1.56	3.35
20-Sep-13	1.32	1.184	1.78
23-Sep-13	0.854	0.792	0.34
26-Sep-13	0.696	-1.18	0
29-Sep-13	0.798	-0.157	0.82

Angular Momentum, Vertical velocity and Rainfall.

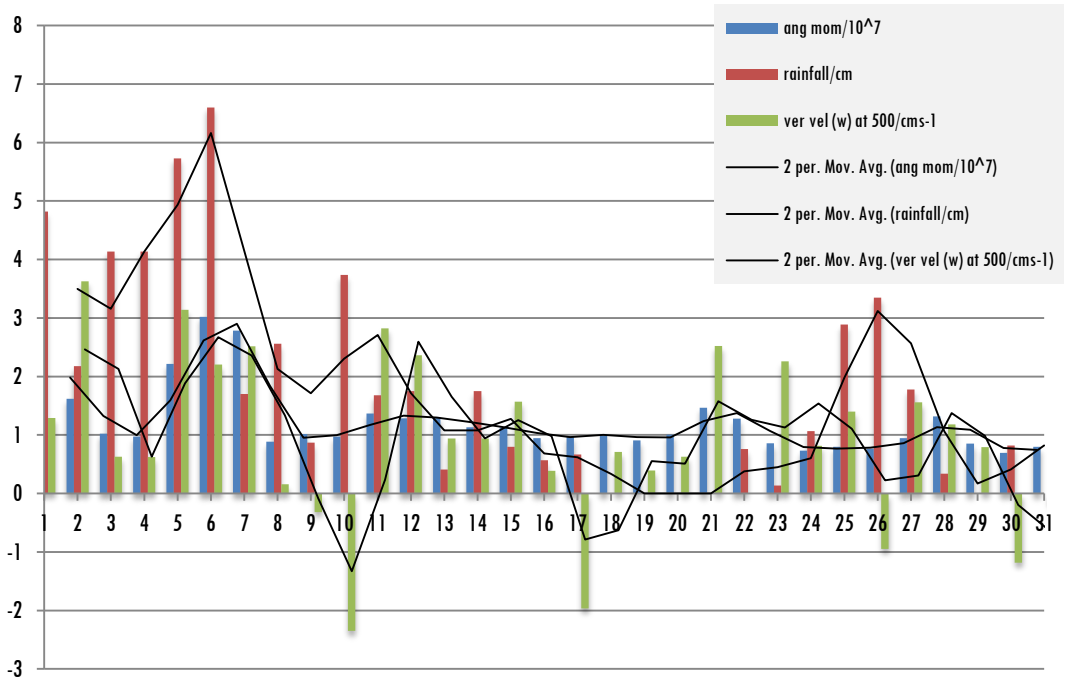

Fig. 3.30: Temporal variation of Ang. Momentum, Vertical velocity and Rainfall.

It is seen that the correlation between angular momentum and vertical velocity is 0.54, while that between angular momentum and rainfall is 0.76. A weak correlation (0.44) was found between vertical velocity and rainfall (Fig. 3.30).

3.5.23 Comparing Cloud top pressure, Cloud fraction, OLR and Angular Momentum

To make further verification upon the validity of determining angular momentum, Era-interim data on Cloud fraction, Cloud top pressure and OLR are taken and these properties do support the results (Fig. 3.31). On those days registering high value in angular momentum the OLR is less than 200 Wm^{-2}; Cloud fraction above 0.8 and Cloud top pressure is just above 200 hPa showing higher level of convection (Table 3.4).

Table: 3.4: Details of Angular momentum and cloud characteristics

2013 - Date	Angular Momentum/10^6	OLR/Wm^{-2}	Cloud fraction	Cloud-top Pressure/hPa
07/06	16.2281	162	0.873	227
13/06	9.7402	192	0.808	273
22/06	30.218	158	0.891	209
28/06		145	0.917	206
01/07	8.8663	173	0.85	247
04/07		187	0.713	233
07/07	10.1967	197	0.65	231
13/07	9.7402	180	0.778	250
16/07		142	0.881	193
22/07	12.8811	188	0.809	291
25/07	13.041	228	0.615	373
31/07		183	0.631	191
03/08	11.3	256	0.436	587
12/08	9.45	197	0.639	231
15/08		266	0.181	451
21/08	9.79	241	0.371	324
24/08	10.2	273	0.231	462
26/08	9.09	252	0.372	399
27/08	10.1	236	0.414	308
28/08		179	0.708	220
30/08	14.7	226	0.483	319
02/09	12.8	174	0.845	240
08/09	7.35	186	0.846	276
11/09	8	227	0.747	441
17/09	9.48	162	0.869	215
20/09	13.2	252	0.278	336
26/09	6.96	267	0.257	468
29/09	7.98	243	0.393	319

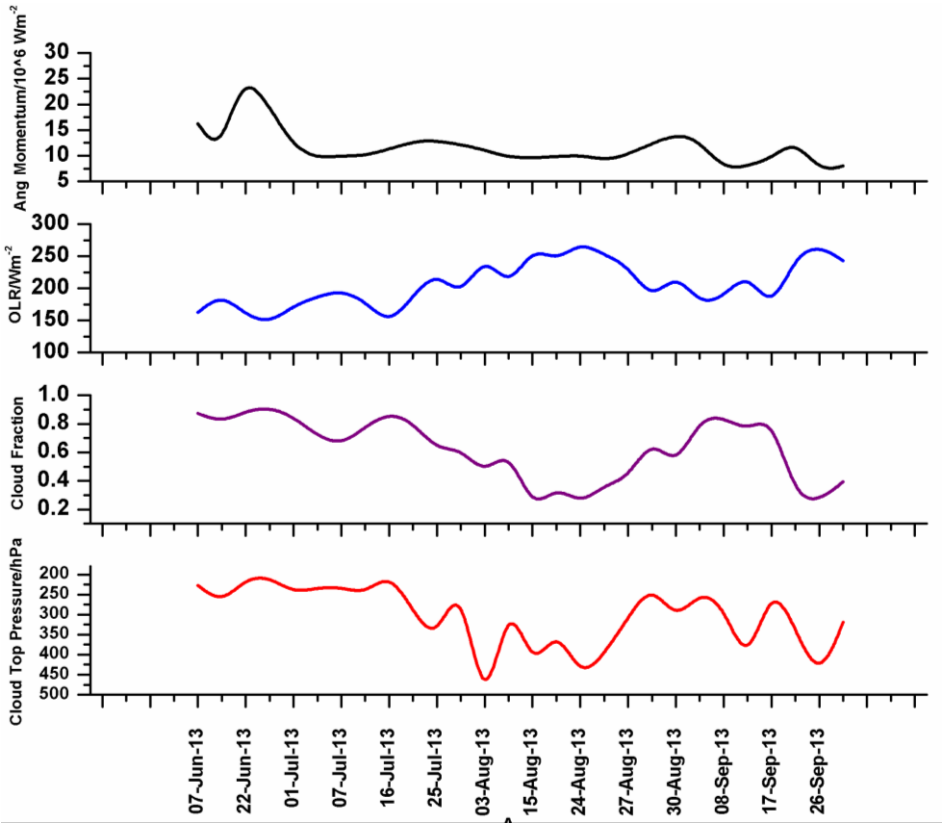

Fig. 3.31: Temporal representation of all four properties – Angular Momentum, OLR, Cloud Fraction and Cloud top Pressure**.**

3.6 Conclusion

The Indian Summer Monsoon 2013, observed over its entire period of active presence from 21st May to 29th September, using the Radiosonde ascents, brought out a significant understanding of the atmospheric features over Cochin. The zonal wind associated with LLJ and TEJ are studied by assessing their core levels, core speeds, shear across their core levels and change- over boundary from westerly to easterly. Also, the Momentum flux, Kinetic energy flux and Moisture flux, brought in by the westerly are calculated and their impact over the rainfall intensity are measured separately. While the analysis upon core levels and its speed over rainfall intensity provided a low correlation- yet not negligible, the moisture flux gains the highest impact over the rainfall. Another factor found influencing the rainfall is the total angular momentum taken over the entire height of the westerly. As 2013 was a good monsoon year, with a series of observations, a good data bank is developed for further analysis.

****

Chapter

4

Characteristics of Low Level Jet Stream and its Relation to Rainfall during Two Contrasting Monsoon Years over Kochi

Contents

4.1 Introduction

The monsoons over India are a much anticipated weather event and their normal onset and distribution are a pre-requisite for the nation's sound economy. Forecasting of monsoons therefore foreruns every policy making initiative in India. Every year, an official forecast on the onset, amount and distribution of rainfall is issued by India Meteorological Department (IMD). Over the past several years, forecasts have generally been successful, yet efforts are on for improving the efficiency. Monsoons have attracted numerous scientific studies and these have generally improved our knowledge of their dynamics; still, underlying mechanisms governing the onset, distribution, intensity, variability need better understanding. The existing large biases in simulation of monsoon behaviour by climate models are an obvious consequence of our limited understanding of monsoon characteristics (Bollasina and Ming 2013; Sandeep and Ajaya Mohan 2014).

One of the main components driving the monsoon rainfall is the monsoon low level jet (MLLJ). It was first observed over the Peninsular India by Joseph and Raman (1966) during the Southwest monsoons. Typically, cross-equatorial in nature, these strong jets emanate as trade wind easterlies in the Southern Indian Ocean which upon crossing the equator as southerly, turns into westerlies over the Arabian Sea before entering the Indian sub-continent (Findlater1969). Since its

discovery, the core of the jet was found lying at 850 hPa with speeds of 20-30 m s^{-1} (Joseph and Sijikumar 2004); however, recent study by Roja Raman et al. (2011) over Southern peninsular India using high resolution GPS radiosonde observations, report the mean core lying at 710 hPa. The moisture influx into the sub-continent via MLLJ has strong bearing on monsoon rainfall. In addition, MLLJ has been observed to have strong inter-annual and intra-seasonal variability (Webster et al. 1998; Krishnamurthy and Shukla 2000; Goswami and Ajaya Mohan 2001). Therefore, MLLJ being a dynamical parameter, its variations can directly be linked to the variability of the Indian summer monsoon.

The Southwest monsoon enters the Indian mainland through Kerala, the southernmost state of India and Cochin in Kerala is popularly known as the gateway of monsoon. Kerala lies flanked by the Western Ghats on its East and the Arabian Sea on its West. Moisture laden Westerlies from Arabian Sea with wind speeds of 15 to 22 m s^{-1} are decelerated by the massive Western Ghats leading to precipitation. Hence, for any studies on monsoon characteristics especially with reference to MLLJ, Cochin would be an ideal location.

There are not many studies on monsoon that look into the characteristics of MLLJ at the region of its onset. In this paper we study the MLLJ characteristics for two contrasting monsoon years, the strong monsoon year of 2013 and deficient monsoon year of 2015. The all India summer monsoon rainfall (June-September) for the year 2013 was 925 mm which is 6.3% in excess of the normal average rainfall. The monsoon season of 2013 is unique for its rapid advance over the entire country. A large portion of the country received excess to normal rainfall with fewer regions recording a deficiency in rainfall. During 2015, the country received a rainfall of 760 mm against a normal average of 887 mm during the monsoon period of June 1 to September 30. Overall, the rainfall was 14% lesser. Deficiency in rain was experienced in almost 40% of the country with near drought situations in parts of UP, Maharashtra and Odisha.

Through a series of dedicated radiosonde observations taken during the monsoon periods of 2013 and 2015, we study the characteristics and dynamics of MLLJ and its impact on rainfall over Cochin. Additionally, the MLLJ modulated

parameters such as momentum flux, kinetic energy flux and moisture flux and their impact on the rainfall amount is also investigated. Furthermore, we also examine whether the variability in rainfall observed over Cochin can sufficiently explain the large-scale distribution of monsoon convective activity over the entire Indian summer monsoon region. For this purpose, satellite observations of upper tropospheric humidity (UTH) were analyzed for the years 2013 and 2015.

The chapter is structured as follows: Section 2 gives the description of data used in this study. Section 3 gives the methodology. Section 4 provides the results and discussion and finally Section 5 presents the summary and conclusions.

4.2 Measurements

4.2.1 Radiosonde data

Data from a dedicated GRAW radiosonde launch campaign conducted during June to September for the years 2013 and 2015 have been used. A DFM 09 model of GRAW radiosonde has been used. The profiles of temperature, humidity, wind speed and wind direction from radiosondes have been used to derive the various MLLJ parameters. The radiosonde launch site is located at Cochin (10.04◦N; 76.32◦E), which is also the site where a novel 205 MHz wind profiling radar has been set up (Kottayil et al. 2016). The rainfall data was also procured for the location during the radiosonde campaign period.

4.2.2 Satellite data

The upper tropospheric humidity derived from 183±1 GHz water vapour channel from the Microwave Humidity Sensor (MHS) sensor onboard the NOAA (National Oceanic and Atmospheric Administration)-18 satellite for the period June-September for the year 2013 and 2015 have been used. The method used for deriving UTH from the brightness temperature of 183±1 GHz channel is described in Buehler and John (2005). Use of microwave measurements has the advantage of providing the UTH distribution under all sky conditions (Buehler et al. 2007, 2008; John et al. 2011). The daily UTH is gridded onto 0.5◦× 0.5◦ latitude–longitude grids . This UTH data finds application in several atmospheric studies (Kottayil et al. 2012, 2013; Kottayil and Satheesan 2015).

4.3 Methodology

The profiles of wind speed and direction obtained from GRAW radiosonde have been used to derive the zonal wind and the various MLLJ parameters such as core speed, core height and MLLJ depth. A zonal wind speed exceeding 8 ms^{-1} is considered as the MLLJ core speed and its corresponding height is recorded as the MLLJ core height. MLLJ depth is determined from radiosonde zonal wind profiles and it is the vertical extent of the westerly winds. The other parameters like moisture flux, momentum flux and kinetic energy flux are derived as follows.

Moisture flux is derived using the following formula,

$$\int_{Z1}^{Z2} \rho q u dz \qquad \text{- (4.1)}$$

where ρ is the density of air in kgm−3, q is the specific humidity in kgkg−1, u is the zonal wind in ms−1, z1 and z2 are the lower and upper height of the Westerly.

Momentum flux is given as

$$\int_{Z1}^{Z2} \rho u dz \qquad \text{- (4.2)}$$

Kinetic energy flux is derived using the following equation,

$$\int_{Z1}^{Z2} \frac{1}{2} \rho u^2 dz \qquad \text{- (4.3)}$$

4.4 Results and Discussion

In this section, we first analyze the changes in the low level jet core speed and core height, for the two contrasting monsoon years of 2013 and 2015. This is followed by an analysis of the variations in the depth of the monsoon westerlies, moisture flux, momentum flux and kinetic energy flux which are the parameters modulated by the strength and depth of the monsoon low level jet. The influence of MLLJ parameters on the observed rainfall amount over Cochin is further investigated, explicitly quantifying the variance in rainfall amount as explained by the MLLJ parameters. We also assess the changes in the convective activity over the Indian summer monsoon region and the Pacific during the two contrasting monsoon years using satellite

datasets of upper tropospheric humidity. The rainfall amount observed over Cochin is related to UTH observed over the whole Indian subcontinent to see whether the variability in rainfall observed over Cochin is in conjunction with the large scale convective activity associated with summer monsoon.

4.4.1 Variations in MLLJ parameters

Fig. 4.1 shows the monsoon low level jet core wind speed and height observed during the years 2013 and 2015. It is clear from the figure that a strong (weak) monsoon of 2013 is characterized by strong (weak) zonal wind speed and elevated (lowered) core height. The MLLJ core speed varies between 9 to 23 ms^{-1} during the observation period of 2013 whereas the observed range in MLLJ core speed is only 8-14 ms^{-1} during the weak monsoon year of 2015.

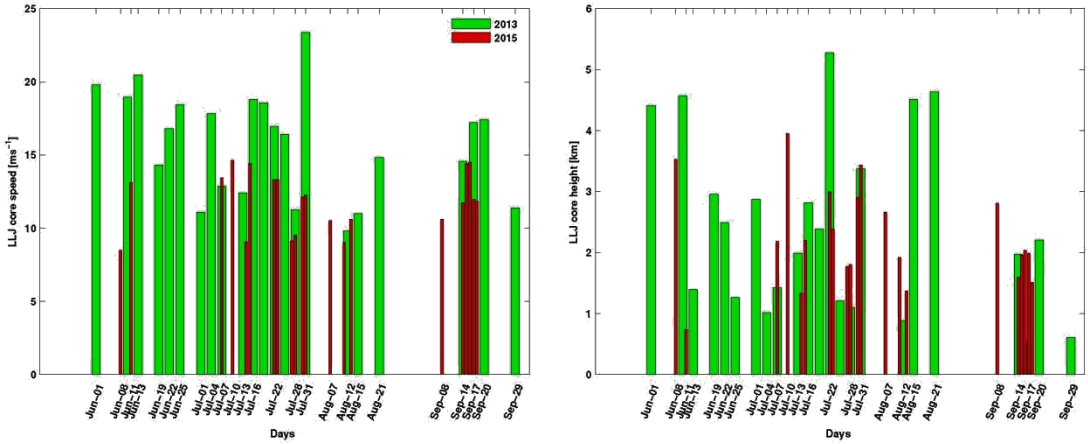

Fig 4.1: Monsoon low level jet core wind speed and height observed during the years 2013 and 2015

It can be seen that the MLLJ core height shows remarkable differences between 2013 and 2015. The core height changes from a minimum value of 0.5 km to maximum of 5.2 km during 2013, while it lies within a range of 0.75 to 3.9 km in 2015. Periodic variations in MLLJ core speed and height in the order of 30–50 days are observed during the strong monsoon year of 2013. These periodic variations in MLLJ core speed and height can be associated to the intra-seasonal variability in the convective band linked to the Indian summer monsoon (Sikka and Gadgil 1980). A strong (weak) MLLJ implies an enhanced (diminished) rainfall activity over the Indian subcontinent (Webster et al. 1998). It is to be noted that this intra-seasonal variability in MLLJ core speed and height is not quite discernible for the weak monsoon year of 2015.

A noteworthy observation here is that the monsoon MLLJ core height variation is not uniformly distributed throughout the Indian subcontinent as suggested by Joseph and Sijikumar (2004). Using reanalysis data Joseph and Sijikumar (2004) had found that the mean MLLJ core height is at 850 hPa (1.7 km) throughout the Indian subcontinent. The mean MLLJ core height observed over Cochin during 2013 and 2015 is 2.03 and 2.2 km respectively. Roja Raman et al. (2011) using high resolution radiosonde had shown that on an average the zonal wind maximum exists at 710 hPa which is equivalent to a height of about 2.8 km. The radiosonde launches were mainly during the evenings and this region has a high convective activity during the time. It is hence possible that the convection could actually be elevating the core height.

The variations in MLLJ core depth (Westerly depth), moisture flux, momentum flux and kinetic energy flux for the years 2013 and 2015 are shown in Fig 4.2. The depth of westerlies is higher during the monsoon period of 2013 than that of 2015 and does not show a marked intra-seasonal variability as observed for MLLJ core speed and core height. The average value of the depth of westerlies for 2013 and 2015 are 7.25 and 6.13 km, respectively. The westerly depth has a strong bearing on the derived flux parameters as evidenced from the figure where they are seen to scale more or less with the depth of westerly.

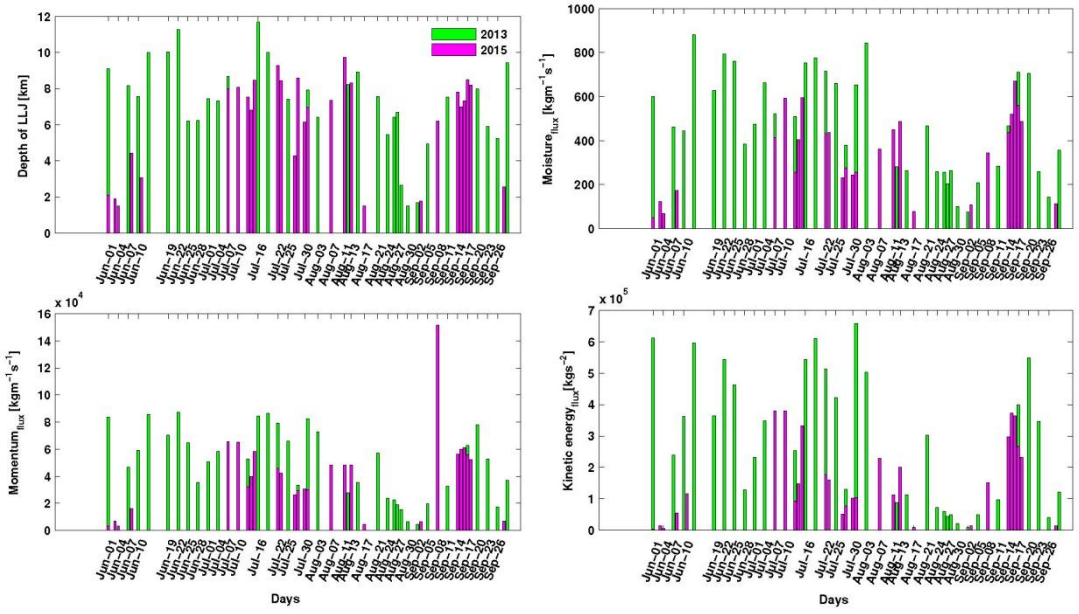

Fig 4.2: The variations in MLLJ core depth (Westerly depth), moisture flux, momentum flux and kinetic energy flux for the years 2013 and 2015.

The moisture flux observed during the strong monsoon year ranges from a minimum of 74 $kgm^{-1}s^{-1}$ to maximum of 884 $kgm^{-1}s^{-1}$, while it is 50 and 671 $kgm^{-1}s^{-1}$, respectively for 2015. The momentum and kinetic energy fluxes also show very high values for 2013 as compared to the weak monsoon year of 2015. The maximum and minimum values of momentum flux observed for 2013 are 87326 and 4590 $kgm^{-1}s^{-1}$ respectively, whereas they are 151651 and 3182 $kgm^{-1}s^{-1}$ for the year 2015. The kinetic energy flux is seen to fluctuate between 8641 and 657337 kgs^{-2} during 2013, while its upper and lower limit for 2015 is 380884 and 2852 kg s^{-2} respectively.

4.4.2 Relation between MLLJ parameters and rainfall

The relationship among rainfall, moisture flux, momentum flux, kinetic energy flux observed over Cochin during the campaign period is shown in Fig 4.3. Note that this relationship is drawn from the combined measurements of the years, 2013 and 2015. Though all these parameters affect rainfall, it is the moisture flux that has the strongest influence on the rainfall. The observed correlations of rainfall to moisture flux, momentum flux and kinetic energy flux are 0.71, 0.51 and 0.59, respectively. The best fit to the relationship between rainfall and moisture flux is given by an exponential fit. This can be given as Rain = 3.136 × exp (0.003077 × moisture flux).

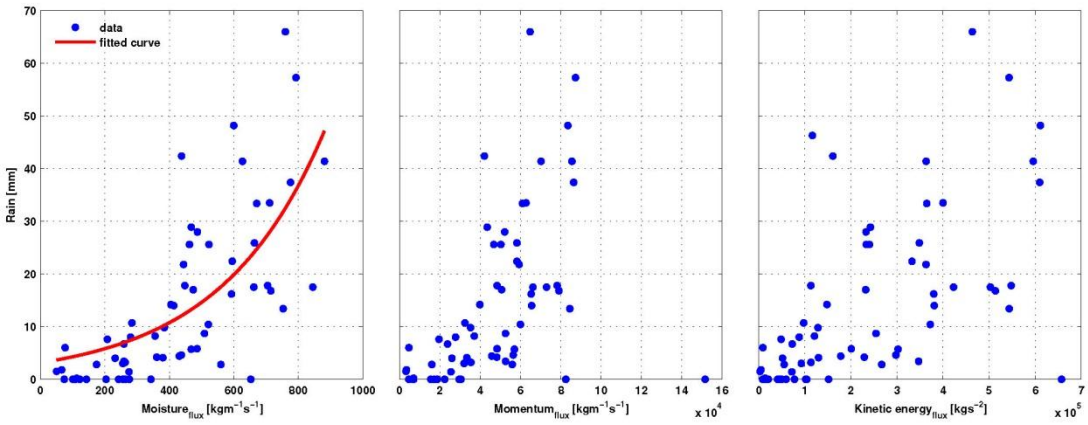

Fig 4.3: The relationship among rainfall, moisture flux, momentum flux, kinetic energy flux observed over Cochin during the campaign period

The moisture flux in turn is modulated by other MLLJ characteristics, such as the depth of MLLJ, its speed etc. It is clear from our analysis that when a weakening of the low level jet occurs, there is reduction in the moisture flux which consequently decreases the rainfall. An interesting inference is that the moisture flux has to attain a threshold limit before it can significantly increase the rainfall owing to their exponential relationship.

With an objective of quantifying the relationship of the various MLLJ parameters to rainfall, a multiple linear regression has been performed. The regression coefficients (Table 4.1) are indicative of rainfall sensitivity to changes in the MLLJ parameters. It is obvious that the most contribution towards rainfall comes from the moisture flux, followed by the monsoon low level jet core speed. The other parameters have minimal contribution to the rainfall amount observed over Cochin. These results reassert the role of monsoon low-level winds over the Arabian Sea which transport moisture to the Indian subcontinent thereby modulating the Indian summer monsoon rainfall.

Table 4.1: Regression coefficients and LLJ characteristics, associated flux and their respective contribution towards rainfall

Parameters	Regression coefficients	Mean value	Rainfall contribution (mm)
MLLJ depth	-7.05×10^{-5} mm/km	6.7 km	0.47
Core speed	0.7818 mm/m s^{-1}	13.91 m s^{-1}	10.88
Core height	-4.59×10^{-5} mm/km	2.33 km	0.10
Moisture$_{flux}$	0.0859 mm/kg m^{-1} s^{-1}	416.3 kg m^{-1} s^{-1}	35.75
Momentum$_{flux}$	-6.98×10^{-5} mm/kg m^{-1} s^{-1}	4.5×10^{4} kg m^{-1} s^{-1}	3.21
KE$_{flux}$	-3.32×10^{-5} mm/kg s^{-2}	2.29×10^{5} kg s^{-2}	7.21

4.4.3 Relation between upper tropospheric humidity and rainfall

In the tropics, the upper tropospheric relative humidity and convection are interrelated. So-den and Fu (1995) have shown that the enhancement of tropical convection is associated with an increased upper tropospheric relative humidity. An analysis of the distribution of upper tropospheric humidity over the Indian subcontinent and the adjoining oceanic regions can thus provide an insight into the changes in the convective activity associated with the Indian summer monsoon.

The June-September mean upper tropospheric humidity for the years 2013 and 2015 is shown in Fig. 4.4. This illustration of the large scale distribution of the UTH clearly shows the differences in the convective activity associated with strong and weak monsoon years. When monsoon was very strong during 2013, the core convective activity is spread over the Indian subcontinent as evident from the high UTH values. The Walker circulation was also strong during this year as seen from the high humidity values over the Maritime continent lying in the tropical warm pool region. The impact of El Nin˜o on the 2015 Indian summer monsoon is clearly visible from the figure. The convective cloud band which otherwise would bring wide-spread rain over Indian subcontinent is seen to have drifted eastward due to the El Nin˜o condition over Pacific. A weakening of Walker circulation as well as subsequent spread of the convective activity towards East Pacific is also apparent from the figure.

The daily average upper tropospheric humidity over the Indian subcontinent (5–20°N; 70–80°E) during the monsoon years of 2013 and 2015 are shown in Fig. 4.5. An intra-seasonal variability in UTH with a periodicity of 30-60 days is especially seen for the year 2013 (Fig. 4.6). An earlier study by Xavier et al. (2010) also depicts an intra-seasonal variability in UTH associated with the Indian summer monsoon. The rainfall observed during the days of the radiosonde launch campaign is also shown in figure as vertical bars. An interesting similarity is apparent in the patterns of rainfall and upper tropospheric humidity (Fig. 4.5). When the convective activity is stronger as depicted by the elevated values in the upper tropospheric humidity over the Indian subcontinent, corresponding rainfall also grows stronger over Cochin. In contrast, a weak convective activity (low UTH values) shows meagre rainfall over Cochin. This is true irrespective of whether monsoon is strong or weak.

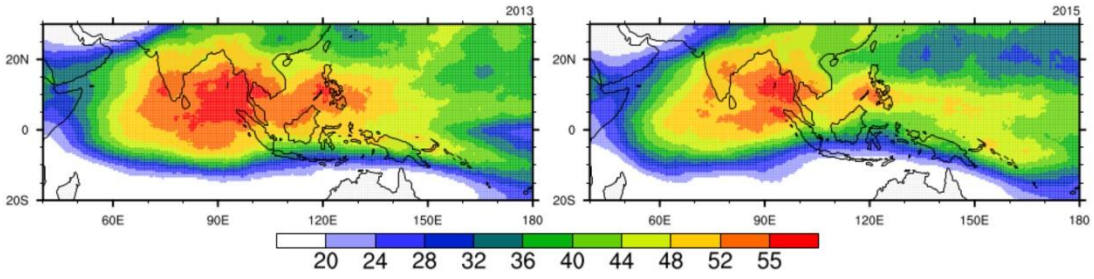

Fig 4.4: The June-September mean upper tropospheric humidity for the years 2013 and 2015

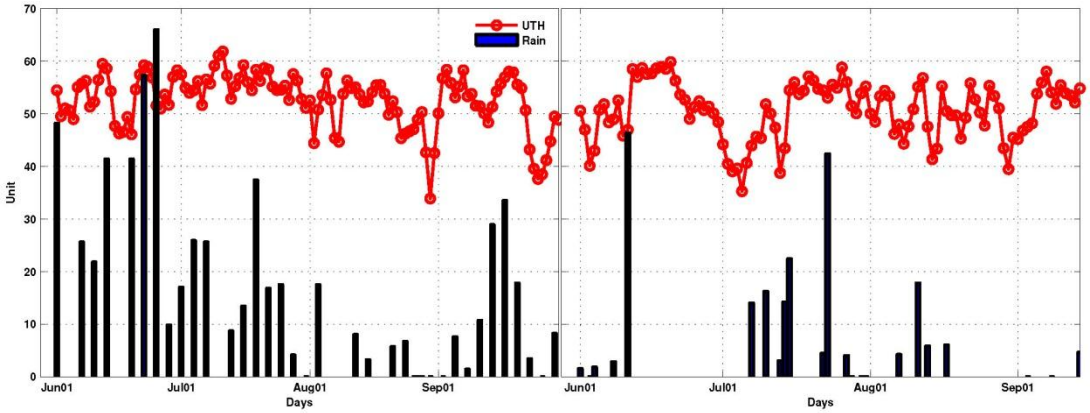

Fig 4.5: The daily average upper tropospheric humidity over the Indian subcontinent (5–20°N; 70–80°E) during the monsoon years of 2013 and 2015

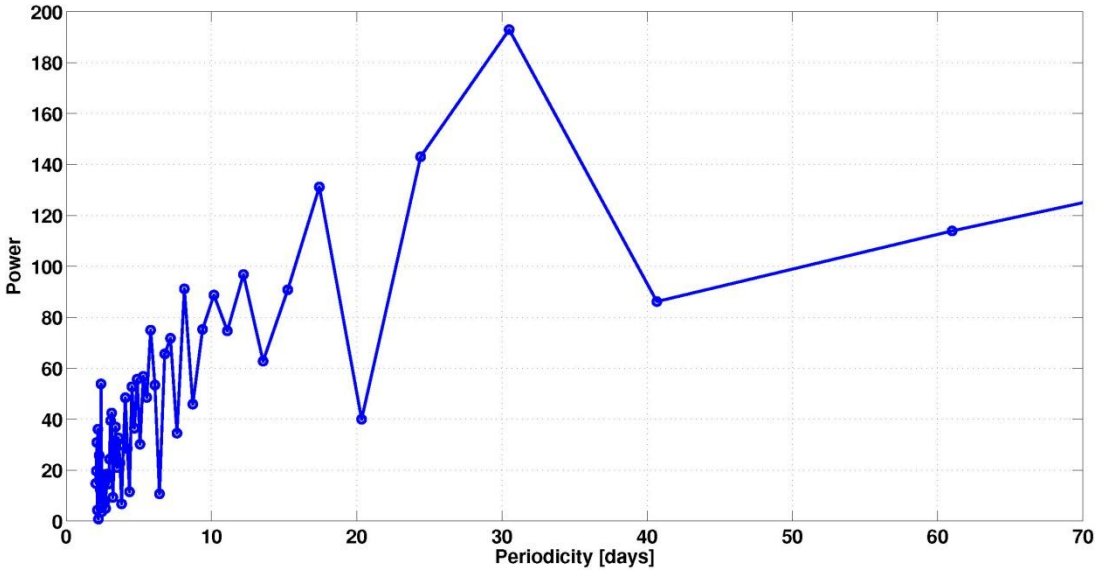

Fig 4.6: Power spectrum of the UTH for JJAS-2013.

4.5 Summary and Conclusions

The monsoon low level jet characteristics over Cochin for two distinct monsoon years of 2013 and 2015 is studied using high resolution radiosonde measurements. 2013 for India was a year of strong monsoon while 2015 was short of normal monsoons. The monsoon low level jet core speed, core height and MLLJ depth vary significantly between strong and weak monsoon years. On an average, the monsoon low level jet's core height remains at 2 km. The MLLJ core height and speed shows a periodic 30–60 day oscillation during the strong monsoon year of 2013. The MLLJ depth, moisture, momentum and kinetic energy fluxes were significantly higher in 2013 as compared to 2015. The westerly depth has a strong

impact on moisture, momentum and kinetic energy fluxes. The effect of MLLJ parameters on observed rainfall over Cochin has been worked out through multiple linear least square regression (Fig 4.6). It was observed that the moisture flux has the strongest influence on rainfall followed by MLLJ core speed. It is also found that the observed rainfall can be related to moisture flux through a first order exponential relationship.

We analyze the reason for the weakening of the monsoon in 2015 by studying the convective activity through the use of satellite derived upper tropospheric humidity. It is inferred from the analysis that the moisture source for rainfall had drifted eastward from the Indian sub-continent due to the prevalent El Nino conditions over the Pacific. It is also observed that the convective activity over the Indian sub-continent is mirrored in the rainfall pattern observed over Cochin.

The study of characteristics of monsoon low level jet and its relationship with rainfall over the monsoon onset region using high resolution radiosonde data for contrasting monsoon years is being done for the first time. Through this study, we trace the effect of MLLJ and its parameters on monsoon rainfall. When resorting to the use of models for rainfall prediction, the biases of MLLJ can determine the accuracy of prediction. Moreover, detailed regional studies of this kind would help in diagnosing the errors in the models which could eventually enhance the prediction of Indian summer monsoon.

****

Chapter

5

Estimation of Vorticity and Divergence using Triangular Method and its Association with Monsoon Rainfall

Contents

5.1 Introduction

Kochi, being the Gateway of Indian Summer Monsoon, presents a predictive set of features in foreseeing the character of forthcoming monsoon all over India. The wind pattern and the cloud coverage provide a general outlook of the onset of monsoon. A detailed observation of features like intensification of Low Level Jet, the divergence pattern, vorticity, temperature and the humidity profiles etc. are predictive parameters for the intensity of the forthcoming monsoon rainfall. Most of these parameters can be derived with Radiosonde experiments.

Such an observation was conducted continuously during the monsoon season in 2013 and a limited study was undertaken during the monsoon period of 2014 as well as 2015. In association with Space Physics Laboratory (SPL), Vikram Sarabhai Space Centre, Thiruvananthapuram, simultaneous observations from three stations (Kochi, Thiruvananthapuram and Coimbatore) was conducted in 2013 and the data is used for analysis to understand the temporal and spatial variation of zonal wind, humidity, temperature, vorticity and divergence.

Among the three stations chosen for the comparative study, Coimbatore lies on the leeward side of Western Ghats and generally receives very less amount of annual rainfall (< than 224 cm). The other two stations are Kochi and Thiruvananthapuram, both being coastal stations. Moisture laden air mass driven by the westerly over the hilly terrain of Western Ghats, undergoes cooling and produces copious precipitation. The

cool air ascending over the mountain and descending on the other side, loses its water content and becomes dry. Hence a rain shadow region is developed over the leeward side of the mountain (Anu and Mohankumar, 2004). Kochi and Thiruvananthapuram are situated at the southern half of Kerala, showing distinct behavior in south west monsoon period because southern Kerala is in the anticyclonic shear zone of LLJ while northern Kerala is in the cyclonic shear zone. Kochi is very much influenced by this cyclonic vorticity over the northern side of LLJ (Krishnamurthy, 1985) and hence its monsoon characteristic is different from that of Thiruvananthapuram.

5.2 Objectives

The major objectives of the present chapter of the Thesis are (i) to estimate the vorticity by triangular method using Radiosonde and (ii) to understand the diurnal and spatial variation of monsoon parameters.

5.3 Data used

i. ***Radiosonde Experiment:***GPS-sonde provided pressure, temperature, humidity, wind speed, wind direction, position of the radiosondeetc, in every 5 s, during the ascent of the balloon. Using this data, the zonal and meridional wind speeds are calculated and the study over the core heights and core speed of the Westerlies and Easterlies are conducted. From the temperature profile the tropopause height and the lapse rate within the tropopause are assessed.

ii. ***ERA-interim data****:* The reanalysis data for the zonal wind speed, for the same experimental dates, was downloaded from ECMWF at a resolution of $0.25^{\circ} \times 0.25^{\circ}$, for the level 850hPa, over the region 8 – 15 N and 75 – 80 E, covering the three stations.

iii. Rainfall data from India Meteorological Department*:* Daily mean rainfall data provided by India Meteorological Department was collected from the Daily Weather Report.

iv. NOAA gridded Data*:* Using this data the outgoing long-wave radiation (OLR) is examined during the same period. It is known that OLR should be well below 200 Wm^{-2} in order to set a proper convective system.

v. Satellite data*:* Satellite image over the region, during the period of observation, is analyzed to assess the persisting weather condition.

5.4 Methodology

(i) *Radiosonde Experiment:*

The launching of balloons carrying GPS sonde, conducted simultaneously from all the three stations – Thiruvananthapuram (Lat 8.85˚N: Lon 76.94˚E), Kochi (Lat 9.93˚N: Lon 76.26˚E) and Coimbatore (Lat 11.01˚N: Lon 76.96˚E), starting from 11:30 IST on 26th August to 05:30 IST on 29th August, with a six hour interval, was organized and monitored by Department of Atmospheric Sciences (CUSAT) and Space Physics Laboratory (VSSC).

GPS-sonde provided pressure, temperature, humidity, wind speed, wind direction, position of the radiosondeetc, in every 5 seconds during the ascent of the balloon. It is using this data that the zonal and meridional wind speeds are calculated and the study over the core heights and core speed of the Westerlies and Easterlies are conducted. From the temperature profile the tropopause height and the lapse rate within the tropopause are assessed. From the processed data of the zonal wind speed, the vertical shear across the westerly and easterly core levels is determined.

A study on Divergence and Vorticity over the triangular region formed by the stations Kochi, Thiruvananthapuram and Coimbatore (Fig. 5.1) is done using the radiosonde data of zonal and meridional wind speeds as well as the X and Y components of locations of the stations, with respect to the centroid of the triangular region.

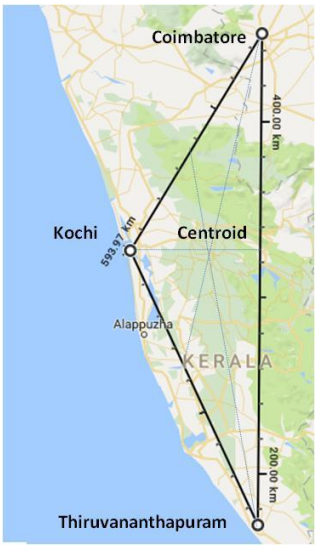

Table 5.1: The X and Y coordinates of the stations are taken with reference to the position of the centroid of the triangular region, shown in the figure.

Location	X	Y
Kochi	-42 km	17 km
Coimbatore	36 km	73.5 km
Thiruvananthapuram	16 km	-148 km

Fig 5.1:Regional Map showing the locations of the three stations

5.4.1 Theoretical Background of estimating vorticity

With three-station data, for zonal wind speed (u_1, u_2, u_3) and meridional wind speed (v_1, v_2, v_3), at the 850 hPa level; location coordinates (x_1, x_2, x_3) and (y_1, y_2, y_3) with respect to the position of the centroid of the triangular region, wind field equations can be formed as,

$$(x_2\text{-}x_1)a + (y_2\text{-}y_1)b = u_2 - u_1 \quad \text{- (5.1)}$$

$$(x_3\text{-}x_1)a + (y_3\text{-}y_1)b = u_3 - u_1 \quad \text{- (5.2)}$$

$$(x_2\text{-}x_1)c + (y_2\text{-}y_1)d = v_2 - v_1 \quad \text{- (5.3)}$$

$$(x_3\text{-}x_1)c + (y_3\text{-}y_1)d = v_2 - v_1 \quad \text{- (5.4)}$$

where $a = \delta u/\delta x$ $b = \delta u/\delta y$

where $c = \delta v/\delta x$ $d = \delta v/\delta y$

Using Cramer's rule (Kreyszig, 1988) the solutions for *a*, *b*, *c* and *d*are calculatedtocomputethe Divergence and Vorticity (Davies and Jones, 1993).

$$a = \frac{\begin{bmatrix} u_2-u_1 & y_2-y_1 \\ u_3-u_1 & y_3-y_1 \end{bmatrix}}{2A} \qquad b = \frac{\begin{bmatrix} x_2-x_1 & u_2-u_1 \\ x_3-x_1 & u_3-u_1 \end{bmatrix}}{2A}$$

$$c = \frac{\begin{bmatrix} v_2-v_1 & y_2-y_1 \\ v_3-v_1 & y_3-y_1 \end{bmatrix}}{2A} \qquad d = \frac{\begin{bmatrix} x_2-x_1 & v_2-v_1 \\ x_3-x_1 & v_3-v_1 \end{bmatrix}}{2A} \quad \text{- (5.5)}$$

where '*A*' represents the area of the triangular network (Gellert et al., 1977) formed by the three stations.

Then, Divergence $\mathbf{D = a + d}$ - (5.6)

Vorticity$\boldsymbol{\xi}$ **= c – b** - (5.7)

5.5 Results and Discussion

Computing the diurnal and spatial variation of various components such as Westerly core speed and core height; Tropical Easterly Jet core speed and core height; surface temperature and Tropopause height, gives a clear picture of how all these variables behaved over these three stations.

Table 5.2: Westerly and TEJ core speed and core height observed over the three stations: Kochi (KCH), Thiruvananthapuram (TVM), and Coimbatore (CMB)

2013		Westerly core speed/ms^{-1}			Westerly core height/m			Tropical Easterly Jet core speed/ms^{-1}			Tropical Easterly Jet core height/m		
Date	Time/IST	TVM	KCH	CMB	TVM	KCH	CMB	TVM	KCH	CMB	TVM	KCH	CMB
26/08	11:30	8.825	7	5.208	2050	1750	550	-81.2	-82.26	-81.64	16050	15350	15050
	17:30		8.123	7.581		2050	750	-81.4	-77.75	-82.47	16150	15850	15450
	23:30	10.44	7.15	6.826	1350	1450	850	-81.65	-70.91	-83.71	16050	15950	14850
27/08	05:30	9.06	6.06	3.4	1250	1550	3850	-82.22		-82.62	15950		14150
	11:30	6.21	5.96	5.02	1150	1350	5150	-79.75	-80.27	-80.84	16350	16450	16250
	17:30	6.27	7.5	6.63	1850	1950	750	-81.06	-80.37	-81.27	15850	15850	16050
	23:30	6.9	6.67	4.83	1450	850	750	-81.43		-83.44	16350		15750
28/08	05:30	8.04	6.04	2.26	1150	1050	550		-79.25	-80.64	15850	15650	15450
	11:30	5.35	4.4	3.87	1450	1050	650	-78.85	-80.35	-81.39	16250	16450	16550
	17:30	7.84	9.06	8.39	1150	850		-82.08	-80.8	-81.16	15250	15550	15750
	23:30	8.06	7.34	7.02	1250	1150	350		-81.17	-82		15650	15450
29/08	05:30	8.97	7.03	2.95	950	550	450	-81.4	-83.75	-81.75	16450	16350	16250

Table 5.3: Surface temperature, tropopause height, and tropopause temperature observed over Kochi (KCH), Thiruvananthapuram (TVM), and Coimbatore (CMB)

2013		Surface Temp/°C			Tropopauseht/m			Tropopause Temp/°C		
Date	Time/IST	TVM	KCH	CMB	TVM	KCH	CMB	TVM	KCH	CMB
26/08	11:30	26	28.8	29.1	16350	16364	17050	-81.2	-82.26	-81.64
	17:30		28.9	28.11	16150	15799	16850	-81.4	-77.75	-82.47
	23:30	25.45	28.5	26.1	16450	16629	16550	-81.65	-70.91	-83.71
27/08	05:30	24.22	25.5	25.76	16350		16550	-82.22		-82.62
	11:30	26.12	29.5	28.76	16050	16433	16450	-79.75	-80.27	-80.84
	17:30		30	29.57	16550	16163	16350	-81.06	-80.37	-81.27
	23:30		26.2	28.08	16350		16250	-81.43		-83.44
28/08	05:30		25.8	25.41		15875	16650		-79.25	-80.64
	11:30	25.94	29.3	28.47	15950	16318	16450	-78.85	-80.35	-81.39
	17:30		28.8	28.78	16450	16474	16450	-82.08	-80.8	-81.16
	23:30	25.91	27.2	24.45		16066	16150		-81.17	-82
29/08	05:30	25.0	26.2	24.72	16350	16124	16350	-81.4	-83.75	-81.75

5.5.1 Diurnal variation of Westerly core speed

The strong cross-equatorial low level jet (LLJ) moving over the Indian subcontinent during the boreal summer monsoon period has its core varying in height and strength due to a number of reasons such as surface friction, differential heating, terrain structure impact and the time of the event observed in a day (Ruchith et al., 2014). The land-sea heating contrast and the topography play major roles in developing the character of LLJ over the coastal belt stations (Winat et al., 1988; Samelson, 1992; Burk and Thompson, 1996) like Thiruvananthapuram and Kochi.

During the campaign period from 26th to 29th August in 2013, it is found that the westerly core speed becomes more than 8 m s^{-1} at Thiruvananthapuram, while at Kochi and Coimbatore it is less than that over Thiruvananthapuram, showing that the westerly is weak (Fig. 5.2). The core speed even comes down to 2 m s^{-1} at Coimbatore, as it is lying on the leeward side of the Western Ghats. The diurnal variation of wind shows similar pattern both at Kochi and Coimbatore with an average value of about 5 m s^{-1}. Even though being coastal stations, Kochi and Thiruvananthapuram do not show any

similar trend while Kochi and Coimbatore being located on opposite sides of Western Ghats, present a similar variation in wind pattern. This can be attributed to i) the latitudinal proximity between the two stations allowing the same band of westerly passing over both stations, and ii) the relative geographical location of Kochi and Thiruvananthapuram with respect to the core of the westerly.

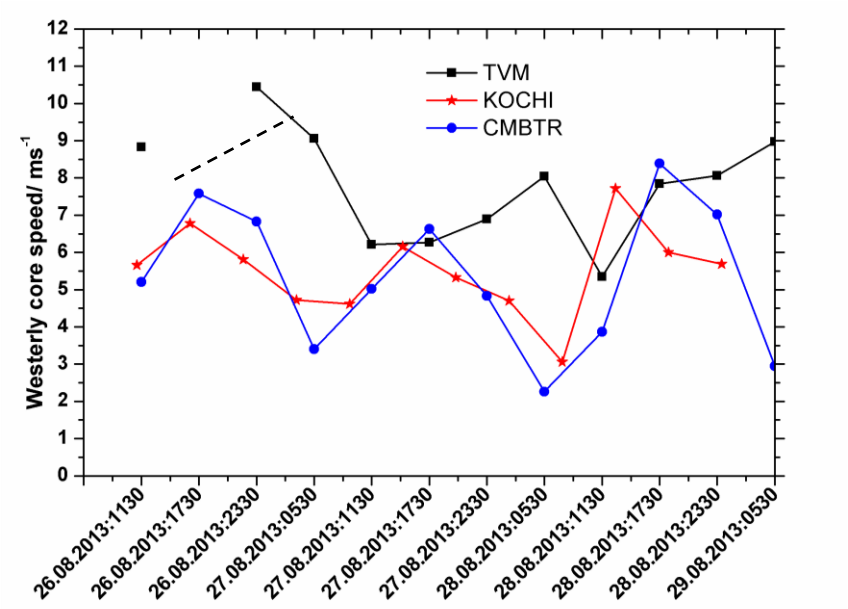

Fig 5.2: Westerly core speed variation at Thiruvananthapuram, Kochi and Coimbatore

5.5.2 Diurnal variation of Westerly core level

Westerly core altitudes at the coastal stations present higher magnitude due to its direct entry from the Arabian Sea, whereas above Coimbatore station lying on the leeward side of the Western Ghats, the core level is low due to the weakening of the wind strength and its interaction with the mountains. Also it can be noted that during night time the core level descends at all stations (e.g., Ruchith et al, 2014). Another feature drawing our attention is the weakening trend of the westerly during the four observing days. The diurnal oscillations of the core height at the coastal stations are found to be of higher amplitude than that at Coimbatore (Weaver and Nigam, 2006). Although we treat all lower tropospheric wind bands as jets, according to the Bonner (1968) classification, certain weak jets cannot be considered as LLJs. Hence the westerly regime over Coimbatore may be considered as non-LLJ.

The westerly core level at Kochi and Thiruvananthapuram maintains a height of 1 to 1.5 km, whereas at Coimbatore it is below 1 km (Fig. 5.3).

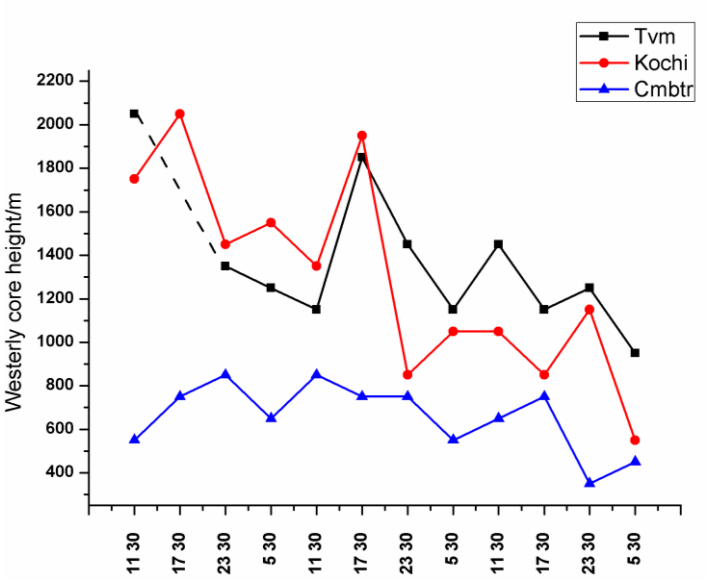

Fig 5.3: Temporal variation of Westerly core height at 3 stations

5.5.3 Diurnal variation of TEJ core speed

The Tropical Easterly Jet (TEJ) core speed above Kochi and Coimbatore are found to be varying in a similar fashion its amplitudes are different (see Fig. 5.4). It should be noted that there exists certain data gap over Kochi due to balloon not reaching up to the height levels of TEJ. The speed of TEJ core goes beyond 50 m s^{-1} on 27th August evening, and by 29th Aug its intensity comes down to 30 m s^{-1}. A continuous weakening of TEJ core speed is observed from 27th to 29th August. This observation is supported by another study by Abish and Joseph (2013).

The TEJ is a strong band of horizontal current of air associated with high vertical wind shear. Referring to World Meteorological Organization (Reiter, 1961) criteria, the TEJ is defined as the zonal wind whose wind speed exceeds 30 m s^{-1} in the upper troposphere.

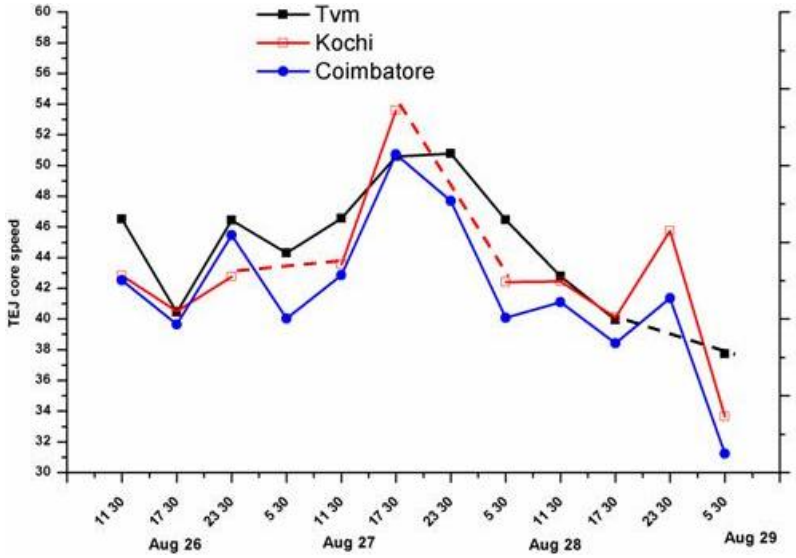

Fig 5.4: Temporal variation of core speed of TEJ

In the month of July, the TEJ is roughly located at two places, one around 10–20°N latitude and 50–85°E longitude at 100 hPa; and 2–14°N latitude and 45–80°E longitude at 150 hPa. During August, the TEJ is located around 10–15°N latitude and 65–80°E longitude at 100 hPa; and 0–10°N latitude and the same longitude at 150 hPa (Rao et al., 2009). In July and August, a slight southward shift is observed in TEJ at 150 hPa (Raman et al, 2009). Both 100 hPa and 150 hPa levels have jet speeds of high magnitude in July and in between, the former level gives the higher strength. It is noted that the TEJ exists between 10° and 15°N during peak monsoon months of July–August (Raman et al, 2009). Also, large diurnal variation in the TEJ over a given location has been reported (Koteswaram, 1958), and there exists large intra seasonal oscillations too (Chen and Yen, 1991).

5.5.4 Diurnal variation of TEJ core level

Earth's atmosphere is encircled with jet streams (over 30 m s^{-1} in upper troposphere and over 15 m/s in lower troposphere), which are narrow horizontal current of air associated with strong vertical wind shear. Jet streams are mesoscale in the cross flow direction (few hundred kilometers) and synoptic scale along the flow direction (may extend for thousands of kilometers around the world) and less than a kilometer thick (Reiter, 1961).

The TEJ is an important parameter of the Asian Summer Monsoon circulation which can be seen in the upper tropospheric levels and completes the

monsoon circulation during the ISM months of June–September (Krishnamurti and Bhalme, 1976). It is reported that the mean jet height is 16.11 ± 0.10 km and the mean wind reversal height is 8.56 ± 0.10 km.

Exempting the problem faced in the continuity of observation at Kochi, from Fig. 5.5, it is seen that all the stations show approximately an average value of 16 km height for the TEJ core level. In general, the diurnal variation is within 15 to 16.6 km height for the core position.

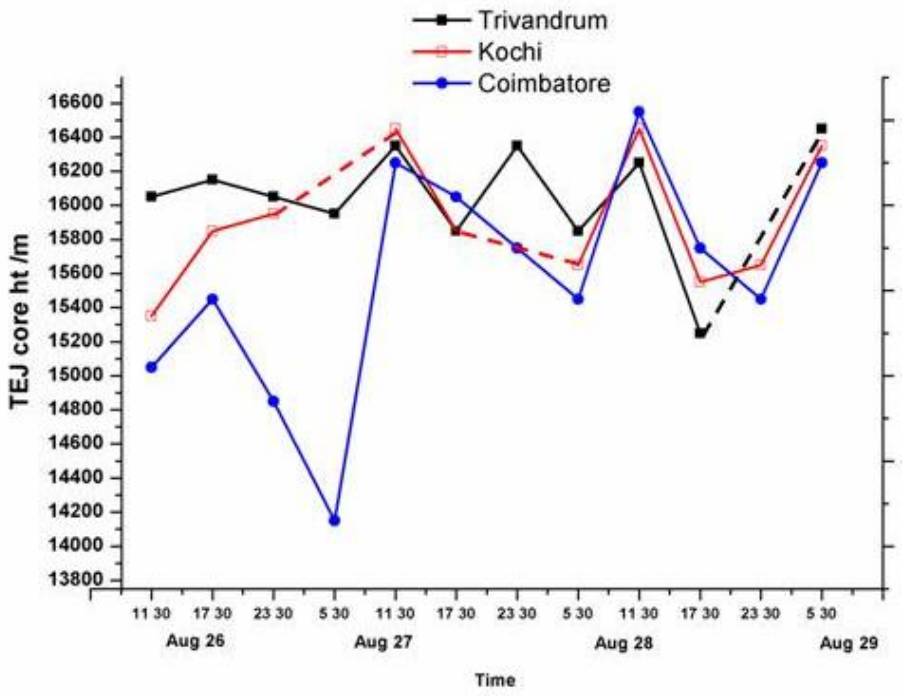

Fig 5.5: Temporal variation of core height of TEJ

5.5.5 Diurnal variation of Surface Temperature

When sea surface temperature (SST) crosses 30°C limit in May, the Arabian Sea turns into a warm pool, pumping vapour into the atmosphere and setting a pressure difference with respect to the land (Joseph, 1990). Within a few days after the onset of monsoon there would be rapid cooling in SST. The mean surface temperature of air at any place is governed by latitude, elevation, distance from the sea, type of prevailing air mass, which in turn determines the pattern of cloudiness and weather. Ananthakrishnan (1979) had reported that the highest maximum temperature above 33° C occurs in April and the lowest minimum temperature of about 22° C occurs in August at coastal stations in the State. The atmospheric characteristics of a mountain terrain like Western Ghats

are modified by its altitude, solar insolation, cloudiness and terrain texture. Over the western and eastern sides of the mountain the atmospheric temperature do not vary much by latitude in a year (Nair, 2009).

The diurnal variation of the surface temperature at Kochi and Coimbatore (except Thiruvananthapuram) show a similar variation, touching a maximum close to 30 °C and a minimum close to 25 °C (Fig. 5.6). The temperature at Thiruvananthapuram shows a relatively lower value compared to both Kochi and Coimbatore.

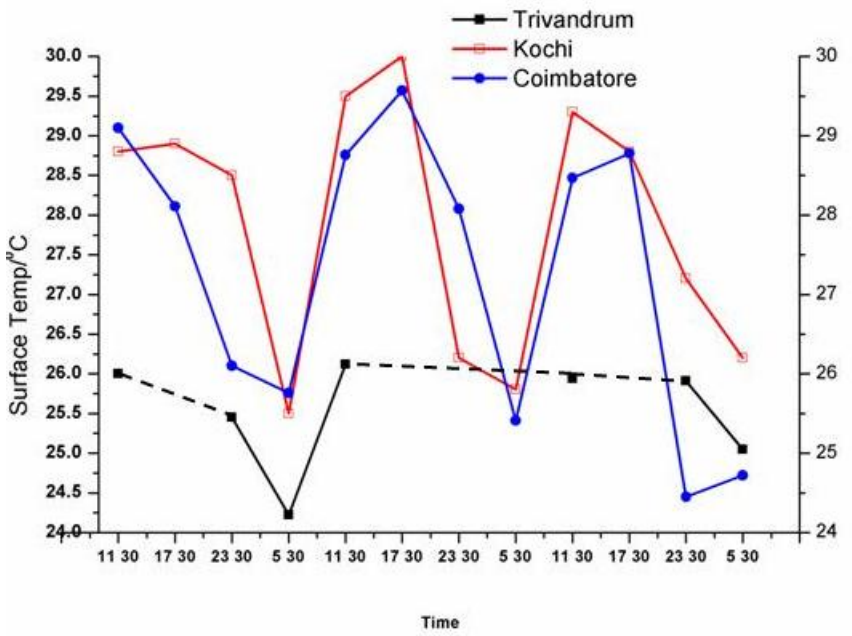

Fig 5.6: Temporal variation of surface temperature

5.5.6 Temperature Profile over the three stations

As high temperature develops over the land, the pressure come down and advection of air mass laden with vapour followed by rainfall will take place. This would lower the surface temperature resulting in reduction in vapour charging. But, as a result of latent heat release in the cloud over the continent, the atmospheric pressure would be kept low to sustain the vapour intake (Soman and Krishna Kumar, 1993). This process gives a feed back to modify the atmospheric temperature.

Temperature profiles at these three stations recorded by GPS sonde during the observation on 26th to 29th August 2013 reveal that the tropospheric height is always around 16 km and lapse rate is identical (Fig. 5.7a-f). However, the vapor content may vary depending on the proximity to ocean, and the strength of the moisture laden wind.

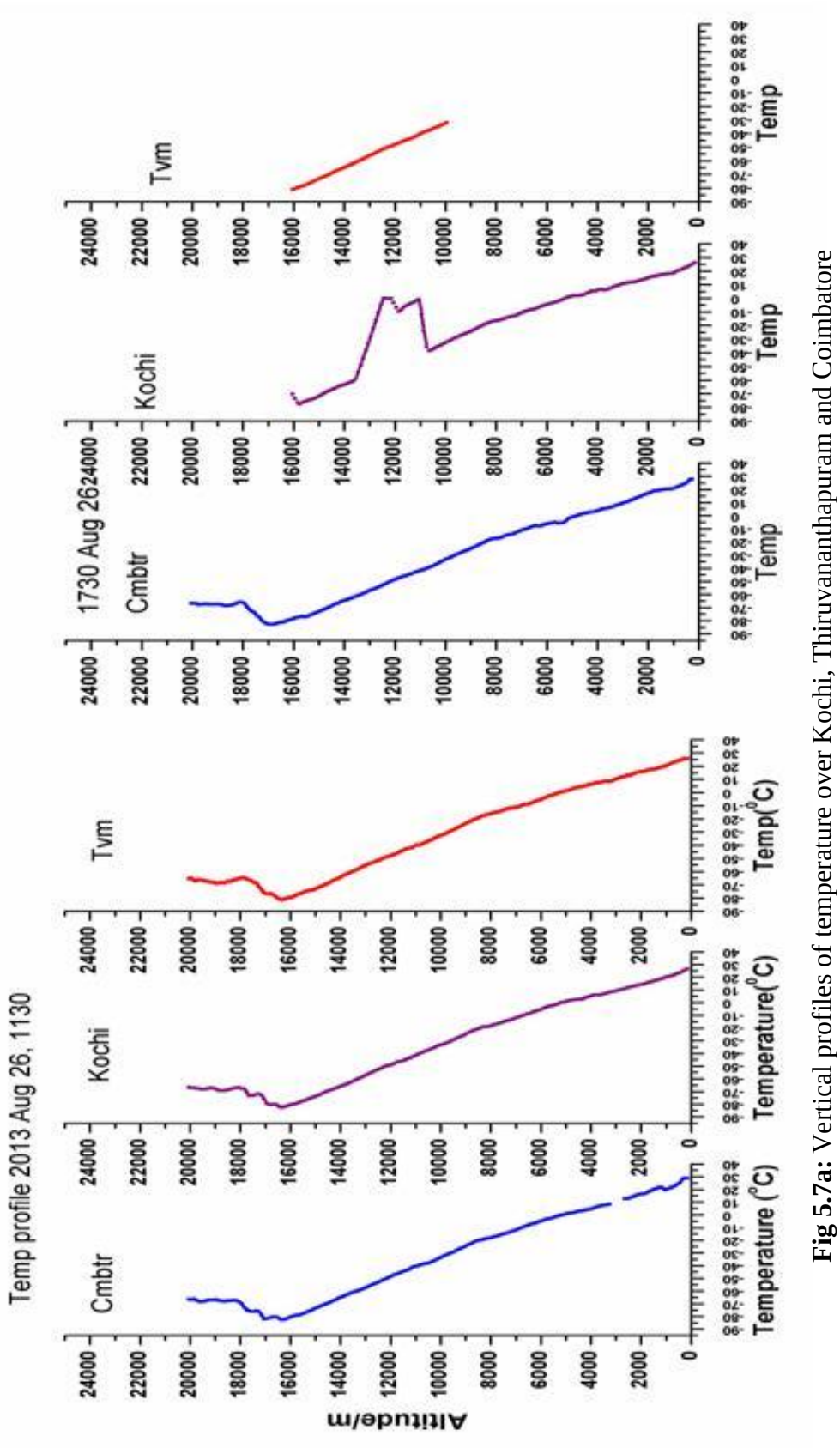

Fig 5.7a: Vertical profiles of temperature over Kochi, Thiruvananthapuram and Coimbatore

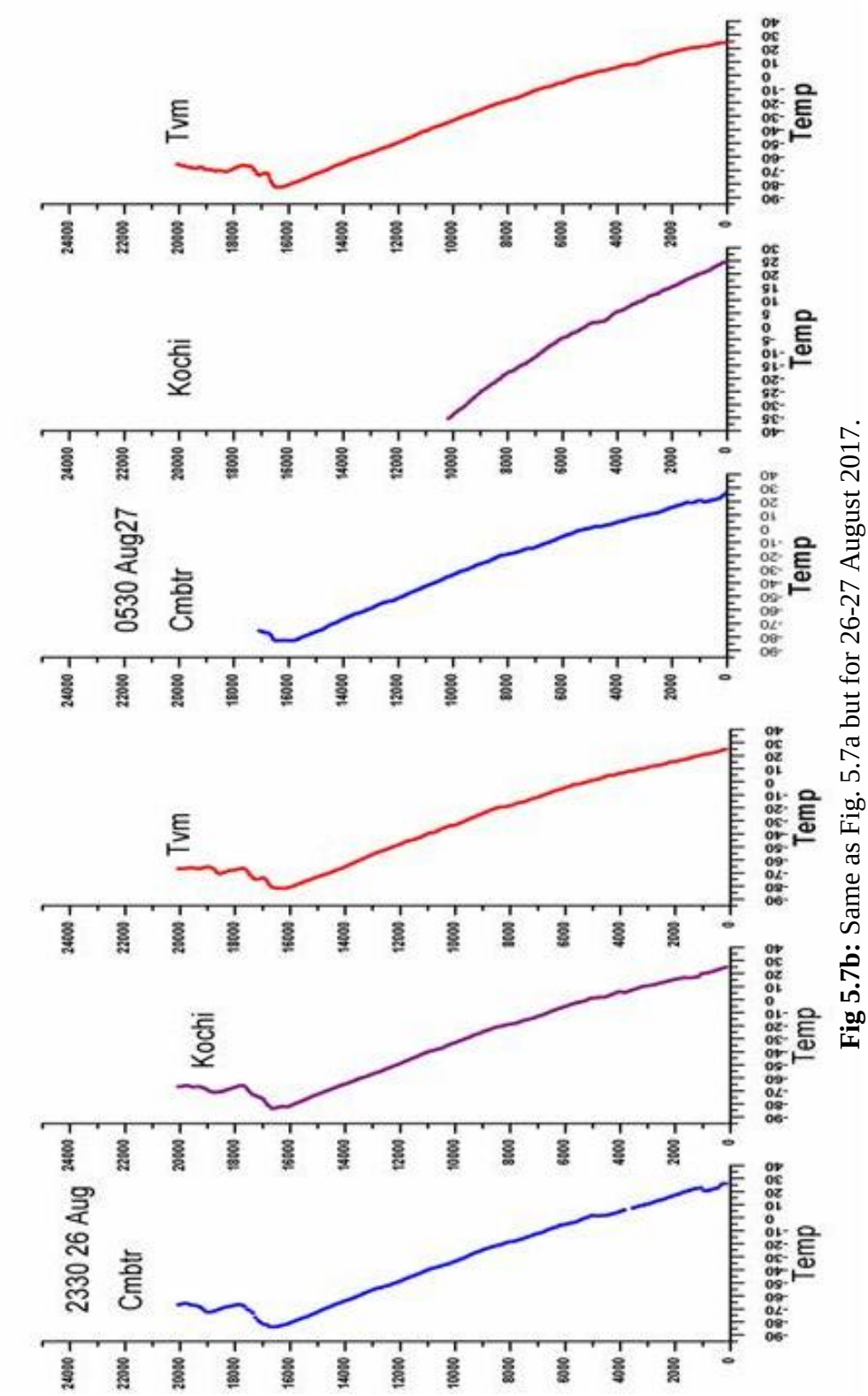

Fig 5.7b: Same as Fig. 5.7a but for 26-27 August 2017.

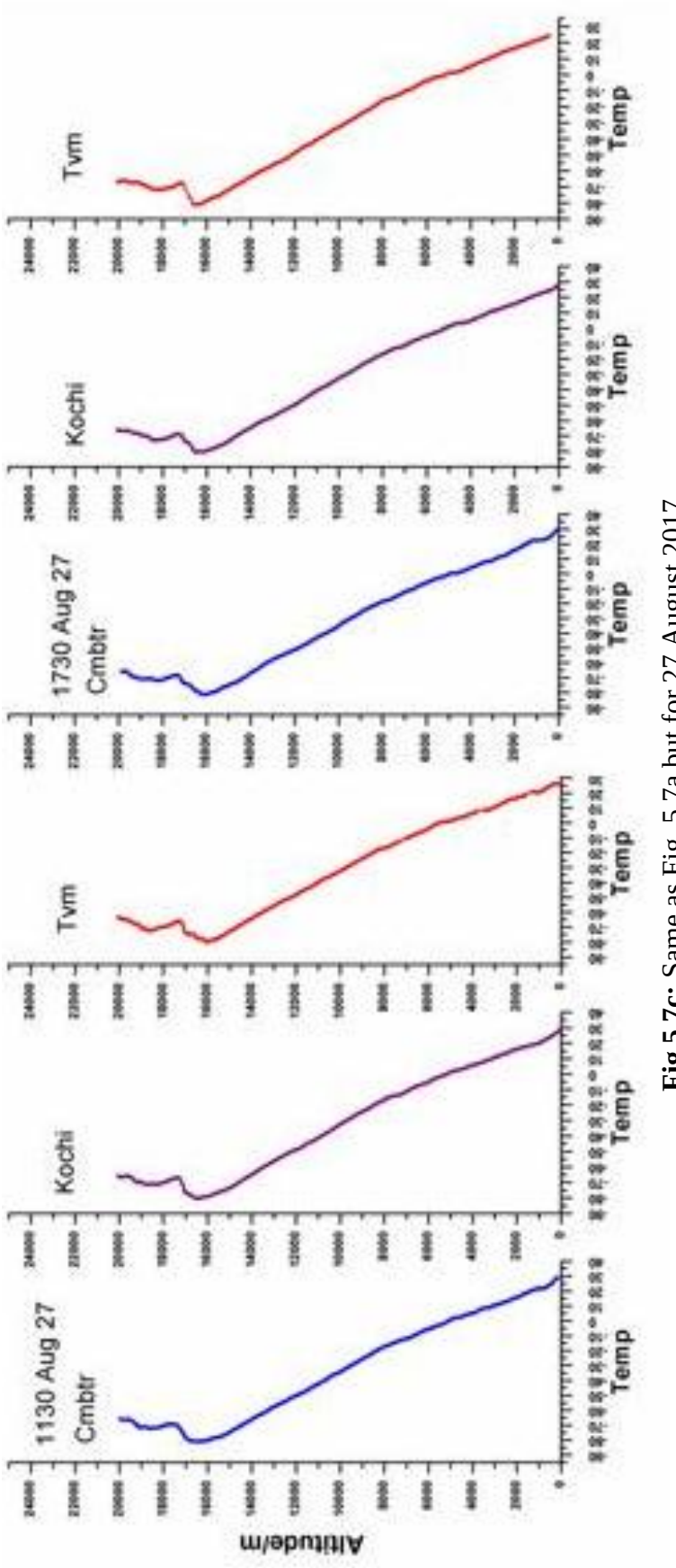

Fig 5.7c: Same as Fig. 5.7a but for 27 August 2017

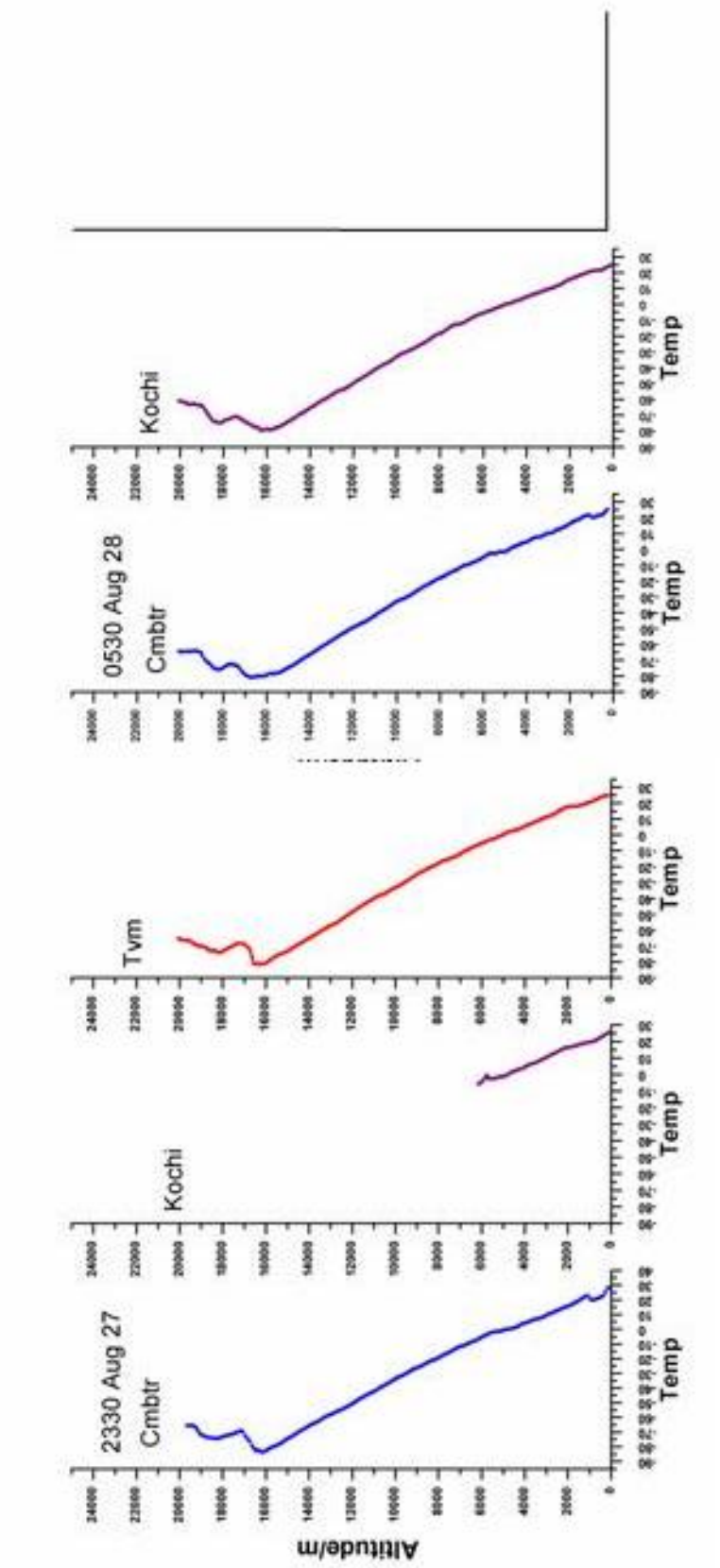

Fig 5.7d: Same as Fig. 5.7a but for 28 August 2017

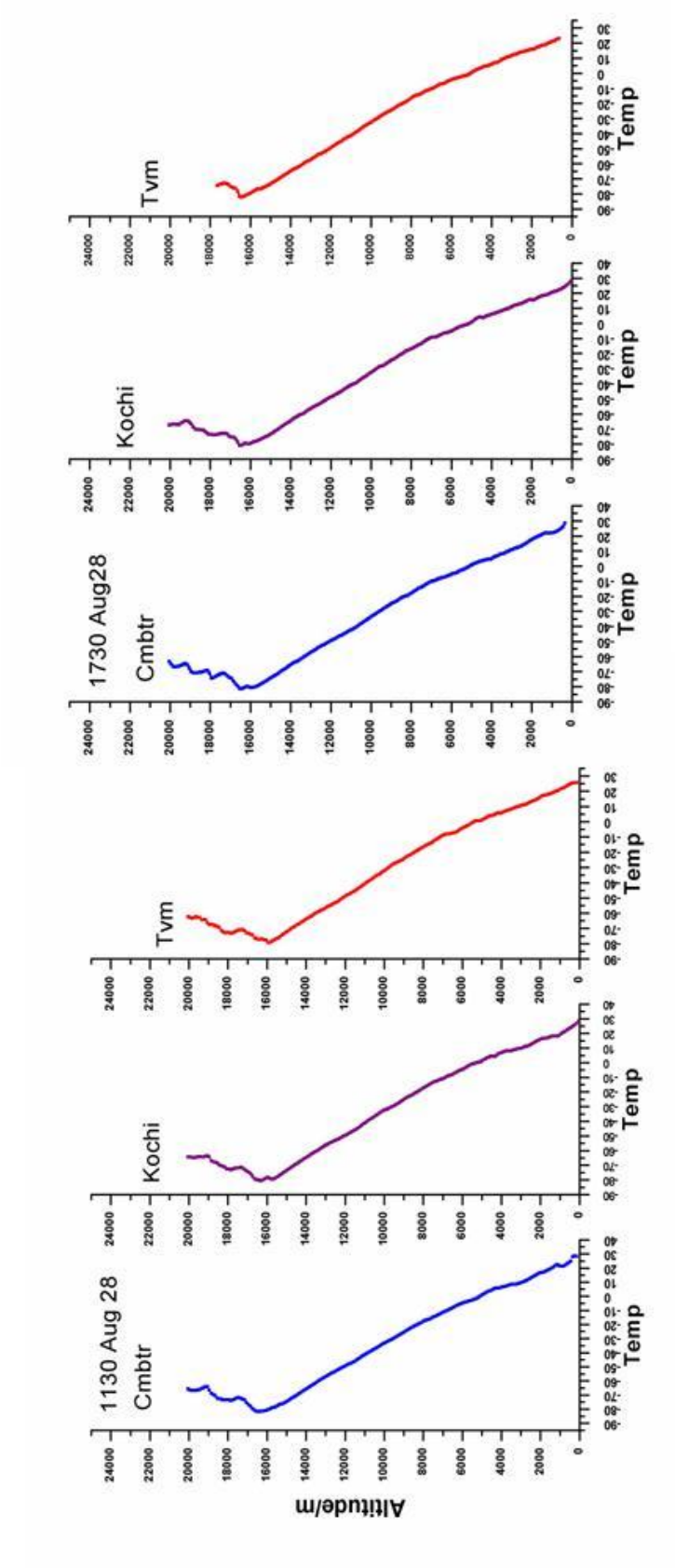

Fig 5.7e: Same as Fig. 5.7a but for 28 August 2017

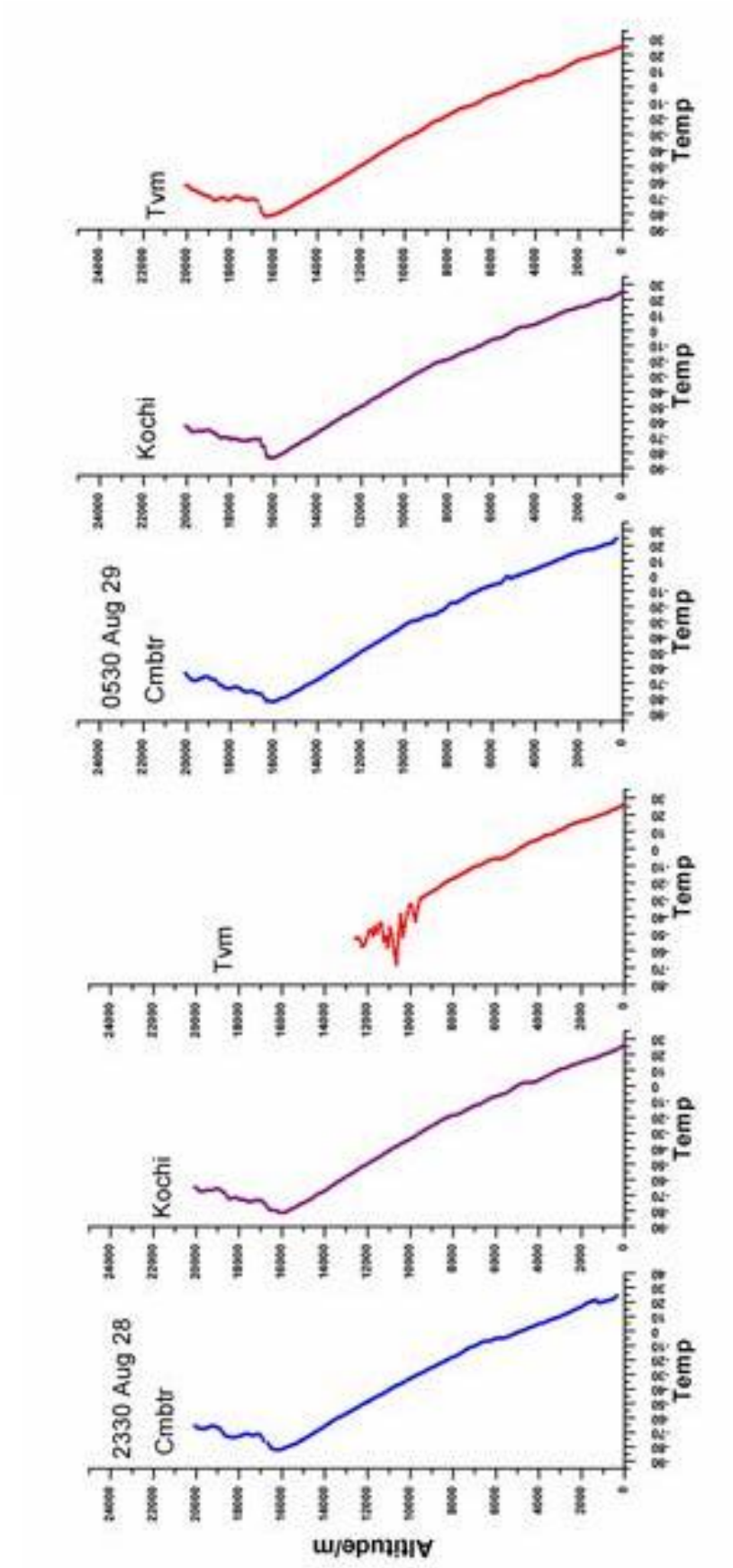

Fig 5.7f: Same as Fig. 5.7a but for 29 August 2017

5.5.7 Diurnal variation of Tropopause height:

Tropopause - the canopy region hovering over the troposphere, maintaining a steady lowest temperature of around -80°C, is at an altitude varying from 16 to 18 km, in the Tropics. The tropopause height normally varies with latitude, longitude and with the propagation of cold troughs and warm ridges during mid-latitude winters (Mohanakumar, 2008). Kulkarni and Verma (1993) had reported that the annual variation of tropopause height over the tropics below 20° N is similar to average variation in SST over ± 20° N and this agrees with the observation of Reid and Gage (1981).

Using the data taken from the three stations, the tropopause height is estimated, and it shows a diurnal variation from 15.8 km to 17 km (refer to Fig. 5.8). The temporal variation in tropopause height has no similarity in all the stations and Coimbatore maintains always a higher value.

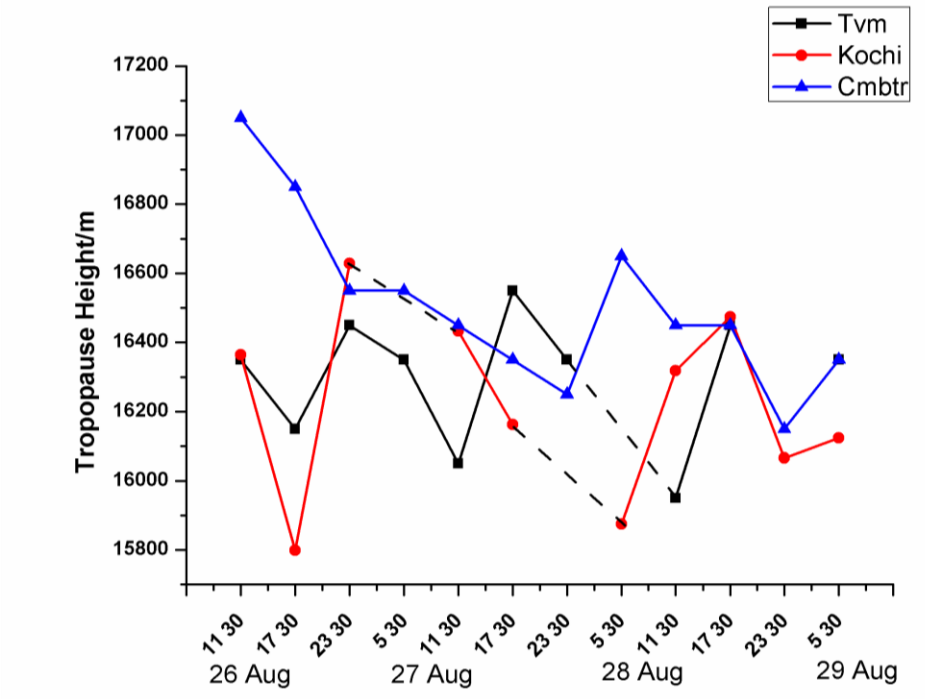

Fig 5.8: Diurnal variation of Tropopause height

5.5.8 Zonal wind at different levels over the three Stations

The variation in zonal wind speed at 850 hPa level at Thiruvananthapuram, Kochi and Coimbatore using Era-interim data is given below (Fig. 5.9). It is seen that Kochi retains the higher values in zonal wind speed, probably due to its

geographical proximity to the gateway of monsoon wind. Fig. 5.9 and Fig. 5.10 depict the variation in zonal wind speed at 500 hPa level observed with Era-interim and Radiosonde data set, respectively.

Table 5.4: Zonal wind speed at 850 hPa level at Thiruvananthapuram, Kochi and Coimbatore using Era-interim data.

Date	Time	Tvm	Kochi	Coimbatore
Aug-26	11:30	3.5	4.5	3.5
	17:30	5.5	4.5	4.5
	23:30	1	2.5	1.5
Aug-27	05:30	3.5	3.5	2
	11:30	2.5	3.5	1.5
	17:30	5.5	5.5	4.5
	23:30	5.5	5.5	4.5
Aug-28	05:30	3	3.5	2.5
	11:30	5	4.5	3.5
	17:30	7.5	5.5	6.5
	23:30	5.5	4.5	3.5
Aug-29	05:30	1.5	3.5	1.5

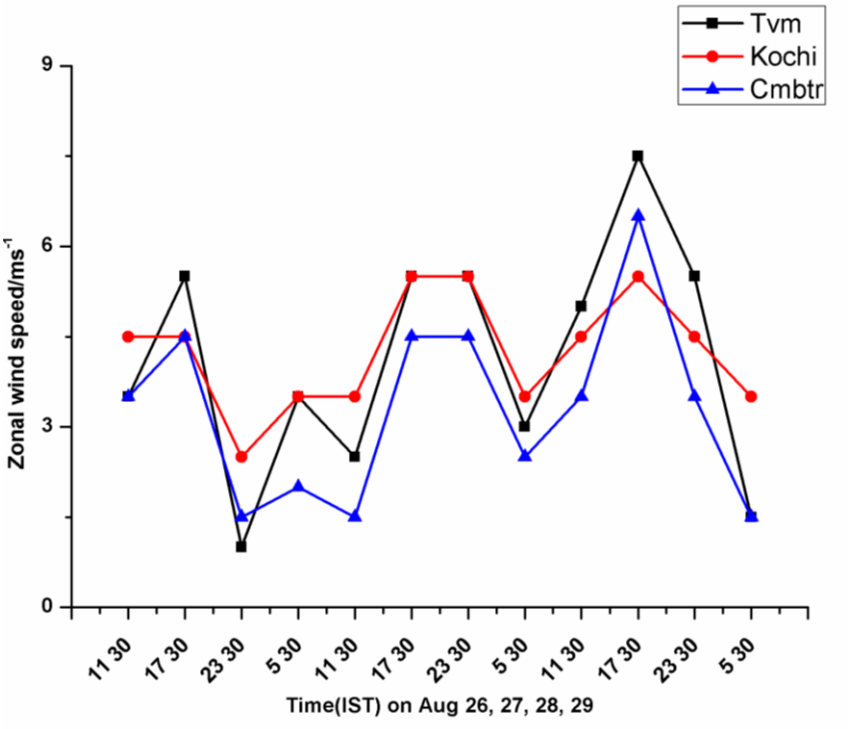

Fig 5.9: Diurnal variation of Zonal wind speed 500 hPa level (Era-interim data)

Table 5.5: Zonal wind speed at 500hPa level at Kochi, Thiruvananthapuram andCoimbatore (Unit in ms^{-1}) from Radiosonde data

Day	TIME	Kochi	TVM	CMB
Aug 26	11:30	4.5	3	3.5
	17:30	4.5	4.5	4.5
	23:30	2.5	1	1.5
Aug 27	05:30	3.5	3.5	2
	11:30	3	2.5	1.5
	17:30	5.5	5.5	4.5
	23:30	5.5	5.5	4.5
Aug 28	05:30	3.5	3	2.5
	11:30	4.5	4.5	2.5
	17:30	5.5	7.5	6.5
	23:30	4.5	5.5	3.5
Aug 29	05:30	3.5	2	2

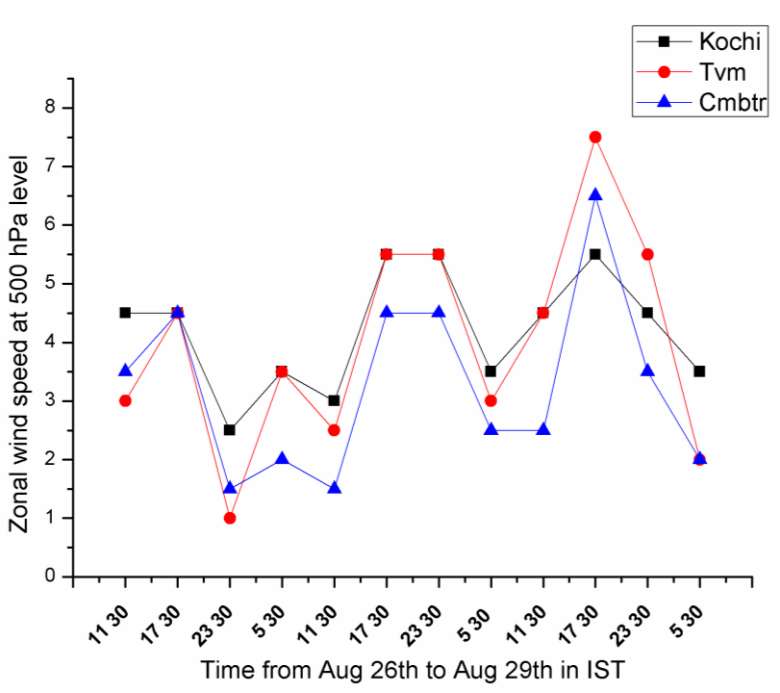

Fig 5.10: Zonal wind speed at 500 hPa (Radiosonde data)

5.5.9 Computing Divergence and Vorticity:

On analyzing the time-series of Divergence and Vorticity at 850 hPa (Fig 5.11) with respect to the centroidof the region formed by connecting the stations,

Kochi, Thiruvananthapuram and Coimbatore, it is found that the divergence is positive and the vorticity is negative with one or two exceptions. This condition shows that the occurrence of rain during this period over this region is rather nil. A negative correlation of 75% is present between the divergence and vorticity.

Table 5.6: Divergence and Vorticity estimated for the centroid of the three stations.

Date	Time/IST	$a/10^{-5}$	$b/10^{-5}$	$c/10^{-5}$	$d/10^{-5}$	Divergence D = a + d	Vorticity ξ = c - b
26-Aug-13	11 30	2.66	0.97	-5.85	1.18	3.84	-6.817
	23 30	4.23	2.21	-9.45	4.25	8.48	-11.67
27-Aug-13	5 30	2.36	1.9	-5.27	-2.57	-0.21	-7.16
	11 30	4.08	0.2	-6.7	-2.64	1.45	-6.9
	17 30	1.24	-1.02	-0.89	-2.36	-1.12	0.13
	23 30	3.58	1.74	-2.36	-1.95	1.63	-4.1
28-Aug-13	5 30	2.19	1.19	-3.7	-1.97	0.22	-4.89
	11 30	2.71	0.46	-3.98	-0.75	1.96	-4.44
	17 30	1.04	0.39	-2.24	-1.55	-0.51	-2.63
	23 30	1.6	1.38	-6.62	-1.44	0.166	-8
29-Aug-13	5 30	5.01	1.47	-6.27	-0.46	4.55	-7.74

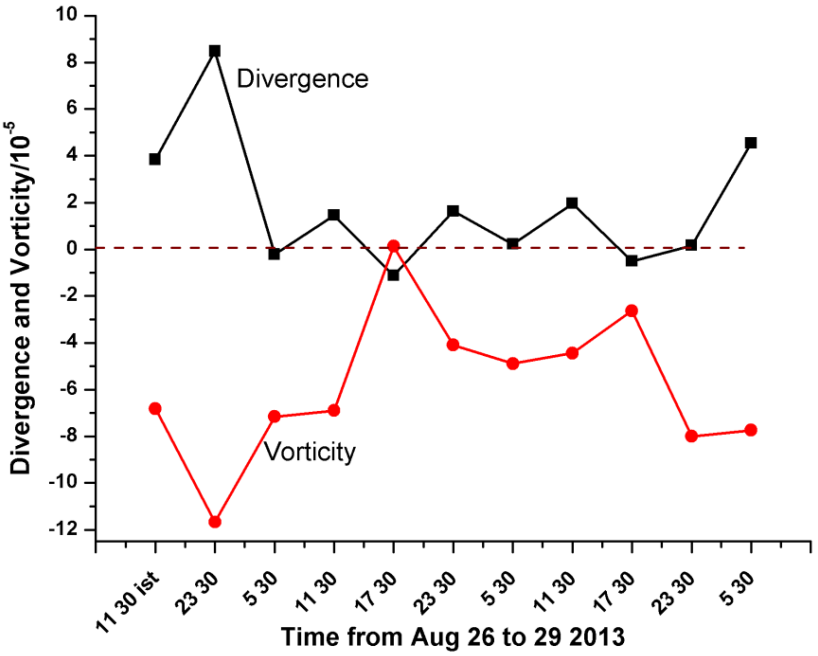

Fig. 5.11: Temporal variation of divergence and vorticity over the three-station region.

This observation is well supported by the rainfall data from the Daily Weather Report published by India Meteorological Department (IMD) during the same period.

Table 5.7: Table showing the distribution of rainfall (mm) received over Kerala during the campaign period

Station	26th Aug 2013	27th Aug 2013	28th Aug 2013	29th Aug 2013
Alappuzha	0	0	0	0
CIAL Kochi	0.2	0	0	0
Kochi AP	0	0	0	0
Kottayam RB	0	0	0	0
Kozhikode	0	0	0	0
Palakkad	0	0	0	1
Punalur	0	0	0	0
Thiruvananthapuram	0	0	0	0

5.5.10 Outgoing Long-wave Radiation

On examining the daily mean of the Outgoing Long-wave Radiation (OLR) from 26th to 29th August 2013, (see Fig. 5.12) (https://www.esrl.noaa.gov/psd/data/gridded/data.interp_OLR.html), it is clearly found that OLR is either very close or above the limiting value 200 Wm^{-2}, confirming the dry condition present in the region.

Table 5.8: OLR values over the region taken from satellite data

OLR (Wm^{-2})	Aug 26	Aug 27	Aug 28	Aug 29
	202	216	193	263

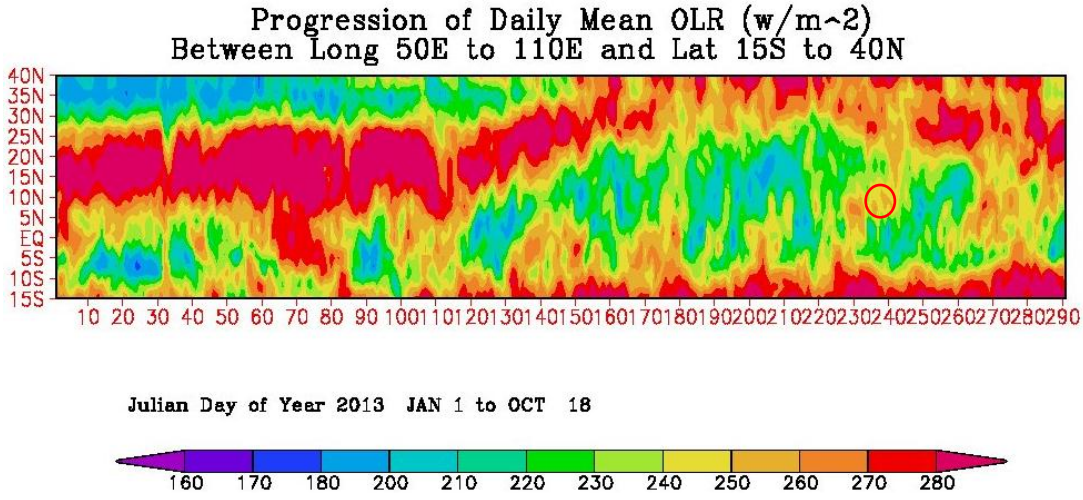

Fig. 5.12: Satellite image by India Met Dept showing OLR

Courtesy : IMD

The region within the red circle in the above pattern of OLR (Fig 5.12) shows that the OLR values were above 240 Wm^{-2} from 26th to 29th August 2013, indicating suppressed convection. In short, the field campaign provided an opportunity to estimate the vorticity and divergence over the centroid of the three stations, which helped in assessing the vigor of convection over the site concerned.

5.6 Summary and Conclusion

The special high resolution radiosonde observations over three stations and subsequent analyses revealed certain basic properties at the three stations:

1) The diurnal variations in westerly core speed and surface temperature at Kochi and Coimbatore are quite similar while that over Thiruvananthapuram is quite different.
2) The diurnal variations in westerly core level, zonal wind speeds at both 850 hPa and 500 hPa, and tropopause height at Kochi and Thiruvananthapuram are found to be similar while that at Coimbatore is smaller in magnitude.
3) The diurnal variation of TEJ core level and speed, and temperature profile at all the three stations are found to be varying in a similar fashion because of the higher height level of TEJ.
4) The positive values of divergence and the negative values of vorticity at 850 hPa level represent the absence of cloud and rainy condition, which is well supported by the rain data taken from the India Meteorological Department and OLR values showing above 200 Wm^{-2} during those observational days.

Thus, there is much similarity in the lower level in the variation of meteorological parameters at Coimbatore and Kochi due to their latitudinal proximity and the opening provided by the Palghat gap in the Western Ghats. Higher altitude properties are similar at all three stations since they lie in the southern.

****

Chapter

6

Lower Atmospheric Features using the Stratosphere-Troposphere Radar at Cochin

Contents

6.1 Introduction

Weather instruments that can observe the air motion of the troposphere with high degrees of accuracy and time resolution are necessary for the remote sensing and weather forecast. Wind profiling radar (WPR) is one such instrument which provides the three-dimensional measurements of wind velocities and directions of each layer of atmosphere in real time, and has become indispensable for high accuracy weather prediction.

ST radars are emerging as powerful tools for atmospheric research and have immense applications in meteorology, cloud physics, thunderstorms, atmospheric electricity, climate change, environmental physics, civil aviation, communications, etc. The principle involved in the atmospheric Radar is to transmit the modulated waveform of electromagnetic energy using antenna array into the atmosphere and processing the backscattered echoes through suitable means by utilizing a chain of signal processors to determine wind components with a high degree of temporal and

spatial resolutions. It can be used for deriving several vital parameters required for studying the structures and dynamics of atmosphere.

Wind profiler radars are vertically directed pulsed Doppler radars capable of analyzing the back scattered signals to determine the velocity vector of air in the beams (Samson et al., 2016). They depend on signals scattered from gradients in the radio refractive index associated with turbulent eddies with scales of one-half the radar wavelength. The goal of detecting the very weak clear air signals dictates the use of long coherent dwell times, low noise system, low antenna side lobes, and careful attention to potential interference.

6.2 Evolution of Wind Profiling Radars

It was not until this century that we began to get a systematic look at the space and time variability of the atmosphere as a function of height above the ground. A significant advance in this area was made some 50 years ago with the development of Radiosonde, a device carried aloft by a balloon to measure temperature, pressure, and humidity and transmits these data back to a ground station. By tracking the motion of the balloon, the winds aloft could also be determined. Although Radiosonde measurements are made every 12 hours interval globally, this is not sufficient to define the significant smaller-scale weather events. Advances in our understanding of the weather are dependent upon obtaining measurements with a higher resolution in both time and space. Many other applications also require more frequent and more closely spaced upper-air measurements. Even though Radiosonde are inexpensive, the relatively high cost of maintaining balloon launching and tracking facilities has precluded more extensive use.

Development of remote sensing technology offers a solution to this problem. In particular, it is now possible to measure vertical profiles of the wind on a nearly continuous basis with accuracy better than that normally obtained with most balloons, and more economically. These revolutionary instruments are known as wind profiling radars (or wind profilers). They are suitable as research tools in assisting scientists in a wide spectrum of research interests, or as operational systems helping to bring practical benefits to users in a variety of applications.

Although the initial applications of radar were for detecting solid objects, such as airplanes, it was soon discovered that radar can also detect hydrometeors (rain, ice, snow etc) in the atmosphere, principally those large enough to precipitate. Remote detection of hydrometeors became the foundation for the science of radar meteorology. Radars are able to detect subtle changes in the frequency of the returned signal from which the radial velocity of the target hydrometeors can be determined using the Doppler principle. If the hydrometeors are moving with the wind, the radial velocity of the wind relative to the radar site is also measured. These conventional weather radars are designed to detect reflections from objects in the air rather than the air itself. On occasion, echoes were noted that did not correspond to any visible object. Some of these were found to be reflections from the warms of insects or birds. Others were shown to be from the air itself. These echoes that originate in "clear air" are the foundation of wind profiling.

6.3 Theory of Wind Profiling Radars

Wind Profiling Radars (WPRs) depend upon the scattering of electromagnetic energy by minor irregularities in the index of refraction of the air. In the atmosphere, minor irregularities in the index of refraction exist over a wide range of sizes. In the lower portion of the atmosphere (troposphere and stratosphere), the index of refraction depends primarily upon the temperature, pressure and humidity of the air. A spatial variation in this index encountered by a propagating electromagnetic (radio wave) causes a minute amount of the energy to be scattered (or dispersed) in all directions. Most of the energy incident on the refractive irregularity propagates through it without being scattered. As mentioned above, radio frequency electromagnetic pulses propagating through air lose part of their energy to scattering from these refractive irregularities. A small portion of this scattered energy is returned to the radar site, where it can be received and analyzed. Backscattering (scattering of energy toward its point of origination) occurs preferentially from irregularities of a size about one-half the wavelength of the probing radio wave. Since these irregularities are carried by the wind, they prove to be good "tracers" of the mean wind.

During its propagation, the electromagnetic pulse waves experience random refractivity fluctuations due to atmospheric turbulence and are scattered (echoes from refractive index gradient- Bragg scattering). Refractive index n (or refractivity N) of air depends on pressure P (hPa), temperature T (K), and water vapor pressure 'e' (hPa).

$$N=(n-1)*10^6=77.6\frac{p}{T}+71.6\frac{e}{T}+3.7*10^5\frac{e}{T^2} \qquad \text{- (6.1)}$$

Parts of the scattered pulse waves (echoes) then return to the radar with time delays proportional to the height where the scattering had occurred, making it possible to relate the scattering intensity to the height by sampling them with proper time intervals. Since turbulence moves with the flow of the wind, the echoes are subjected to the frequency shifts (Doppler shifts) proportional to the wind velocity (V) at the height where the scattering took place.

6.4 Doppler Radar Principle

In 1842, the Austrian physicist Johann Christian Doppler developed the theory and supporting mathematical equations to explain the relationship between motion and frequency changes in sound. Application of Doppler theory was first recorded in the late 1950's; however, it wasn't until the early 1990's that Doppler technology became the standard mechanism to measure radar imagery. Doppler provides a rich suite of automated algorithms allowing meteorologists to more definitively identify and track thunderstorm/precipitation intensity, severe weather signatures, micro bursts, wind shear and precipitation accumulation.

The Doppler Effect can be defined as *the observed change in the frequency of sound or electromagnetic waves due to the relative motions of the source and observer.*

Electro-Magnetic travelling wave can be represented as

$$S_t(t)=A\cos(\omega t-kr-\phi_0) \qquad \text{- (6.2)}$$

Where A = amplitude in volts

ω = angular frequency (radians per second)

k = Propagation Constant (rad/meter)

$\emptyset_o$ = initial phase offset (radian)

r = distance (meter)

In a Radar, the received signal from a target at a distance R can be represented by

$$S_t(t) = A'\cos(\omega t - 2Rk - \phi_0) \qquad \text{- (6.3)}$$

The phase of the received signal with respect to the transmitted signal is given by

$$\phi = k.2R = \left(\frac{2\pi}{\lambda}\right).2R = \left(\frac{4\pi}{\lambda}\right).R \qquad \text{- (6.4)}$$

The rate of change of ∅ is given by

$$\omega_d = 2\pi f_d = \frac{d\phi}{dt} = \frac{4\pi\ dR}{\lambda\ dt} = \frac{4\pi}{\lambda} v_r \qquad \text{- (6.5)}$$

Therefore, Doppler shift in frequency is given by,

$$f_d = \frac{2}{\lambda} v_r \qquad \text{- (6.6)}$$

6.5 Atmospheric Scattering

Scattering from atmospheric target may be due to: (i) Irregularities in the index of refraction of air: Three types - Bragg's Scattering, Fresnel Reflection, Fresnel Scattering (ii) Hydrometeors, particularly wet ones (rain, melting snow, water coated ice): Rayleigh Scattering (iii) Birds and insect (frequency dependent) and (iv) Smoke plumes

Multitude of targets may introduce serious errors. In the case strong precipitation, the measured velocity is that of rain, not wind interfering signals are mainly due to: (i) Ground and sea clutter (ii) Aircraft and migrating birds

The principle scattering mechanism in Wind Profiler Radar is called "Bragg scattering" (Gossard and Strauch, 1983), rather than turbulence scattering. This term results from the physical mechanism of constructive interference of backscatter from spatial spectrum components at the Bragg wave number $k = 4\pi/\lambda$ of refractive index fluctuations in a turbulent layer, which is much wider than many radar wavelengths

λ. The Bragg scatter can be isotropic, i.e., without causing a radar aspect sensitivity, if the turbulent irregularities of refractive index are homogeneously random and statistically similar in all directions. Bragg scatter can also be anisotropic, causing an aspect sensitivity if the statistical properties of the irregularities, namely their correlation distances, are dependent on direction. Although the angular (spatial) dependence of the radar echoes, i.e., the aspect sensitivity for these two processes - isotropic and anisotropic Bragg scatter - is different, the temporal variations of the radar echoes should be similar because of the randomly fluctuating irregularities. The Doppler spectrum should approximately reveal a Gaussian shape.

The received echo power, P_r, is calculated as

$$P_r = (\text{constant}) \{P_t \tau A_e / r^2\} [\eta] \qquad \text{- (6.7)}$$

Where the 'constant' is a combination of constants, both mathematical and physical (such as system efficiency), P_t is the transmitted power, and η is the reflectivity.

In the inertial sub-range, the radar reflectivity is proportional to C_n^2 and is given by

$$\eta = 0.38 \lambda^{-1/3} C_n^2 \qquad \text{- (6.8)}$$

Where λ is the radar operating wavelength. By combining equations (1) and (2), we see that a measurement of P_r can be converted into C_n^2. The wind profiler is therefore also a C_n^2 profiler. The height range of useful returns depends on the operating frequency and degree of turbulence. Obviously the stronger the turbulence, the stronger is the echo.

6.6 Applications of ST Radar

The VHF wind profiler can be used for both research and operational purposes.

Operational Purpose: It has many applications in Weather Forecasting, Aviation, Wind support for Satellite launches, and Air quality meteorology.

Research purpose: Atmospheric boundary layer processes, Turbulence, Atmospheric stability and waves, Tropical convection and precipitation, Stratosphere-

Troposphere exchange, Vertical wind, Temperature and Humidity profiling (in association with RASS), Mesospheric and Ionosphere dynamics etc.

6.7 System Overview

This section presents the specifications and technical aspects and of the design and development of a 205 MHz VHF Wind Profiler Radar installed at Cochin (10.04^o N, 76.33^o E) India for the troposphere and lower stratospheric studies in the tropical monsoon region.

The 49 Element Mini-wind profiler system is a miniature model of the 619 element ST Radar main system at CUSAT. The Mini-profiler contains all the sub-systems of the final system, which helps in evaluating the overall integrated functionality of the system. The Mini-profiler consists of 49 antenna elements, corresponding to 49 Transmit-receive (TR) modules, which are interfaced to the Radar processing computer by means of 2 stage power combiners (RF) and Tile interface module (Digital). The Radar processing computer is a major subsystem of the Mini profiler radar. This sub-system consists of signal generators, coherent digital receivers and signal processing section of the radar. This entity generates the control signals based on the commands issued by the radar controller, and distributes them to the other sub-systems of radar. The transmission, reception and digitization of the received signals are synchronous with a master reference clock. The digitized data is processed and stored in the memory. The stored data is manipulated for ON line and OFF line analyses.

6.8 Wind Profile Measurements

6.8.1 Horizontal Velocity Measurement

The Doppler wind profiler measures horizontal wind from two or more fixed beams directed obliquely in orthogonal planes. The profiler measures the radial component of the wind in each beam direction. The oblique beams are typically directed about 15 degrees off the zenith (vertical). Since mean vertical motions are typically less than about 0.1 m/s, vertical motions are usually ignored in determining the horizontal wind from the radial component. But, such vertical components are still taken into consideration for calculating horizontal component at high precision.

Wind profiles are typically deduced from a consensus of many samples of individual wind measurements taken over about 10 to 30 minutes. Individual samples are typically obtained on each beam in about three minute. When three beams are used for wind profiling, about ten values will be in a consensus to form the profile for the zonal and meridional components of the velocity. The consensus process compares velocities and discards outliers that do not agree with other values.

6.8.2 Vertical Velocity Measurement

Vertical velocity is measured with the vertically directed beam of a wind profiler. Unlike the horizontal velocities, the expected range of vertical velocities is usually less. Thus, it is possible to adjust the maximum unambiguous velocity to be much less than that required for measurement of horizontal velocities. As a consequence, the spectral resolution is much better for vertical velocity measurement.

6.8.3 Spectral Moments

It is well established that the first three moments of the Doppler power spectral density or the "power spectrum" are directly related to the desired atmospheric base parameters: radar reflectivity, radial velocity, and velocity spectrum width.

The spectral moments can be directly related to the reflectivity, velocity and dispersion parameters desired for further analysis. Computing these moments has historically been performed using classical moment calculations based on techniques from probability theory when considering the power spectrum as a density function of frequency or velocity components of the desired signal (Keeler and Passarelli, 1990).

The zeroth moment (M_0) is the area under the curve of S (f) (the power spectrum of the received signal) and represents total signal clutter, and noise power. Of course, we are usually interested only in the signal power, so the clutter and noise powers must be estimated and removed. Noise power is generally easy to remove, but clutter removal causes difficulties to the parameter estimation process.

The classical normalized first moment (M_1) represents mean velocity and is given by the linear weighting of S(f) over the Nyquist interval. Note that white noise biases the velocity towards zero and for a pure noise spectrum the mean velocity is identically zero. The normalized second central moment (M_2) represents the velocity

dispersion within the pulse resolution volume. Shear, turbulence and precipitation motion contribute to a distribution of radial velocities. The velocity dispersion (width) is the square root of the second central moment of the spectrum estimate.

The Zeroth Moment is given by

$$M_0 = \sum_{i=m}^{N-1} P_i \qquad \text{- (6.9)}$$

Where, P_i = Power spectral Value of i^{th} Point

The first moment or Mean Doppler

$$M_1 = \frac{1}{M_0} \sum_{i=m}^{N-1} P_i f_i \qquad \text{-- (6.10)}$$

$$f_i = \frac{\left(i - N/2\right)}{\left(IPP * n * N\right)} \qquad \text{-- (6.11)}$$

Second moment or variance

$$M_2 = \frac{1}{M_0} \sum_{i=m}^{N-1} P_i (f_i - M_1)^2 \qquad \text{-- (6.12)}$$

Doppler width (Full) = $\sqrt[2]{M_2}$ -- (6.13)

Signal to Noise Ratio (SNR) = $10 \log \left[\frac{M_0}{N * L} \right]$ -- (6.14)

Where,

N = Number of FFT points

L = Noise Level (Computed Using Hildebrand and Sekhon Noise Level Estimation)

i = Bin Number (Height)

IPP = Inter Pulse Period

n = End index of Doppler data

m = Start index of Doppler data

6.8.4 Wind Speed (u, v, w) Computation

One of the important applications of the wind profiling is the computation of wind speed. By using the Doppler profiles of the radar returns, wind speed can be calculated at different heights. For computing the wind speed, wind profiles for minimum of three directions is a must. The wind profiles in North, South, East and West directions with an oblique angle θ are obtained. The wind profiles in the zenith direction (vertical wind velocity) shall also be obtained. If there is a relative motion between the source of the waves and an object encountering the waves, the frequency measured at the object will be different from that at the source. This is called the Doppler Effect. If the object is approaching the source, the frequency will be higher, if it receding, the frequency will be lower. The amount of frequency change is called the Doppler shift which is directly proportional to the relative radial velocity between the source and the object and inversely proportional to the wavelength. In the case of wind profiling, the source is the wind profiler and the object is the refractive irregularity that scatters the waves. A double Doppler shift is encountered here: one shift as the pulse impinges upon the scattering volume and other as the pulse is scattered back towards the wind profiler.

The Doppler Shift is given as

$$f_d = \frac{2}{\lambda} v_r \operatorname{Sin}\theta \qquad \text{-- (6.15)}$$

From Doppler shift, the radial velocity is given as

$$v_r = \frac{f_d \lambda}{2 \sin\theta} \qquad \text{-- (6.16)}$$

For the directions of Zenith-X and Zenith-Y, the radar is operated in vertical direction. So the related equation for Doppler frequency is

$$f_d = \frac{2}{\lambda} v_r \qquad \text{---- (6.17)}$$

6.9 Observational Results of Atmospheric Features with WPR

6.9.1 Validation Wind Profiler Radar data using Radiosonde Measurements

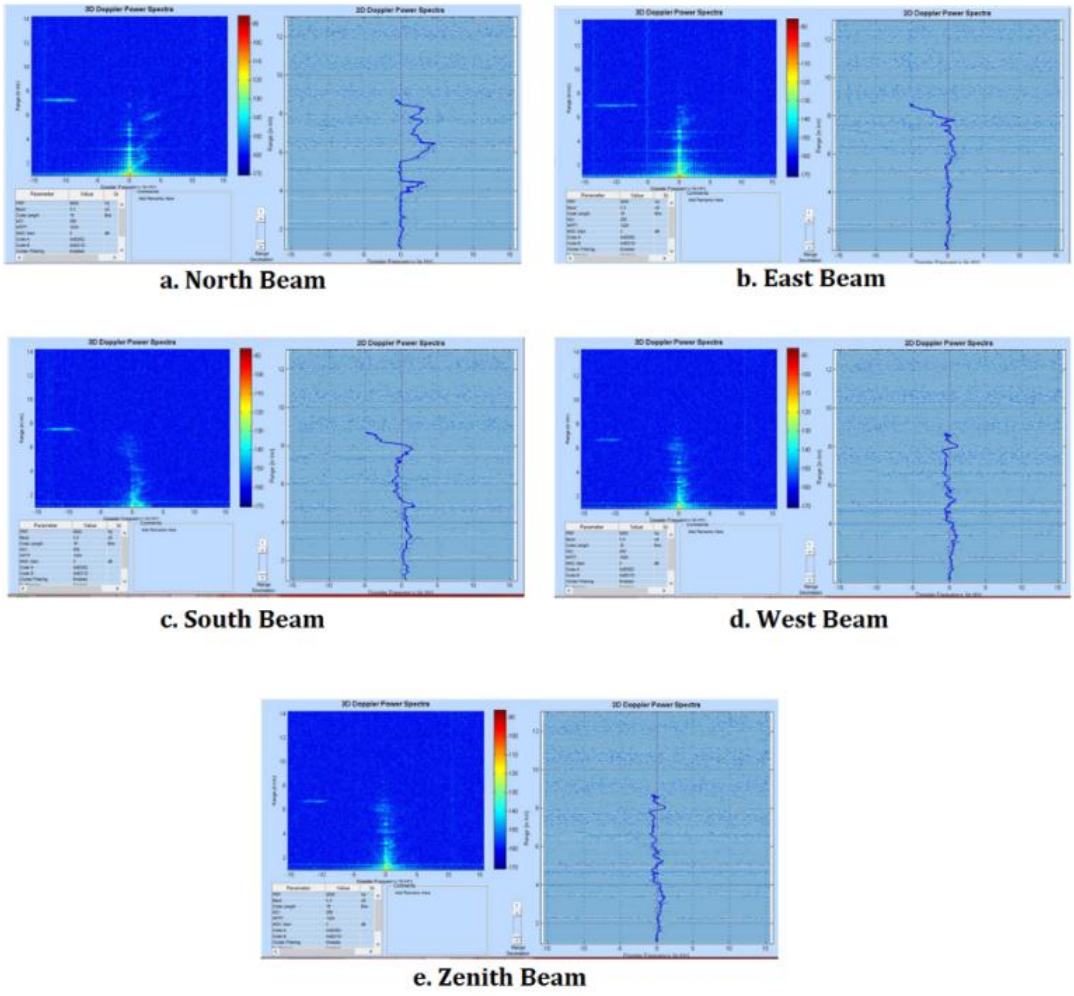

Fig. 6.1: 3D power spectra observed on 04th June 2015

Given above is the sample power spectra (Fig. 6.1) obtained on June 04, 2015, from which the *u*, *v*, and *w* profiles have been derived.

In order to validate the radar wind profiles, the Radiosonde wind measurements were spatially and temporally collocated with radar data. The radar profiles are generated every three minutes and the Radiosonde yields data every five seconds for different levels. The collocations with radiosonde are based on the radar data acquisition time. For each radar data acquisition, collocations are made with radiosonde. Therefore, it is possible to have collocated pairs with nearly the same

altitude coverage but a few minutes apart. The collocated pairs having a maximum altitude difference of 25 m and a maximum temporal difference of 300 s have been retained. From the collocated radiosonde wind speed and direction, the zonal (u) and meridional wind (v) components have been calculated and then compared with the radar's zonal and meridional winds for the altitude range. Note that our collocation criteria do not take into account the radiosonde drift during its ascent; only the differences in vertical altitude and data acquisition time are considered.

Before doing a one to one comparison between radiosonde and radar, some data points were excluded based on certain criteria of wind speed and direction. The first criterion adopted takes into account the collocated radar and radiosonde's wind direction offset, which if more than 90^{O}, removes the corresponding data of both the instruments from the analysis. This directional offset is found when light winds with speeds less than 2 m s^{-1} occur in either radiosonde or radar and the differences in the wind speeds between them is large. Some data points were also removed by applying a threshold on the difference in wind speeds between collocated Radiosonde and radar. Only those data points having wind speed difference less than 7 ms^{-1} have been retained for analysis. The reason will be dealt in the result section. The large wind speed difference can arise when radiosonde drifts farther away (~8 km) from the radar location. However, this does not imply that a large spatial separation can result in inferior comparison of radar and radiosonde winds. But if there is a local modification in temperature or pressure field due to turbulence, then large wind speed differences may occur.

To validate the functionality of ST Radar Mini Profiler during Monsoon season, experiments have been conducted during month of June, 2015. As part of the experiments, ST Radar Mini Profiler has been operated continuously for 15 days and the radar data products have been collected. To cross check the ST Radar Mini Profiler data products, Radiosonde has been used. Radiosondes have been launched and the data products of the ST Radar Profiler has been compared with the data products of Radiosonde.

6.10 Preliminary results of WPR observations

In this section we present the results of comparisons between radiosonde and radar's zonal wind, meridional wind, wind speed and wind direction.

6.10.1 Radiosonde Trajectory

Fig. 6.2 shows the trajectory of the radiosondes launched from a region proximal to the radar location. The colour bar in the figure shows the distance between the radiosonde and radar locations. The horizontal distance covered by the radiosonde is a non-linear function of height. The variations in the horizontal wind speed cause the radiosonde to drift farther and farther away from the radar location with ascent. For instance, at an altitude of 1 km, the Radiosonde drift is approximately 1 km as compared to an altitude of 6 km where the Radiosonde drift is around 10 km. However, this drift in the radiosondes does not affect the radiosonde-radar wind comparison as long as the wind field is homogeneous.

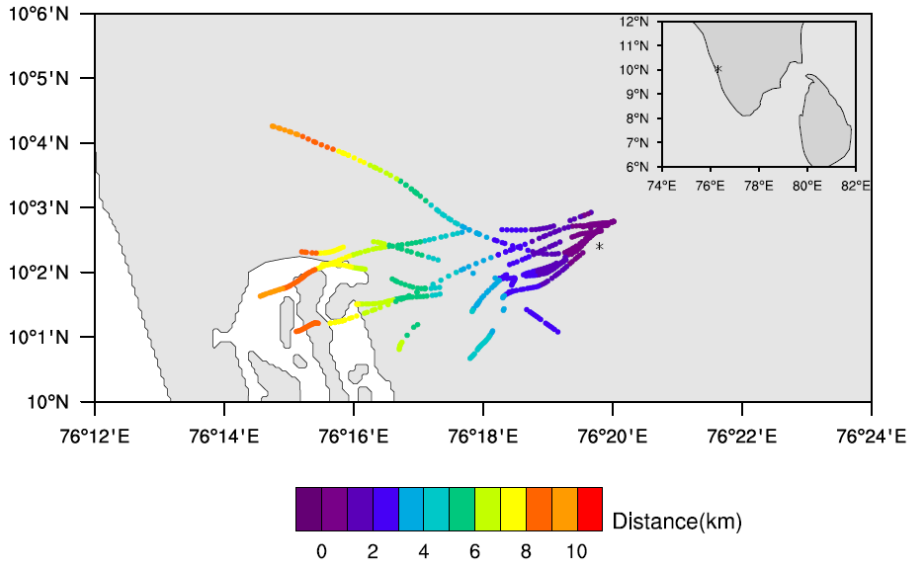

Fig. 6.2: Trajectories of Radiosonde during the validation period

6.10.2 Radar v/s Radiosonde Comparison

A comparison of daily zonal and meridional wind profiles between radar and radiosonde is shown in Fig. 6.3a and 6.3b. In general, the radar wind profiles match very well with the radiosonde wind profiles and the radar is seen to capture the day to day wind variations quite well. The mean value of the collocated zonal and

meridional wind as a function of height from Radiosonde and radar is shown in Fig. 6.4. The standard deviation of the mean zonal and meridional wind from Radiosonde is shown as horizontal error bar. The mean zonal and meridional wind from radar closely follows the radiosonde both in terms of magnitude and direction, and is well within the variability of the radiosonde. The mean zonal wind from both radar and radiosonde are easterly attaining maximum value of around ~14 m s^{-1} at 3 km whereas the meridional winds are northerly below 3 km and changes to southerly above 3 km. These transitions are reflected in radar and radiosondes.

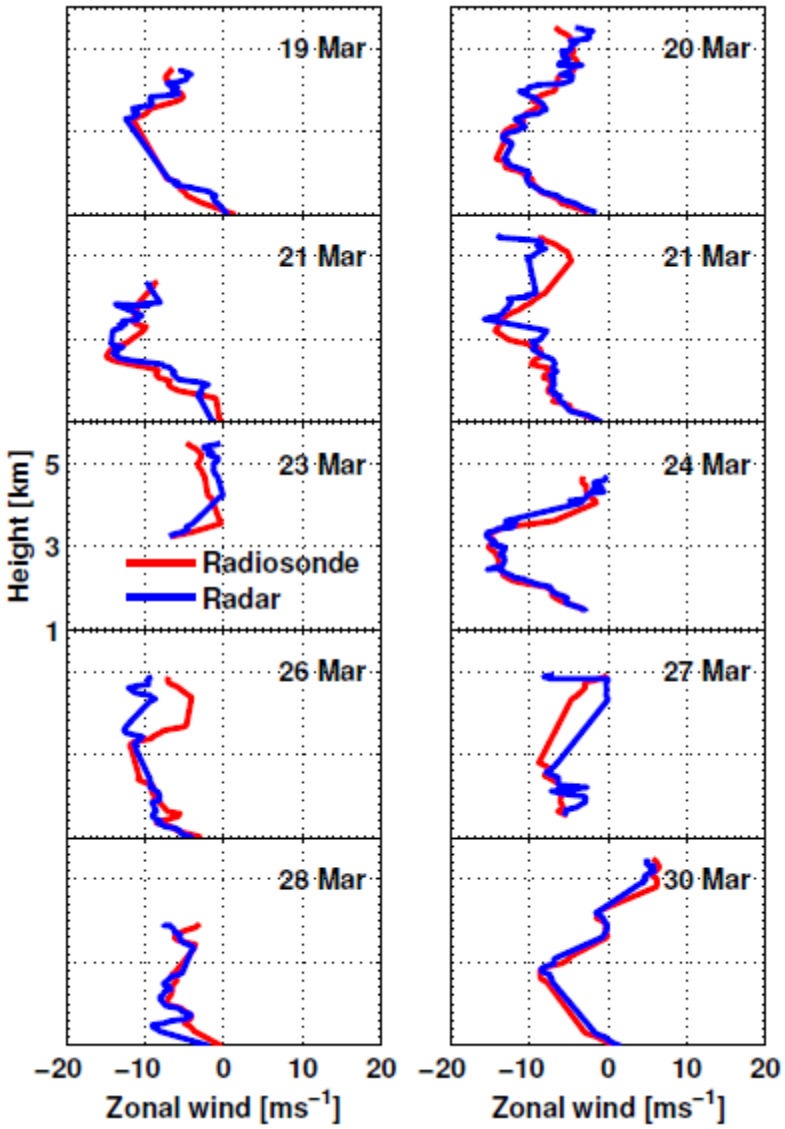

Fig. 6.3a: Comparison of zonal component of winds from WPR with those observed from co-located Radiosonde measurements in 2015.

A one to one comparison between zonal and meridional wind from radar and radiosondes for an altitude range of 1 - 6 km is shown in Fig. 6.5a. Each point corresponds to measurements made at almost the same time and height for both the instruments. The radar zonal wind shows very good agreement with radiosonde having a correlation coefficient of 0.91.The linear regression slope is 0.93±0.019 which is very close to unity. The mean bias and Standard Error of Estimate (SEE) found in the zonal wind comparison is 0.08±1.95 ms^{-1} and 1.92 ms^{-1}, respectively.

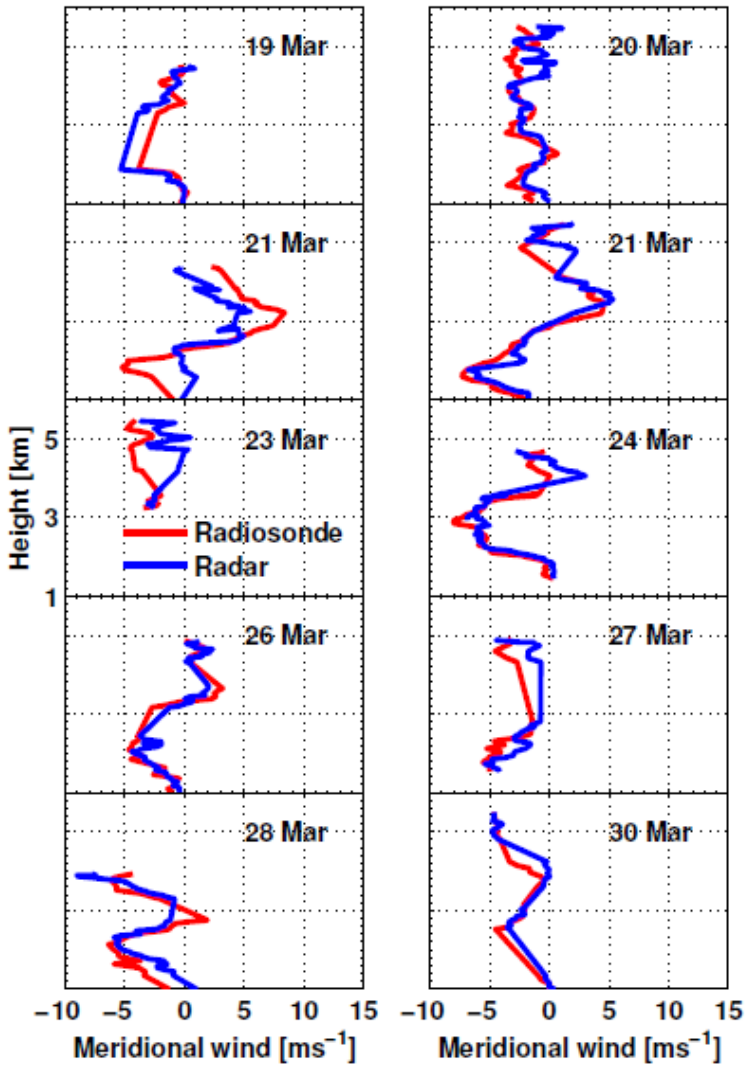

Fig. 6.3b: Same as Fig. 6.3a, but for meridional winds.

The zonal wind comparisons have also been performed for the different altitude ranges of 1 - 3 km and 3 - 6 km and the observed correlation values are 0.92 and 0.90, respectively. The SEE and mean bias in radar zonal wind observed at 1 - 3

km are 1.42 m s^{-1} and -0.59±1.43 m s^{-1}, respectively, whereas the corresponding values at 3 - 6 km are 2.20 ms^{-1} and 0.63±2.28ms^{-1}.

The radar meridional wind also shows a good agreement with radiosondes and the observed correlations are 0.85, 0.89 and 0.82 for the altitude ranges of 1 - 6, 1 - 3 and 3 - 6 km, respectively. The SEE for the three altitude ranges are 1.38, 1.18 and 1.52 m s^{-1}, respectively while the mean bias values correspond to -0.44±1.56, 0.45±1.45 and -0.38±1.66 ms^{-1}.

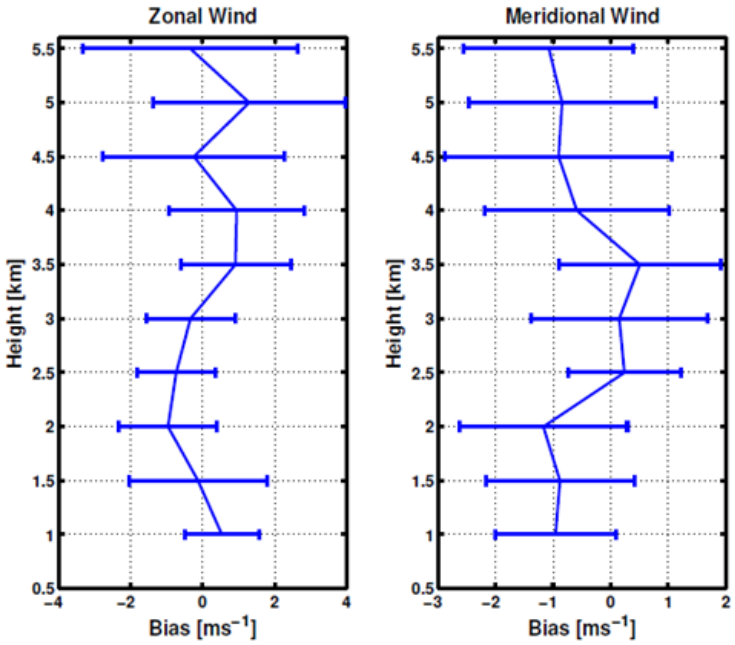

Fig. 6.4: The mean difference and standard deviation between collocated radar and radiosondezonal and meridional wind as a function of height.

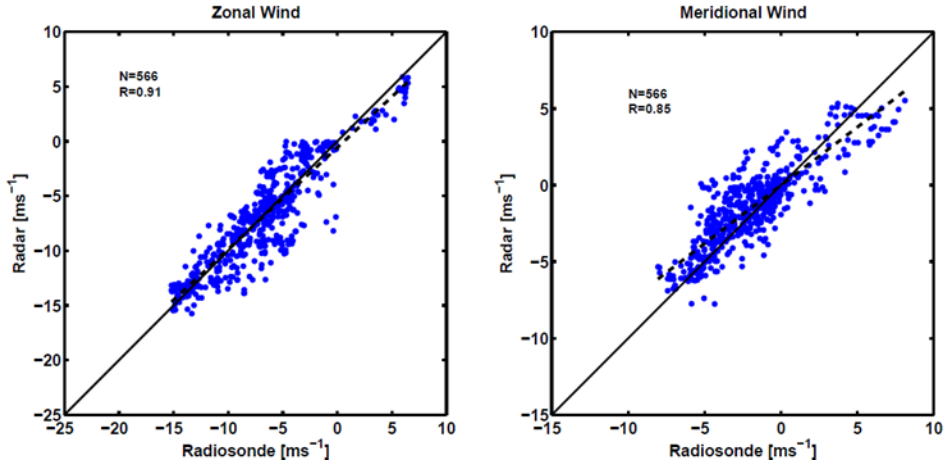

Fig. 6.5a: Scatter plot of zonal and meridional wind speeds from Radar and Radiosonde

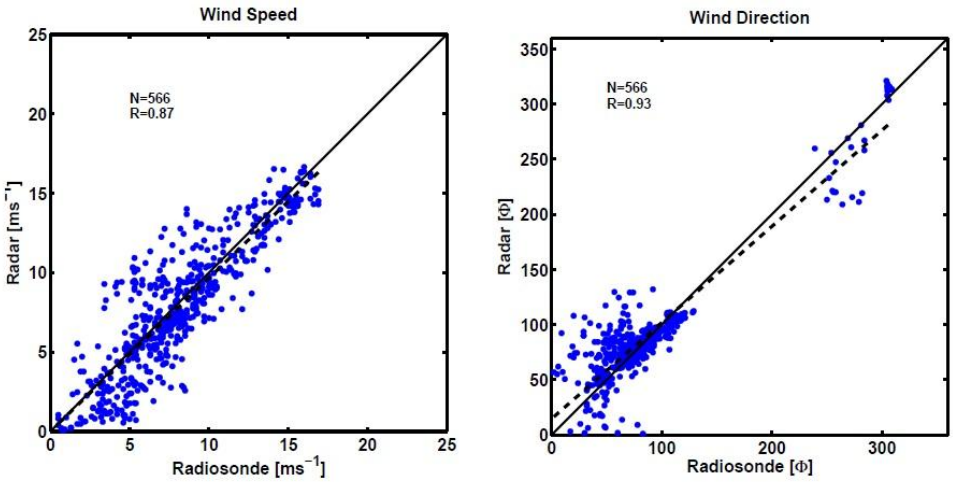

Fig.6.5b: Same as Fig. 6.5a, but for total horizontal wind speed and direction

Comparisons were also performed for wind speed and wind direction obtained from radiosondes and radar and the result is shown in Fig. 6.5b. The observed correlation for wind speed is 0.87 with mean bias of 0.27±1.99 ms^{-1} for the 1 - 6 km altitude range. The wind direction comparison also shows very good correlation of 0.93 with a mean bias of -3.9±19.7^{O}. The correlation of wind direction between radiosonde and radar is slightly lower in the 1 – 3km altitude range possibly due to relatively larger bias in the zonal and meridional winds.

In nutshell, the first time validation of the mini Wind Profiler using collocated radiosonde wind measurements is presented here. The wind profiles within 1-6 km altitude range have been validated. The radar wind profiles match very well with the Radiosondes both in terms of magnitude and direction and ideally captures the day to day variations in wind. The correlation between radar and Radiosondeszonal and meridional wind is 0.91 and 0.85, respectively. The standard deviation of the difference between radiosonde and radar for zonal wind is found to be 1.95 m s^{-1}, and that for meridional wind is 1.56 m s^{-1}. These observations are seen to agree quite well with other established wind profiler radars operating elsewhere in the World.

6.10.3 Observation of pre-monsoon features of atmosphere

The Mini Profiler was used to validate the functionality of all the sub system of ST Radar as well as the signal processing algorithms. The expected height coverage for the 49 element Mini Profiler is 4 to 6 km. However, during the thunderstorm event, it is expected to have enhanced height coverage, during pre- and post-thunderstorm event. This experiment shows that during the thunderstorm, the 49 element ST Radar Mini-Profiler is able to profile the atmosphere up to 12 km.

This section provides a brief account of a thunderstorm event observed on 24th April 2015. The configuration of the experiment conducted on this day is provided in Table 6.1.

Table 6.1 Experiment Configuration for 24th April 2015

Sl.No:	Parameter	Value
1.	Operating Frequency	205 MHz
2.	Number of Antenna elements	49
3.	Radiated Peak Power	24.5 KW
4.	Pulse Repetition Frequency	8000 Hz
5.	Baud	0.3 µs
6.	Code length	16 bits
7.	Pulse Width	7.8 µs
8.	Duty Ratio	3.84 %
9.	Code Type	Complementary codes
10.	Number of coherent Integration	250/128
11.	Height Coverage	0.8 km to 12.0 km
12.	Beams	5
13.	Number of FFT points	1024

Fig. 6.6 depicts the vertical profiles of *u*, *v*, and *w* components of the thunderstorm event. It is interesting to note that there is an increased height coverage up to about 12 km during this particular event. Further, the zonal winds vary within ±10 ms^{-1} in the lower levels below 1 km, while the meridional winds vary within ±15 ms^{-1} in the same height levels during the heavy precipitation period of around 1

hour duration. However, the zonal and meridional components at times cross a threshold of 45 ms^{-1} at the upper height levels around 10 km. The change in the wind direction is rapidly random. The vertical winds are mostly negative (downward directed) during the precipitation time, and is within -10 ms^{-1} at the lower height levels, while it crosses +10 ms^{-1} at a height level of 10 km. All the three orthogonal components show high variability at upper levels compared to lower heights.

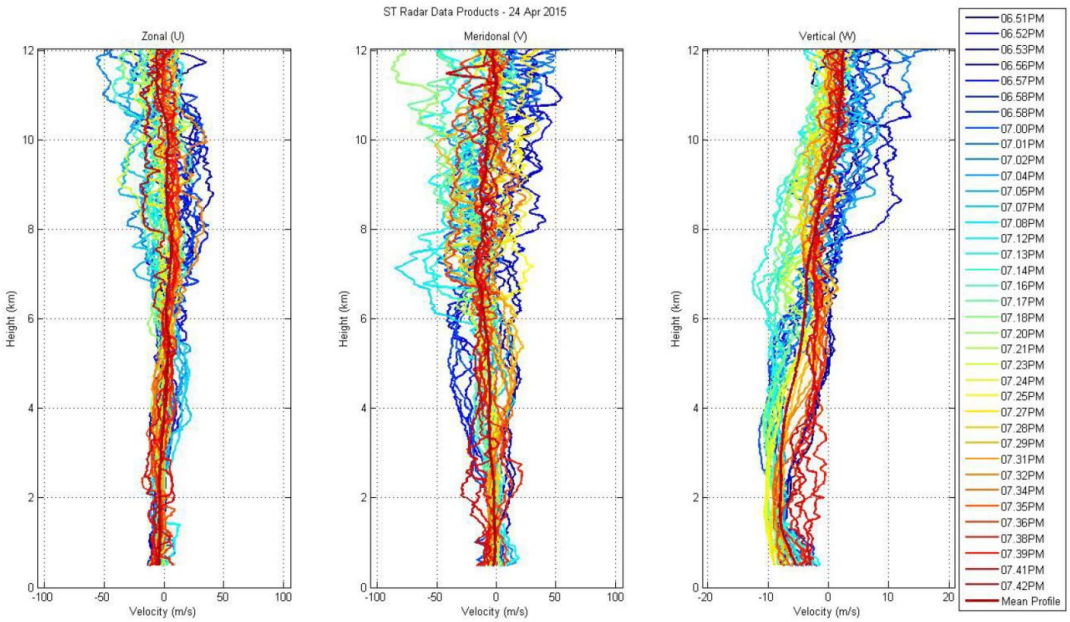

Fig. 6.6: UVW Components for 24th April 2015

While examining the time evolution of total horizontal wind, the rapid changes associated with thunderstorm environment could be seen evidently from Fig. 6.7. The lower heights up to about 3 km is seen to be turbulent while upper levels witness relatively slow changes in both magnitude and direction. However, there is evident intensity in magnitude of wind. This could be attributed to sudden updrafts and downdrafts associated with stormy environment as part of transformation of latent heat to kinetic energy.

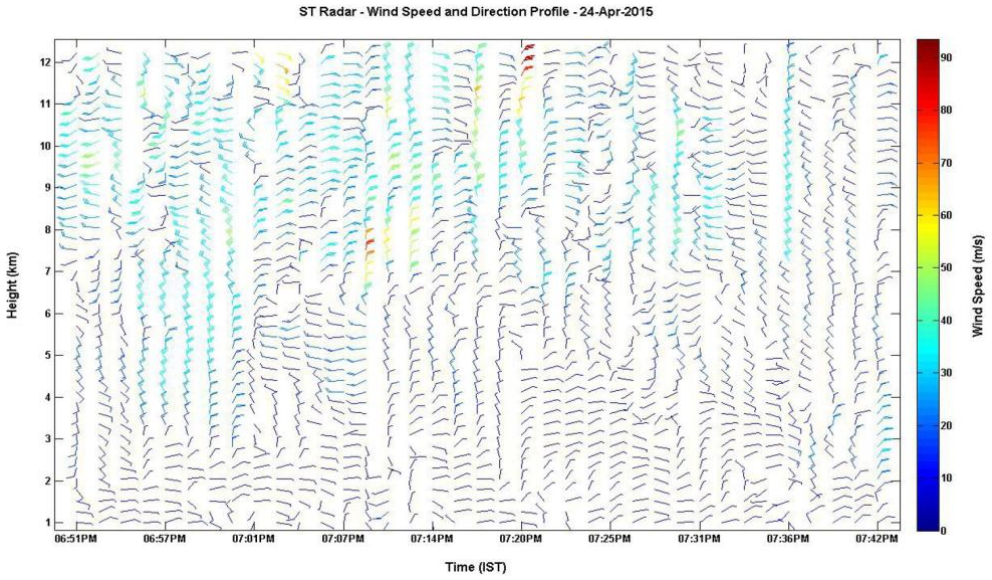

Fig. 6.7: Wind Speed & Wind Direction Profiles 24th April 2015

Fig. 6.8 represents the wind shear calculated at each level during the fag end of the storm's life time. Higher positive and negative intensity in wind shear is observed above ~7 km. The change in the strength of wind with height is a desirable factor for increasing the vigor of the storm. The wind shear aids updrafts by creating a relatively low pressure at higher levels, and also by wind removal of precipitation from the updraft summit, and in some case, introduction of updraft rotation. Chaudhari et al. (2010) reported that high and low instability conditions along with moderate to high vertical wind shear play a significant role in longevity and strength of the storm. Thus the vertical wind shear can be considered as a stability index to examine the thunderstorm strength and associated impacts.

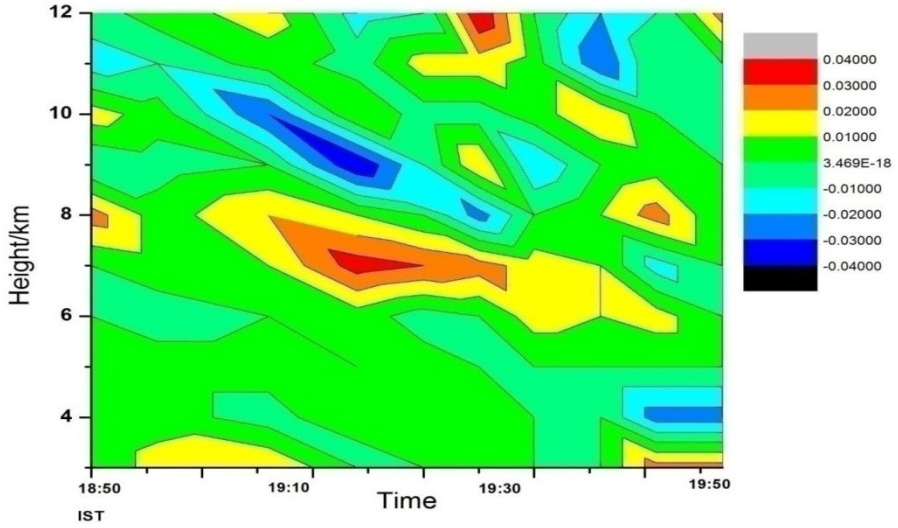

Fig. 6.8: Wind shear inside the Thunderstorm observed on 24th April 2015

6.10.4 Wind Profiler Observation of Monsoon -2016

While the Indian sub-continent witnessed a normal south-west monsoon in 2016 with a rainfall just less than 3 % of the normal rainfall, certain regions like Kerala received 33 % less rainfall than usual. The onset of monsoon was on 8th June over the Kerala coast and the withdrawal commenced around the last week of September. With the onset of Indian summer monsoon, the monsoon circulation also experiences substantial changes among which are the establishments of a tropical easterly jet (TEJ) and the formation of a low level jet. The TEJ plays an active role in the advancement of monsoon disturbances (Chen and van Loon, 1987) while the low level jet stream is instrumental in significant moisture influx from the Ocean to the Indian landmass (Joseph and Sijikumar, 2004).

TEJ is a an upper tropospheric and northern hemispheric summer phenomenon with its core in the North Indian Ocean between 5N and 10N and flowing at speeds greater than 30 ms^{-1} (Wang, 2006). The summer time differential heating occurring over the Indian sub-continent in contrast to the cooler Indian Ocean and the subsequently developing pressure gradient is the driving factor behind this jet.

The low level jet stream or monsoon low level jet (MLLJ) flows at wind speeds exceeding 15–20 ms^{-1} at about 850 hPa, and it regulates the moisture influx across the Indian region (Goswami et al., 1998). A well-documented coupling

between TEJ and low-level jet has been observed and this is essential for incidences of heavy precipitation in South Asia (Chen et al. 1989). The 205 MHz radar can simultaneously look into both TEJ and MLLJ and a comprehensive study of their dynamics and vertical coupling during monsoon period can be studied.

The observed core speed and height of monsoon low level jet over Cochin during June – September, 2016 is shown in Fig. 6.9. During the observation period, the MLLJ core speed varies between 9–50 m s^{-1}, showing a decreasing trend towards the end of September when the monsoon is in its withdrawal phase. The MLLJ core height also shows variations with maximum and minimum values of 0.76 km and 4.95 km, respectively (refer to Fig. 6.9). The mean core speed and height lies at 11.64 ms^{-1} and 2.79 km during the observation period.

The MLLJ depth, which is defined as the vertical span of westerly wind is shown in Fig. 6.10. The westerly depth has an association with the monsoon rainfall as it regulates the moisture influx into the Indian sub-continent from the Arabian Sea (Narayanan et al., 2016). The rainfall observed over the radar location for the observation period is also shown in the same figure. A lack of coherence between the rainfall and MLLJ depth despite the prevalence of westerlies could be because of deficient moisture supply over the Kerala coast during the monsoon of 2016.

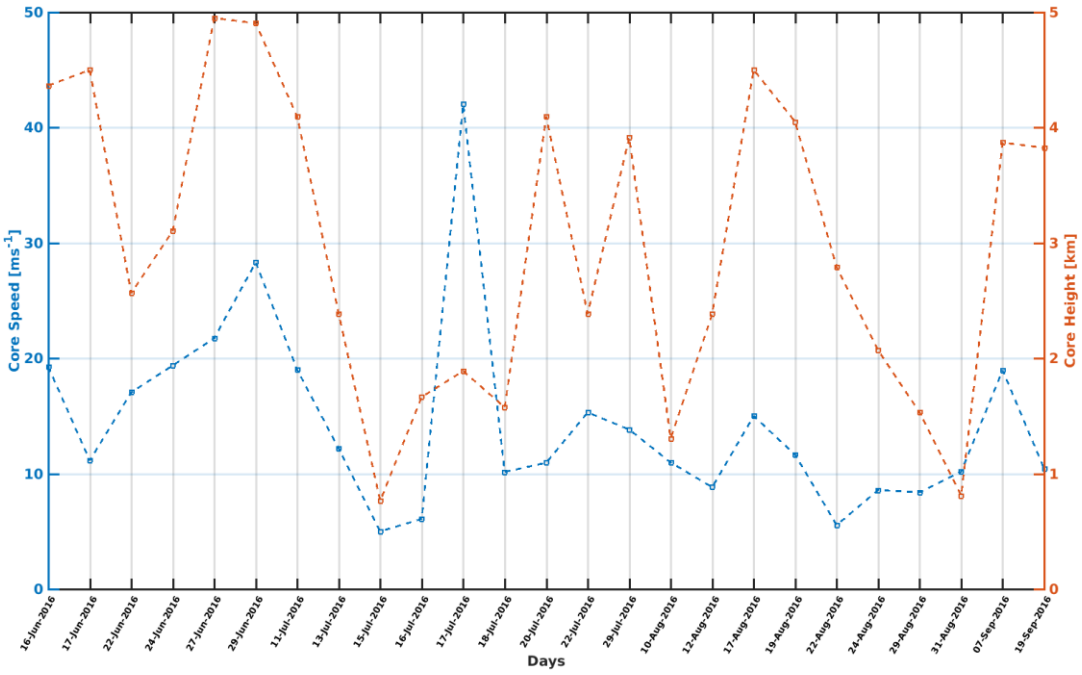

Fig. 6.9: The MLLJ core speed and height observed by 205 MHz radar in JJAS-2016.

Fig. 6.11 shows the TEJ core speed and core height during the observation period. The range observed for core speed lies between -56 and -15 ms^{-1} whereas the core height lies within a range of 14–19 km.

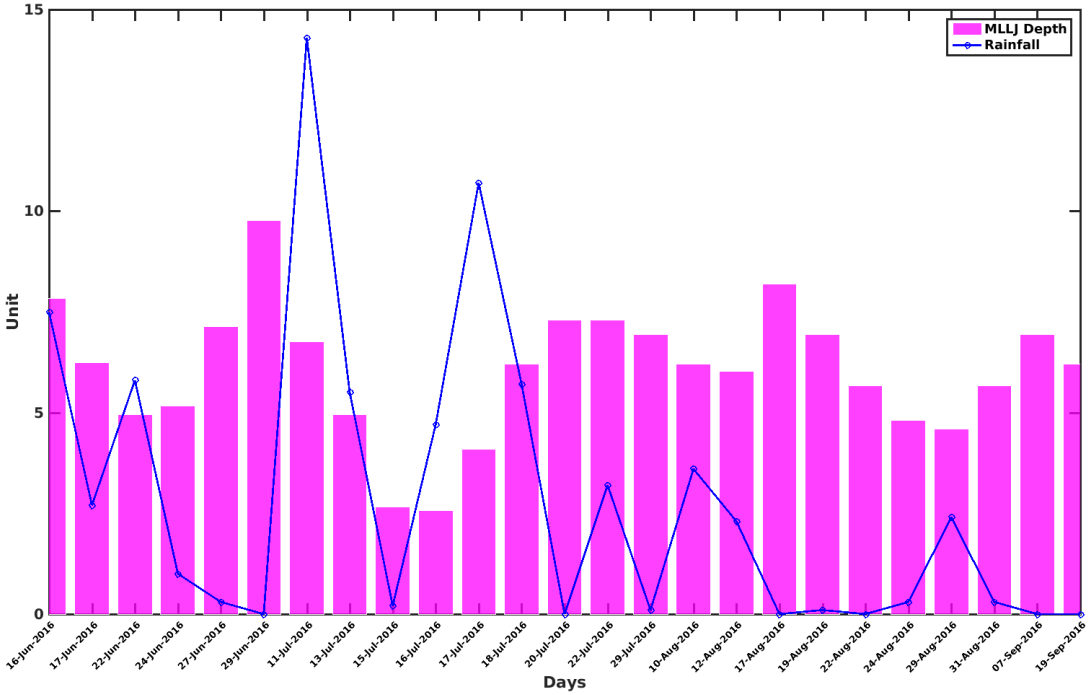

Fig. 6.10: The depth of MLLJ and rainfall over Cochin during monsoon season of 2016.

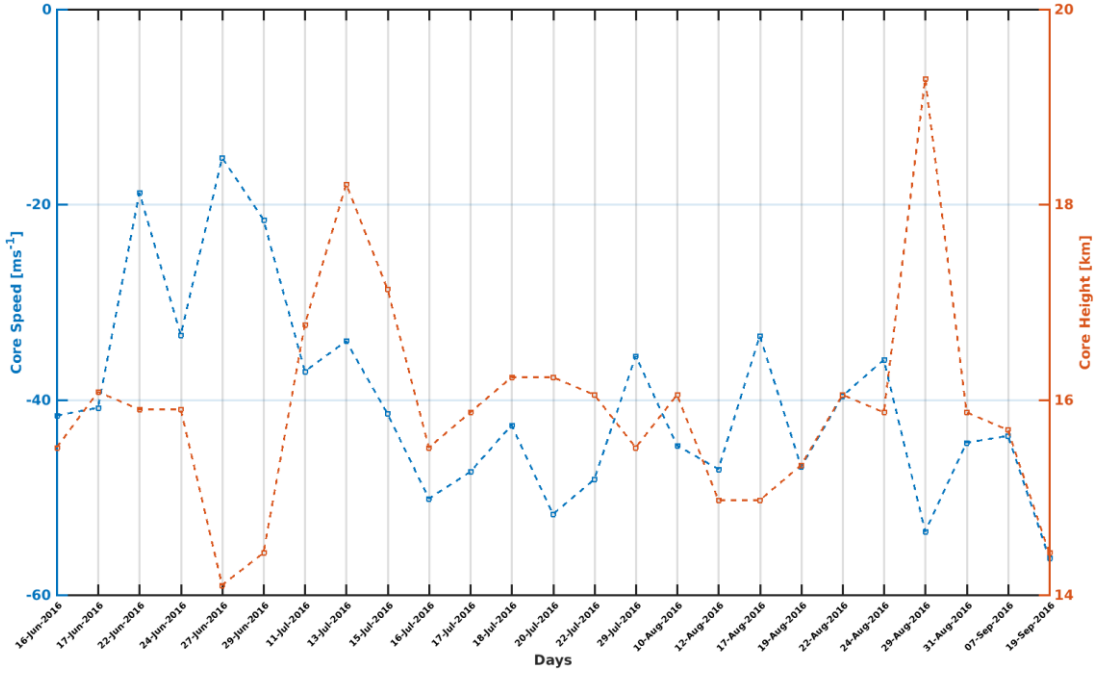

Fig. 6.11: The TEJ core speed and height observed by 205 MHz radar

The coupling between TEJ and MLLJ can induce a vertical motion, eventually leading to formation of precipitating clouds during the monsoon period. In order to demonstrate this, we have investigated the difference between the core speeds of TEJ and MLLJ as a function of vertical velocity at 850 hPa (1.79 km). It shows an increasing trend in the ascending motion as wind shear increases, which shows the link between MLLJ and TEJ and consequent development of vertical motion. Fig. 6.12.

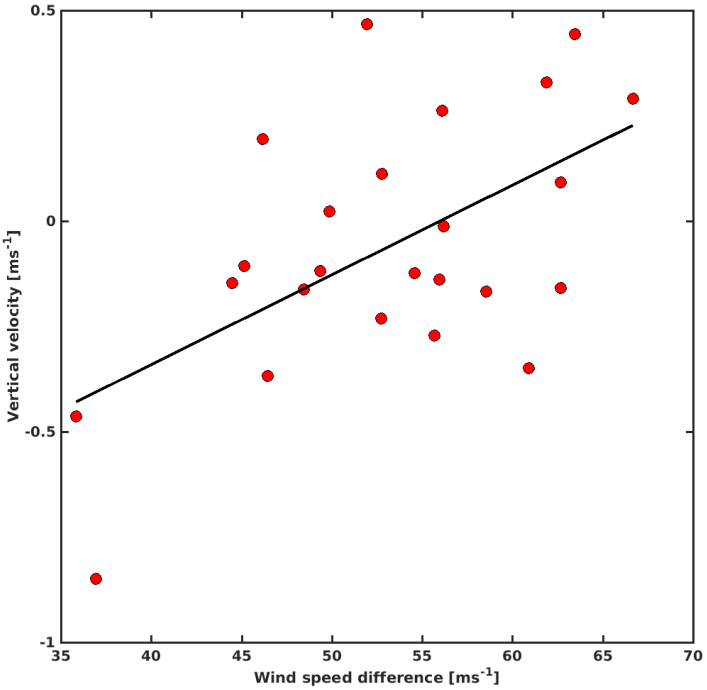

Fig 6.12: Relation showing the difference in the core speeds of TEJ and LLJ with vertical velocity.

The daily variation of vertical profiles of zonal winds obtained from the WPR is plotted in Fig. 6.13a. A wind core extending up to about 4 km could be seen, which corresponds to the LLJ which acts a source of vapour influx. However, the maximum wind speed is observed until mid-July, thereafter maintaining only a weak current until its withdrawal phase. Similarly, Fig. 6.13b represents the daily evolution of vertical velocity which illustrates that the vertical wind was mostly directed upward during the entire period. This upward velocity is helpful in the formation of clouds, but its magnitude is relatively low (within ± 0.5 m s^{-1}). We believe that the relatively low magnitude of both of these components could be

attributed to the below normal rainfall over Kerala, which led to severe drought condition in the State.

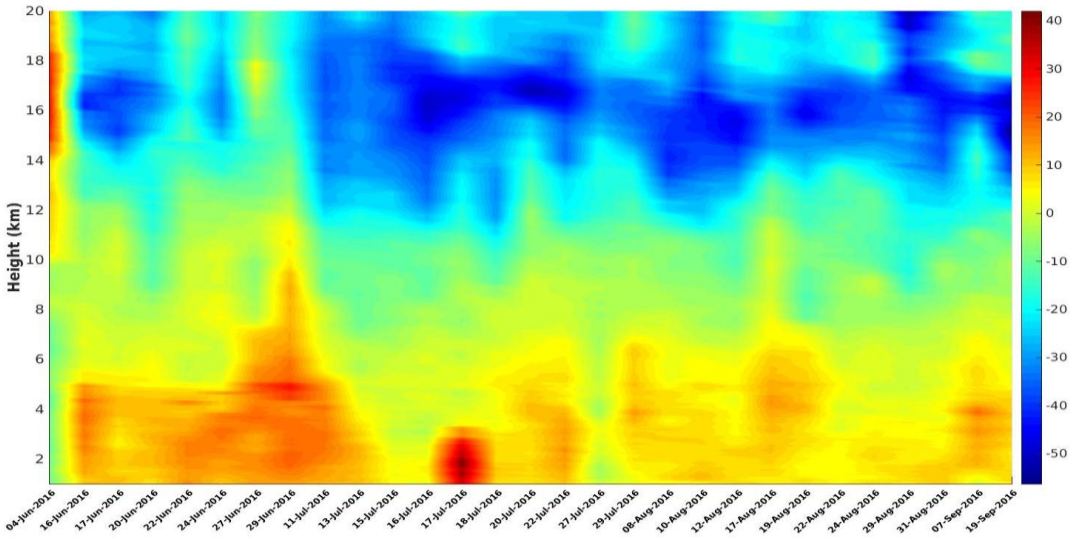

Fig. 6.13a: Variation of vertical profiles of zonal wind over Cochin during 2016 Monsoon

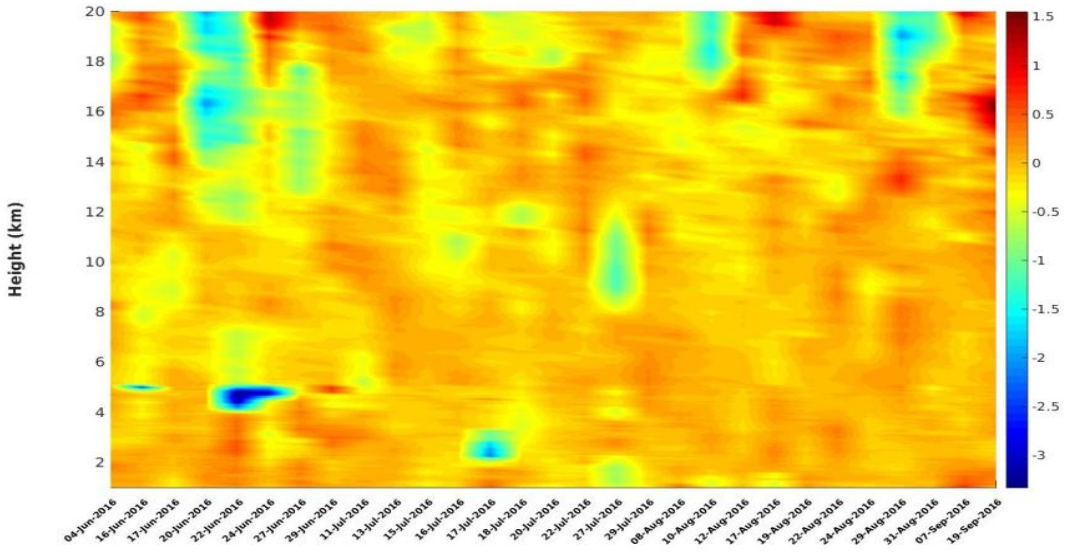

Fig. 6.13b: Same as Fig. 6.12a, but for vertical wind with height.

6.11 Conclusion

WPR at CUSAT, Cochin would be the first radar with this frequency that is being used for wind profiling rather than its stereotypic application in communication and broadcasting. This radar has been set up as an experimental trial to assess the feasibility of using the 205 MHz frequency for wind profiling and also

determine the scientific quality of the data product. This is being run as a predecessor to an even bigger wind profiler radar with 619 three element Yagi-Uda antennae capable of providing wind profiles in the altitude range of 315 m to 20 km.

The validation of the wind profiler has been performed by comparing with collocated radiosonde measurements. The wind profiler shows good capability in measuring the atmospheric wind variability with altitude. The standard deviation of the difference between radar and radiosonde for zonal wind is 1.95 ms^{-1} while it is 1.56 ms^{-1} for meridional wind. Our results agree quite well with studies using other wind profiler radar operating in different UHF and VHF ranges. These results assert the practicality of using the 205 MHz radar for wind profiling and consequent meteorological applications including monsoon studies. Several features of the dynamical filed such as wind core strength, wind shear, turbulence and conditions leading to local convection could be undertaken with the help of this Radar. A preliminary assessment of the 2016 monsoon season with a careful analysis of the wind strength with height could throw some light into the poor performance of monsoon in 2016. The results are encouraging as it gives the confidence that the wind profiler with 619 antennae provides, good quality wind profiles with high temporal and spatial resolution. More in-depth studies of monsoon on a multi-dimensional scale would come forth from this radar facility in the coming years.

****

Chapter

7

Summary and Future Direction

Contents

7.1 Summary

The main objective of the thesis has been to explore the features of southwest monsoon right over its gateway to the subcontinent by employing a suite of observational facilities like Radiosonde, Radar and complementary instruments. Even though several studies have focussed on analyzing the monsoonal features using satellite or re-analysis data set over Kerala, it hasn't been more precise until the installation of a new Stratosphere-Troposphere Wind Profiling Radar (operating at 205 MHz) along with high-resolution GPS Radiosonde which helped in comprehending the minute fluctuations of the monsoon weather over this tropical coastal station. The timely onset, intensification and northward propagation phases of the monsoon are crucial not only for the food security and drinking water needs, but also for the economy of the country as a whole. The strength of monsoon LLJ and TEJ are two important dynamical factors that complete the monsoon circulation, whose properties decide the fate of the monsoon. Satellite and re-analysis data sets are limited either spatially or temporally, and a continuous monitoring of the above dynamical field is mandatory to accurately assess and predict the nature of monsoon circulation. It is this point that has been addressed to some extent in the present doctoral thesis. The major highlights of the study are as follows:

Chapter -1 provides an overview of the observed features of Indian summer monsoon and its semi-permanent nature. Furthermore, the recent trend in the performance of monsoon has also been reviewed. Chapter-2 is a description of the

location of the study, instruments employed for data collection, and details of various data set used for undertaking the research work.

Chapter-3 provides the characteristics of monsoon circulation and associated meteorological parameters during an active monsoon year-2013. The diurnal evolution of LLJ and TEJ shows an increase in strength close to the onset of monsoon over Kerala. Subsequently, the wind shear also increases favouring large–scale organization of convection. The chapter also reveals that the level of westerly to easterly boundary has a substantial bearing on the subsequent rainfall intensity. The zonal momentum and kinetic energy fluxes associated with LLJ show higher magnitude, and they support development of convection in association with transport of moisture content.

Chapter-4 presents the contrasting performance of monsoon during two different years, one being a good monsoon year while the other being a drought year. The Radiosonde data have been utilized to estimate the wind components, and the features of MLLJ such as core speed, core height and depth of westerlies were computed. Subsequently, their role in the intensity of monsoon precipitation was investigated. The correlations of rainfall with fluxes of moisture, momentum and kinetic energy are 0.71, 0.51, and 0.59, respectively. In addition, a positive relation between rainfall and upper tropospheric humidity was brought out. The intra-seasonal variability in monsoon LLJ core height and speed was examined, and they show a periodicity of 30-60 day oscillation during the strong monsoon year of 2013.

Chapter-5 provides an account of the special method of estimating vorticity using triangular grid observations to assess the strength of monsoon rainfall. The triangular grid method employs a special field campaign involving three station observations taken at the vertices of a triangle. The convergence and cyclonic vorticity being the decisive factors of the vigour of convection could thus be analysed for their role in the intensity of precipitation. Furthermore, the diurnal variation of several parameters such as the height of tropopause, core height levels and intensity of LLJ and TEJ could be investigated in association with variability in rainfall.

Chapter-6 yields the preliminary observations of pre-monsoon and monsoon dynamical field using the mini wind profiler operating at 205 MHz. As a first step,

the validation of Radar derived winds was undertaken with the help of radiosonde wind observations. It was found that the zonal and meridional wind components show correlations of 0.91 and 0.85, respectively, with their counterparts obtained from radiosondes. The standard error and mean bias in both zonal and meridional winds have been brought out. Subsequently, time evolution of vertical properties of winds and wind shear causing turbulent mixing associated with pre-monsoon thunderstorm event could be explored. In the later part, the characteristic properties of monsoon dynamical environment, and their effect in producing rainfall could be investigated with finer temporal resolution of a few minutes.

7.2 Future Direction

The present thesis is a diagnostic understanding of the relation between monsoon dynamical field and precipitation. This is only a preliminary assessment of its kind using the latest but advanced observational techniques available over Cochin. However, there is immense scope in both diagnostic and prognostic studies of the present topic. A few of them are listed below:

i. Continuous operation of the 205 MHz wind profiler and complementary instruments during the pre-monsoon to monsoon transition period for investigating how the sudden transition in both thermodynamical and dynamical fields help rapid advancement of monsoon.

ii. Rational use of the recently installed Doppler Weather Radar of India Meteorological Department at Cochin for understanding the off-shore trough formation and characterizing monsoon convection with complementing facilities.

iii. Use of a meso-scale model (Weather Research and Forecasting –WRF model) for prognostic study of pre-monsoon and monsoon convection with incorporation of radar-derived products for the betterment of prediction.

****

References

Abhilash, S., and Mohanakumar K (2009):Vertical structure and evolution of a supercell storm: observations using VHF radar, *International J. RemoteSensing*, **30**, pp 1441-1454, doi: 10.1080/01431160802448950.

Abish B, Joseph P V and Johannessen O M, (2013): Weakening Trend of the Tropical Easterly Jet Stream of the Boreal Summer Monsoon Season 1950–2009, *J. Climate*,**26**, pp 9408-9414. American Meteorological Society.

Alavez A T,Cavazos T and Turrent C (2014): Land-Sea Thermal contrast and Intensity of the North American Monsoon under Climate Change Conditions; *J. Climate*,; **27**, pp 4566-4580Am Met Soc.doi: 10.1175/JCLI-D-13-00557.1.

AnanthakrishnanR.and Soman M K (1988): Indian lnstitute of Tropical Meleorology. Pune 41 1005, India; The Onset Of The Southwest Monsoon Over Kerala:1901-1980; *International J. Climatol*. **8**(3), pp 283-296

Ananthakrishnan R, Acharya U R and Ramakrishnan A R (1967): On the criteria for declaring the onset of the southwest monsoon over Kerala, *IMD, Forcasting Manual*, No IV – 18.1.

Anbar, U., Wang, S., Sobel, A. (2016):Response of Atmospheric Convection to Vertical Wind Shear: Cloud-System-Resolving Simulations with Parameterized Large-Scale Circulation. Part II: Effect of Interactive Radiation**,** *J. Atmos. Sci.*,**73**, pp 199-209,DOI: 10.1175/JAS-D-15-0151.1

Andras S,Czerski H, Zapponi N, and Castro I (2013): Notes on Meteorological Balloon Mission Planning; American Institute of Aeronautics and Astronautics (AIAA) 2013-1295

Annamalai Hand Slingo (2001): Active/break cycles: diagnosis of the intraseasonal variability of the Asian Summer Monsoon, *Clim. Dyn*,**18**, pp 85–102.

Annual Report(2013 and 2017): India Meteorological Department, Ministry of Earth Sciences, Govt. of India.www.imd.gov.in.

Anu Simon and Mohankumar K (2004): Spatial variability and rainfall characteristicsof Kerala. *Proc. Indian Acad. Sci.(Earth Planet. Sci.)*, **113** (2), pp.211 – 221.

Anjaneyalu, T. S. S.(1969): On the estimates of heat and moisture over the Indian monsoon trough zone. *Tellus*,**21**, 64–75.

Asnani, G (1993):Tropical Meteorology, Volume I, edited by Lighthill J and. Pearce P R, pp. 309-319, CambridgeUniversity Press.

Balaji B, Prabha T V, Rao J Y, Kiran T, Dinesh G, Chakravarty K, Sonbawne S M and Rajeevan M (2017):Potential of collocated radiometer and wind profiler observations for monsoon studies; *Atmos. Res.*,**194**, pp 17-26, doi:10.1016/j.atmosres.2017.04.023, 17-26.

Balsley B B and Gage C (1980): The MST Radar Tecnique; Potential for Middle Atmospheric Studies. *PAGEOPH.***118**, pp 452–493.

Bansod SD, Singh HN, Patil SD, Singh N (2012): Recent changes in the circulation parameters and their association with Indian summer monsoon rainfall. *J. Atmos Sol Terr Phys* **77**, pp 248–253.

Battan L. J.(1973): Radar observation of the atmosphere; The University of Chicago Press, 324pp.

Bhat G S (2006): Near-surface temperature inversion overthe Arabian Sea due to natural aerosols, *Geophys. Res. Lett.***33,** pp 826-833.AGU.doi: 10.1029/2005 GL02415.

Bhide U. V., Muzamar, S. P., Ghanekar, O. K., Paul, T. C., Chen and Rao, G.V., (1997): Adiagnostic study on heat sources and moisture sinks in the monsoon trough area during active –break phase of the Indian monsoon of 1979, *Tellus*,**49A**, pp 455 – 473.

Blanford H F (1886): Rainfall of India; *Memoirs of, Ind. Met. Dept*, **2**, 668 pp.

Bollasina, M. A., and Ming Y. (2013): The general circulation model precipitation bias over the southwestern equatorial Indian Ocean and its implications for simulating the South Asian monsoon. *ClimDyn.,***40**, pp 823–838.doi:10.1007/ s00382-012-1347-7.

Bonner W D (1968): Climatology of Low Level Jet, *Mon Wea Rev*, **96**,pp833-850.

Buehler, S. A., and John V. O.(2005): A simple method to relate microwave radiances to upper tropospheric humidity.J Geophys Res 110.doi:10.1029/ 2004JD005111.

Buehler, S. A., Kuvatov M., John V. O.,.Milz M, Soden B. J., Jackson D. L., and Notholt J. (2008): An upper tropospheric humidity data set from operational satellite microwave data. *J Geophys Res* **113,** pp1-13,.doi:10.1029/ 2007JD009314.

Burk, S. D., and Thompson W. T. (1996): The summertime low-level jet and marine boundary layer structure along the California coast, *MonWea Rev*., **124**, pp668–686.

Charney, J.G. and Shukla, J (1981): Predictability of monsoons. Monsoon Dynamics, J. Lighthill and R.P. Pearce, Eds.,Chambridge University Press, pp99-109.

Chaudhari, H.S.,. Sawaisarje, G K Ranalkar, M R and Sen P N (2010): Thunderstorms over a tropical Indian station, Minicoy: Role of vertical wind shear. *J. Earth System. Sci*., **119**(5), pp 603-615.

Chen, T. C. and van Loon, H. (1987):Interannual variation of the tropical easterly jet *Mon. Wea. Rev*, **115**, pp.1739–1759

Chen T and Yen M (1991): Interaction between Intraseasonal oscillations of the Midlatitude Flow and Tropical Convection during 1979 Northern Summer: The Pacific Ocean, *J. Climate*, **4**, pp635-671.

Cheston T C, Frank J (1990): Phased array Radar antennas, Radar Handbook; McGraw Hill Publication.

Choudhury and Krishnan, (2011): Dynamical Response of the South Asian Monsoon Trough to Latent Heating from Stratiform and Convective Precipitation, Centre for Climate Change Research, Indian Institute of Tropical Meteorology, Pashan, India

Colon, J. A.(1964): On interactions between the Southwest Monsoon Current and the Sea Surface over the Arabian Sea, *Indian J. Met. Geophys*., **15**, pp183–200.

Davies-Jones R (1993): Useful Formulas for Computing Divergence, Vorticity and their Errors from Three or More Stations; Monthly Weather Review; NOAA's National Severe Storms Laboratory (Norman, United States).

Dee D P, Uppala S M, Simmons A J., and co-authors(2011):The ERA-Interim reanalysis: configuration and performance of the data assimilation system; *Quart. J. Roy Met Soc*., **137**, pp 553–59; doi**:** 10.1002/qj.828.

ExpeditionIIOE, 1963–1966, (2008): Handbook of Exploration and Environmental Geochemistry, Vol.**10**, 2008, Elsevier B.V. ISSN 1874-2734, DOI: 10.1016/S1874-2734(07)10001-2.

Findlater J (1969): A major low level air current near the Indian Ocean during the northern summer,*Quart. J. Roy. Met. Soc*.**95**,pp362–380.

Findlater, (1971): Mean monthly airflow at low levels over the western Indian Ocean. *Geophys.Memo*., **16**, pp1–53.

Flohn H(1960):Recent investigations on the mechanism of the summer monsoon of southern and eastern Asia. *Symp.on Monsoons of the World.* New Delhi, India, India Meteorology Department, pp 75–88.

Flohn H. (1964): Investigations on the Tropical Easterly Jet.DümmlersVlg. Contract No. DA-91-591-EUC-2781, Final Report No. l. Meteorological Institute, University of Bonn: Germany

Gadgil, S., and Joseph P. V. (2003): On breaks of the Indian monsoon. *Proc. Indian Acad. Sci*., **112**, pp 529–558.

Geerts B and Linacre E (1997): The height of the tropopause, University of Wyoming (*www.das/ geerts/ cwx/notes/chap01/trop height01.gif*).

Gellert W, Kustner H, Hellwich and KastnerH (1977): The VNR concise Encyclopedia of Mathematics; Van Nostrand Reinhold, 760pp

Ghosh S, Vittal H, Sharma T, Karmakar S, Kasiviswanathan KS, Dhanesh Y, et al. (2016): Indian Summer Monsoon Rainfall: Implications of Contrasting Trends in the Spatial Variability of Means and Extremes. PLoS ONE 11(7): e0158670. https://doi.org/10.1371/journal.pone.0158670

Gossard, E. E. and Strauch, R. G. (1983); Radar Observation of Clear Air and Clouds, Elsevier, New York, United States of America, 280 pages.

Goswami, B. N., and Ajaya Mohan R. S.(2001): Intraseasonal Oscillations and Interannual Variability of the Indian Summer Monsoon. *J. Climate***14**, pp1180–1198.doi:10.1175/1520-0442(2001)014(1180:IOAIVO)2.0. CO;2.

Goswami B N and Xavier P K (2005): ENSO control on south Asian monsoon through the length of the rainy season, *Geophys. Res. Lett.*,**32**, pp 1-7, L18717, doi:10.1029/2005GL023216.

Goswami, B. N., G. Wu, and Yasunari, T(2006): The annual cycle, intraseasonal oscillations, and roadblock to seasonal predictability of the Asian Summer monsoon. *J. Climate*, **19**, pp5078-5098.

Gupta A (2006) Monsoon, basically a large scale sea breeze system; Spectrum - *www.tribuneindia.com/2006/20060618/spectrum/main3.htm*

Halley, E., (1686): Historical account of the trade winds and monsoons, *Phil. Trans Roy. Soc., London*, **116**, pp153-168.

Hongbo L, Mingyang H, Bin W, and Qinghong Z (2014): Advances in Low-Level Jet Research and Future Prospects, *J. Meteor. Res.***28**, pp57-75

Hoskins, B. J., and Rodwell M J (1995): A model of the Asian summer monsoon. Part I: The global scale. *J. Atmos. Sci.*, **52**, pp1329–1340.

ITU Report © 2013 ITU International Telecommunication Union; ISBN 978-92-61-14401-2.

IIOE:www.docstoc.com/docs/2201151/A-brief-history-of-oceanographic-studies-in-the-Indian-Ocean-47)

Jayaram, M. (1965): A preliminary study of an objective method of forecasting heavy rainfall over Bombay and neighbourhood during the month of July, *Indian J. Met. Geophys*.,**16**,pp557-564.

JinHua Y, Zhe-Min T, Wang Y (2010): Effects of Vertical Wind Shear on Intensity and Rainfall Asymmetries of Strong Tropical Storm Bilis (2006); *Adv. Atmos. Sci*., **27**, pp 552-561.

Jin Q and Wang C (2017): A revival of Indian summer monsoon rainfall since 2002. *Nature Climate Change*, **7**, pp597-594..doi: 10.1038/NCLIMATE3348

John, V. O., Holl G., Allan R. P., Buehler S. A., Parker D. E., and Soden B. J. (2011): Clear-sky biases in satellite infrared estimates of upper tropospheric humidity and its trends. *J Geophys Res*,**116**.doi: 10.1029/2010JD015355.

Joseph P V and Pillai P V (1988): 40 Day Mode of Equatorial Trough for long range forecasting of Indian Summer Monsoon Onset; *Current Sci*,**57**, pp 951-954,.

Joseph, P. V., and Raman P. L.(1966): Existence of low level westerly jet stream over peninsular India during July.*Ind J Meteor Geophys***17**, pp407–410.

Joseph, P. V. and Sijikumar S.(2004): Intraseasonal Variability of the Low-Level Jet Stream of the Asian Summer Monsoon. *J. Climate*,**17**, pp1449–1458. doi:10.1175/1520-0442(2004)017(1449:IVOTLJ)2.0.CO;2.

Joseph P V, Eischeid J K and Pyle R J (1994): Interannual variability of the onset of Indian summer monsoon and its association with atmospheric features, El Nino and sea surface temperature anomalies; *J. Climate*,**7**pp81–105.

Joshi R R, Singh N, Deshpande S M, Damle S H and PantG B (2006): UHF wind profiler observations of monsoon low level jet over Pune, *Indian J. Radio & Space Phys.*,**35**, pp. 349-359.

Kalapureddy M. C. R. D. N. Rao , A. R. Jain , and Y. Ohno (2007): Wind profiler observations of a monsoon low-level jet over a tropical Indian station; *Ann. Geophys*., **25**, pp 2125–2137.

Kamae Y, Watanabe M, Kimoto M and Siogama H (2014):Summertime land–sea thermal contrast and atmospheric circulation over East Asia in a warming climate—Part II: Importance of CO2-induced continental warming; *ClimDyn.*, **43**, pp1-15, doi 10.1007/s00382-014-2146-0

Kanamitsu M, Krishnamurti TN. (1978): Northern summer tropical circulation during drought and normal rainfall months. *Mon Wea Rev*, **10**, pp 331–347

Kaur S and Purohit M K (2015): Rainfall Statistics of India; India Meteorological Department (Ministry of Earthsciences) Report NO. ESSO/IMD/HS R. F. REPO RT/04(2016)/22.

Keeler R J and Passeralli R E (1990): Signal Processing for Atmospheric Radars, pp 199-229, Radar in Meteorology, D Atlas, ed Boston, American Meteorological Society.

Keshavamurthy, R., S. Kasture, and V. Krishnakumar (1986): 30-50 day oscillation of the monsoon: A new theory, *Beitr. Phys. Atmos*, **59**, pp443-454.

Keshavamurty, R. N. (1968): On the Maintenance of the Mean Zonal Motion in the Indian Summer Monsoon, *Mon WeaRev*,**96**, pp. 23-31.

Keshavamurthy R N, Sathyan V, Dash S K and Sinha H S S (1980): Shift of quasi-stationary featuresduring active and break monsoons; *Proc. Indian Acad. Sci, (Earth Planet. Sci.)***97**, pp127-136.

Kikuchi K.,and Wang B (2009): Global perspective of the quasi-biweekly oscillation, *J. Climate*, **22**, pp1340–1359.

Koteswaran P. (1958):The Easterly Jet Stream in the Tropics, *Tellus*, **10**, pp43 – 57.

Koteswaram, P. (1960): The Asian summer monsoon and the general circulation over the tropics, paper presented at Symposium on Monsoons of the World, India Meteorol. Dep., New Delhi.

Kottayil, A., and. Satheesan K (2015): Enhancement in the upper tropospheric humidity associated with aerosol loading over tropical pacific. *AtmosEnviron***122,** pp148 – 153.doi:http://dx.doi.org/10.1016/j.atmosenv.2015. 09.043.

Kottayil, A., Buehler S. A., John V. O, Miloshevich L. M., Milz M., and Holl G. (2012): On the Importance of Vaisala RS92 Radiosonde Humidity Corrections for a Better Agreement between Measured and Modeled Satellite Radiances. *J Atmos Oceanic Technol.*,**29**, pp48–259. doi:10.1175/JTECH-D-11-00080.1.

Kottayil, A., John V. O. and Buehler S. A. (2013): Correcting diurnal cycle aliasing in satellite microwave humidity sounder measurements. *J Geophys Res* **118**, pp101–113. doi:10.1029/2012JD018545.

Kottayil, A., Mohanakumar K., Samson T., Rebello R.,.Manoj M. G, R. V, Santhosh K. R., Mohanan P., and Vasudevan K. (2016): Validation of 205 MHz Wind Profiler Radar Located at Cochin, India Using Radiosonde Wind Measurements. *Rad Sci.* **51**. pp 106-117.doi:10.1002/2015RS005836.

Kreyszig E (1988): Cramer's Rule; Advanced Engineering Mathematics; John Wiley & sons, inc.

Krishnan R, Kumar V, Sugi M and Yoshimura J (2009): Internal Feedbacks from Monsoon–Midlatitude Interactions during Droughts in the Indian Summer Monsoon,*J. Atmos. Sci*., **66** (3), pp 553-578. ;doi: 10.1175/2008JAS2723.1.

Krishnamurti T N (1971): Tropical East-West Circulation Duringthe Northern Summer, *J. Atmos. Sci*..,**28**, pp1342-1347.

KrishnamurtiT N and Bhalme H N (1976): Oscillations of a Monsoon System. Part I. Observational Aspects, *J. Atmos. Sci*.,**33**, 1937-1954.doi.org/10.1175/1520-0469(1976)033<1937:OOAMSP>2.0.CO;2

Krishnamurti T N, Ardanuv P, Ramanathan and Pasch R (1981):On the Onset Vortex of the Summer Monsoon,*Mon Wea Rev*., **109**, pp344-363.doi.org/10.1175/1520-0493(1981)109<0344:OTOVOT>2.0.CO;2

Krishnamurthi T N 1985 Summer monsoon experiment – a review; Mon. Weather Rev. 113 1590–1626

Krishnamurthy, V.(2011): Extreme Events and Trends in the Indian Summer Monsoon, COLA Technical Report 314, July 2011.

Krishnamurthy, V. and Shukla, J. (2000): Intraseasonal and Interannual Variability of Rainfall over India. *J. Climate*,**13**, pp4366–4377.doi:10.1175/1520-0442(2000)013(0001:IAIVOR)2.0.CO;2.

Kulkarni J R and Verma R K(1993): On the Spatio-Temporal Variations of the Tropopause Height over India and Indian Summer Monsoon Activity, *Adv. Atmos. Sci.*, **10**(4), pp481-488.

Lane T. P. and. Reeder M. J, (2001): Convectively Generated Gravity Waves and Their Effect on the Cloud Environment. *J. Atmos. Sci.*, **58**, pp2427–2440.

Loo Y Y, Billa L, and Singh A (2015):Effect of climate change on seasonal monsoon in Asia and its impact on the variability of monsoon rainfall in Southeast Asia*, Geoscience Frontiers,***6,**pp817-823

Madden and JulianOscillaion, (1994): The Life Cycle of the Madden Julian Oscillation; doi.org/10.1175/1520-0469(1994)051<2225:TLCOTM>2.0.CO;2

Misra V, Moeller L, Stefanova S, Chan S, O'Brien JJ, SmithIII TJ, & Plant N (2011) The influence of the Atlantic Warm Pool on the Panhandle Florida Sea Breeze. Journal of Geophysical Research (Atmospheres), doi:10.1029/2010JD01, 1-x.

Misra V, Krishnamurti T N, Stefanova L (2013): Tropical Meteorology, An Introduction; Springer, New York,

Mohanakumar K (2008):Stratosphere Troposphere Interactions: An introduction; Springer, Netherlands; 414 pp. doi: 10.1007/978-1-4020-8217-7

Muraleedharan P M, Mohankumar K, Sivakumar K U, (2013): A study on the characteristics of temperature inversions in active and break phases of Indian summer monsoon; *J.Atmos.Solar-Terr.Phys*. **93**; pp 11 – 20

MurtyK P R V andSamN V (2002): Characteristics of monsoon low level jet (MLLJ) as an index of monsoon activity; *Proc. Indian Acad. Sci. (Earth Planet. Sci.)*, **111**, pp. 453–457.

Nair V G and Mohankumar K, (2009): Impact of Western Ghats Orography on the Weather and Climate Over Southern Peninsular India – A Mesoscale Modelling Study. PhD Thesis, Dept.of Atmospheric Sciences, CUSAT, India.

Narayanan S, KottayilA,MohanakumarK.(2016): Monsoon low-level jet over the gateway of Indian summermonsoon: a comparative study for two distinct monsoon years, *MeteorolAtmos. Phys*., **128**, pp 689-696.doi 10.1007/s00703-016-0459-8.

NASA Technical Report (1984), NASA Technical Memorandum, ntrs.nasa.gov/ search.jsp?R=19860009480.

Nithya, K., Manoj M.G., and Mohanakumar K (2017) Effect of El Niño/La Niña on Tropical Easterly Jet stream during Asian Summer Monsoon Season, *Theor Appl. Climatol*,**37**(15), pp4994-5004. DOI: 10.1002/joc.5137.

Ogwang B A, Ongoma V, Xing, Ogon F K (2015): Influence of Mascarene High and Indian Ocean Dipole on East African Extreme Weather Events; *Geographical Pannonica*. **19**, pp 64-72

Raghavan K., (1973): Break monsoon over India. *Mon Wea. Rev*. **101**, pp33–43

Rai P and Dimri A P. (2017): Effect of changing TEJ, LLJ and QBO on Indian Summer Monsoon; *Atmos. Sci. Lett*.,**18,** pp52-59.Doi:10.1002/asl.723

RajanC K (1989): Climate of Kerala, National Library No 551.6;

Rajeevan M, Gadgil S, and Bhate J (2008): Active and Break Spells of the Indian Summer Monsoon, NCC Research Report No7/2008, 45 pp.

Ramage C S (1971): Monsoon Meteorology.International Geophysics Series, vol. 15. San Diego, CA: Academic Press.

Ramage C S and Raman C R V.(1972): Meteorological Atlas of the IIOE, Part 2 Upper Air, University of Hawaii, Honolulu; National Science Foundation, Washington, D.C.

Raman R, Raman M. R ,Rao V. V. M. J, Ratnam M. V, Rajeevan M.,. Rao S. V. B,. Rao N D and Rao N. P. (2009): Characteristics of the Tropical Easterly Jet: Long-term trends and their features during active and break monsoon phases; *J. Geophys. Res. Atmosphere*, **114** (D19). 0148-0227/09/2009JD012065.

Raman, C. R. V., and Dixit, C. M. (1964): Upper air climatological Atlas of the Indian Ocean, Int. Met. Centre, Bombay.

Raman, R. M., M. V. Ratnam, M. Rajeevan, V. V. M. J. Rao, *and* S. V. B. Rao(2011):Intriguing aspects of the monsoon low-level jet over peninsular India revealed by high-resolution GPS radiosonde observations, *J. Atmos. Sci.*,**68**, pp1413–1423.

Ramaswamy, C (1962)**:**Breaks in the Indian summer monsoon as a phenomenon of interaction between the easterly and the sub-tropical westerly jet streams; *Tellus*,**14**, pp 337–349,;DOI: 10.1111/j.2153-3490.1962.tb01346.x.

Ramaswamy, C., (1965): On synoptic methods of forecasting the vagaries of southwest monsoonover India and neighbouring countries, *Proc. Symp. IIOE*, pp 317 - 326.

Ratnam M. V, MurthyB. VK and. JayaramanA (2013): Is the trend in TEJ reversing over the Indian subcontinent?, *Geophys. Res.Lett.*,**40**, pp3446-3449, doi: 10.1002/grl.50519.

Rao, Y. P., 1976, "Southwest Monsoon, Met. Monography", Synoptic Meteorology India Met. Dept. Pune, 367 pp.

Rao R.R (1986): Cooling and deepening of the mixed layer in the central Arabian Sea during MONSOON-77: observations and simulations.*Deep Sea Research Part A. Ocean. Res. Papers*, **33**, pp 1413-1424:doi.org/10.1016/0198-0149(86)90043-9.

Rao, G.K., and Goswami, B.N.,1988: Interannual variations of sea surface temperature over theArabian Sea and the Indian Monsoon: A new perspective. *Mon. Wea. Rev.***116**; pp 558-568.

Rao, P. S., and D. R. Sikka (2005): Intraseasonal variablity of the summer monsoon over the north Indian Ocean as revealed by the BOBMEX and ARMEX field programs, *Pure Appl. Geophys*., **162**, pp 1481 – 1510, doi:10.1007/s00024-005-2680-0.

Rao RR, Sivakumar R (1999): On the possible mechanisms of the evolution of a mini-warm pool during the pre-summer monsoonseason and the genesis of onset vortex in the south eastern Arabian Sea. *Q J R MeteorolSoc*., **125:** pp787–809.

Raman M R, Rao V V M J, Ratnam M.V, Rajeevan M, Rao S. V. B, Rao D N, Rao N. P. (2009): Characteristics of the Tropical Easterly Jet: Long-term trends and their features during active and break monsoon phases; Journal of Geophysical Research, vol. 114, d19105, doi:10.1029/2009jd012065.

Rao, V. B., C. C. Ferreira, S. H. Franchito, and S.S.V.S. Ramakrishna (2008), In a changing climate weakening tropical easterly jet induces more violent tropical storms over the north Indian Ocean, Geophys. Res. Lett., 35, L15710, doi:10.1029/2008GL034729

Rao YP(1976), Southwest monsoon India Meteorological Department. Meteorological Monograph Synoptic Meteorology, No.1/1976, Delhi, 367 pp.

Remedio A R C (2013): Connections of low level jets and mesoscale convective systems in South America; *Reports on Earth System Science*, International Max Planck Research School on Earth System Modelling.

Reid G C and Gage K S (1981): On the Annual Variation in Height of the Tropical Tropopause, *J. Atmos. Sci*., **38**, pp1928-1938.

Reiter, E. R.(1961): Jet stream meteorology, pp. 265-271, University of Chicago Press,.

Roja Raman, M., Ratnam M V, Rajeevan M., Rao V V M J, and Rao B S V (2011): Intriguing Aspects of the Monsoon Low-Level Jet over Peninsular India Revealed by High-Resolution GPS Radiosonde Observations. *J. Atmos. Sci.*,**68**, pp1413–1423. doi:10.1175/2011JAS3611.1.

Roxy M K, Ritika K, Terray P, Murtugaudde R, Ashok K and Goswamy B N (2015): Drying of Indian subcontinent by rapid Indian Ocean warming and a weakening land-sea thermal gradient; *Nature Communications* **6**, Article number: 7423 (2015) doi:10.1038/ncomms8423

Routray A, Mohanty U C, Rizvy S R H, Niyogi D, Osuri K K and Pradhan D (2010):Impact of Doppler weather radar data on numerical forecast of Indian monsoon depressions, *Q J R Meteorol Soc.,* **136**, Part A, pp1836–1850.

Ruchith, R. D., Raj P. E., Kalapureddy M. C. R, Deshpande S. M., and Dani K. K. (2014): Time evolution of monsoon low-level jet observed over an Indian tropical station during the peak monsoon period from high-resolution Doppler wind lidar measurements, *J. Geophys. Res. Atmos.,***119,**pp 1786–1795. doi:10. 1002/2013JD02075.

Ruchith R D, Deshpande S M and Raj P E (2016): UHF wind profiler observations of monsoon low-level jet (MLLJ) and its association with rainfall over a tropical Indian station; *Atmosfera*, **29**, issue 1, pp 1-9; doi.org/10.20937/ATM. 2016.29.01.01.

Samson T K , Manoj M G, Kottayil A , Rakesh V, Rebello R, Babu B, Vasudevan K, Santosh K R, Mohanan P, and Mohankumar K (2016):Technical Aspects of 205 MHz VHF Mini Wind Profiler Radar for Tropospheric Probing; *IEEE Geosci. and Remote Sensing Lett*,**13(**7), pp 1027-1031.

SamelsonR M (1992), Supercritical Marine-Layer Flow along a Smoothly Varying Coastline, *J. Atmos. Sci.*, **49**, pp1571-1584.

Sandeep S and Ajayamohan R S (2014); Poleward Shift in Indian Summer Monsoon Low Level Jetstream under Global Warming.*Clim. Dyn.*,**45**, pp337-351. Doi10.1007/s00382-014-2261-y

SathiyamoorthyV. (2005):Large scale reduction in the size of the Tropical Easterly Jet, *Geophys. Res. Lett.***32**, pp 312-316 doi: 10.1029/2005GL022956.

SathiyamoorthyV, Pal P K and Joshy P C (2007): Intraseasonal variability of the Tropical Easterly Jet; *Meteorol. Atmos. Phys*., **96**(3): pp305-316. doi 10.1007/ s00703-006-0214-7

Sikka D R. (2012): Scientific Studies on the SW Monsoon – Past, present and prospects; Monsoon Monograph (Vol 1); India Meteorological Department,.

Sikka, D. R., and Gadgil S.(1980): On the Maximum Cloud Zone and the ITCZ over Indian, Longitudes during the Southwest Monsoon. *Mon Wea. Rev.*,**108,** pp1840-1852. doi:10.1175/1520-0493(1980)108(1840: OTMCZA)2.0.CO;2.

Singhvi A K and Krishnan R (2014): Past and Present Climate of India. *Landscapes and Landforms of India*, World Geomorphological Landscapes, pp 15-23 doi 10. 1007/978-94-017-8029-2_2, @ Springer Science + Business Media Dordrecht 2014.

SivaramakrishnanS, Saxena S and Vernekar K G (1992): Characteristics of turbulent fluxes of sensible heat and momentum in the surface boundary layer during the Indian Summer Monsoon, Proc. Workshop on preliminary scientific results of MONTBLEX, IISc, Bangaluru, pp 95-108

Soden, B. J., and Fu R.(1995): A Satellite Analysis of Deep Convection, Upper-Tropospheric Humidity, and the Greenhouse Effect. *J. Climate*,**8**, pp2333–2351. doi:10.1175/1520-0442(1995)008(2333:ASAODC)2. 0.CO;2.

Soman M K and Krishna Kumar K (1993): Space-time evolutionof meteorological features associated with the onset of the Indian summer monsoon; *Mon. Wea. Rev.* **121,** pp1177–1194.

Srilaxmi P, Kullayamma, I.,and Rao, M.D. (2012):Removal of Clutter by Using Wavelet Transform For Wind Profiler. *International Journal of Modern Engineering Research (IJMER),***2**(6), pp4591-4594.

Srivastava, A. K., K. C. Sinha Ray, and U. S. De (2000): Trends in frequency of cyclonic disturbances and their intensification over Indian seas, *Mausam*, **51**, pp 113–118.

Swapna P, Krishnan R, Wallace JM (2013): Indian Ocean and monsoon coupled interactions in a warming environment. *Clim. Dyn*., **42**, pp2439-3454. doi:10. 1007/s00382-013-1787-8.

Turner, A., and Stein, T. (2016): Understanding monsoon cloud development using Doppler weather radar andhigh-resolution modelling, (inCOMPASS Field Campaign),*http://www.met.reading.ac.uk/nercdtp/home/available/desc/entry 2018/ SC201811.pdf*

Vasantha, B., M. VenkatRatnam, K. Mohan, S. Kamala, and D. NarayanaRao(2002): Characteristics of tropical easterly jet over Gadanki: Comparison with radiosonde and rawinsonde,*Indian J. Radio Space Phys*., **31**, pp130–139.

Vinayachandran P. N, (2004): Summer cooling of the Arabian Sea during contrasting monsoons, *Geophys. Res. Lett*., **31** (13), doi: 10.1029/2004GL019961

VishnuS , Francis1 P A, ShenoiS S C and RamakrishnaS S V S, (2016), On the decreasing trend of the number of monsoon depressions in the Bay of Bengal. *Environ. Res. Lett.***11,** pp 14-21.

Wang B. (2006). The Asian Monsoon. Springer.

Wang B, Ding Q and Joseph P V (2009): Objective Definition of the Indian SummerMonsoon Onset; *J. Climate*, **22**, pp3303-3316. doi.org/10.1175/2008 JCLI2675.1.

WangB, Liu J, Kim H J, Webster P J,Yim S Y, and Xiang B (2013), Northern Hemisphere summer monsoon intensified by mega-El Niño/southern oscillation and Atlantic multidecadal oscillation, vol. 110 no. 14, Bin Wang, 5347–5352, doi: 10.1073/pnas.1219405110, *Proc. of the National Academy of Sciences* of the United States of America.

Weaver S J and Nigam S (2006), Variability of the Great Plains LLJ: Large Scale Circulation Context and Hydroclimate Impacts, *J. Climate*,**21**, pp1532-1551.

Webster, P. J., Magana V. O., Palmer T. N., Shukla J., Thomas R. A., Yanai M., and Yasunari T. (1998) Monsoons: Processes, predictability, and the prospects for prediction.*J.Geophys.Res*.,**103**(C7).pp14451-14510.doi:10.1029/97JC02719.

Winat, C. D., Dorman C. E., Freeze C. A, and Beardsley R. C. (1988), The marine layer off northern California: An example of supercritical channel flow, *J. Atmos. Sci*., **45**, pp3588–3605.

Wu T (2004): Life on the High Tibetan Plateu; High Altitude Medicine & Biology. July2004, **5(1),**pp1-2. https://doi.org/10.1089/152702904322963609.

Xavier, A., Manoj M.G., and Mohanakumar K (2017): On the dynamics of an extreme rainfall event in northern India in 2013, *Journal of Earth System Science* (In Press).

Xavier, P. K., John V. O.,. Buehler S. A, Ajayamohan R. S., and Sijikumar S.(2010): Variability of Indian summer monsoon in a new upper tropospheric humidity data set.*Geophys Res Lett.,* **37**(5).doi:10.1029/ 2009GL041861.

Yanai M, Li C, Song Z. 1992): Seasonal heating of the Tibetan Plateau and its evaluation of the Asian summer monsoon. Journal of Met.Soc. Japan **70**(1B): pp 319–351.

****

List of Publication

Narayanan S, KottayilA,MohanakumarK.(2016): Monsoon low-level jet over the gateway of Indian summermonsoon: a comparative study for two distinct monsoon years, *MeteorolAtmos. Phys*., **128**, pp 689-696.doi 10.1007/s00703-016-0459-8.

****